



Error Estimation and Adaptive Mesh Refinement for Problems with Complicated Geometries

Marian Nemec

ELORET Corp.
Advanced Supercomputing Division
NASA Ames Research Center

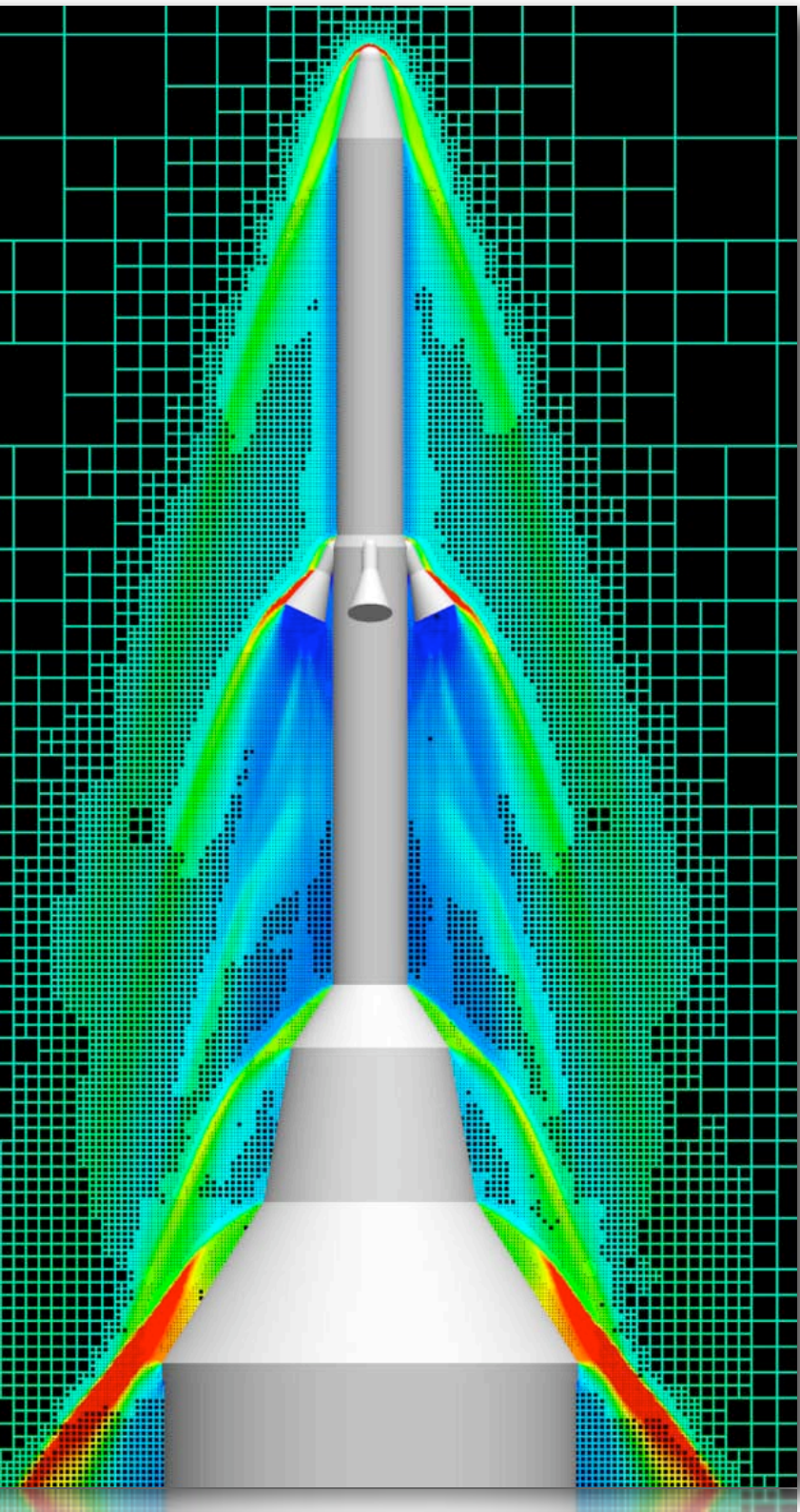
Joint work with Michael Aftosmis (NASA Ames) and Marsha Berger (NYU)

MIT ACDL Seminar
May 9, 2008



Objectives

Toward automation of CFD analysis



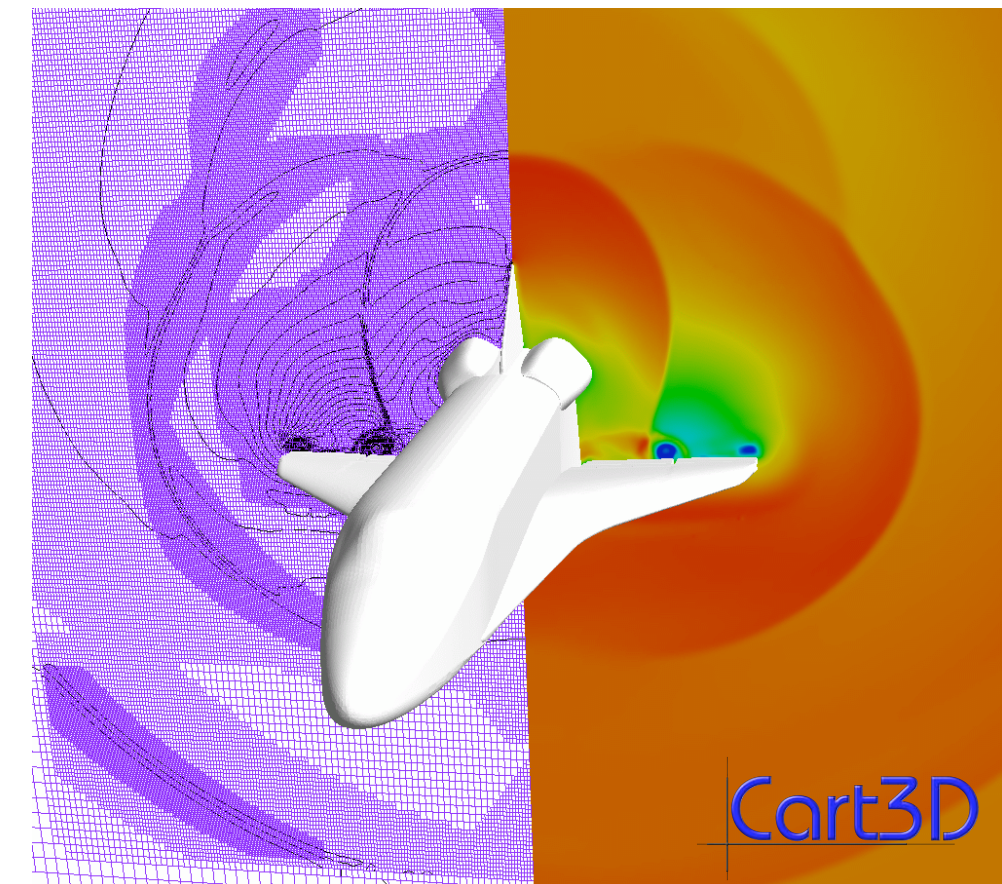
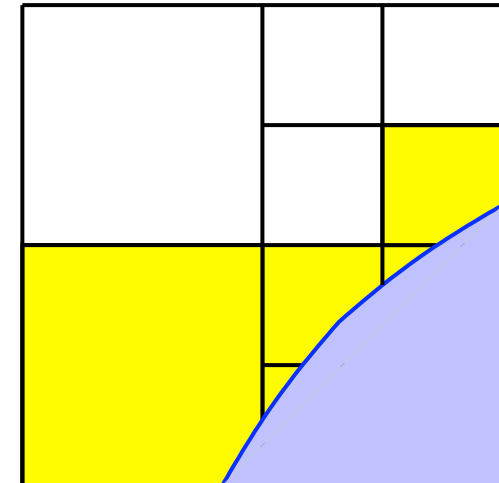
- Handle complex geometry problems
- Control discretization errors via solution-adaptive mesh refinement
- Focus on aerodynamic databases of parametric and optimization studies
 1. **Accuracy**: satisfy prescribed error bounds
 2. **Robustness** and **speed**: may require over 10^5 mesh generations
 3. **Automation**: avoid user supervision
- Obtain “expert meshes” independent of user skill
- Run every case adaptively in production settings



Approach

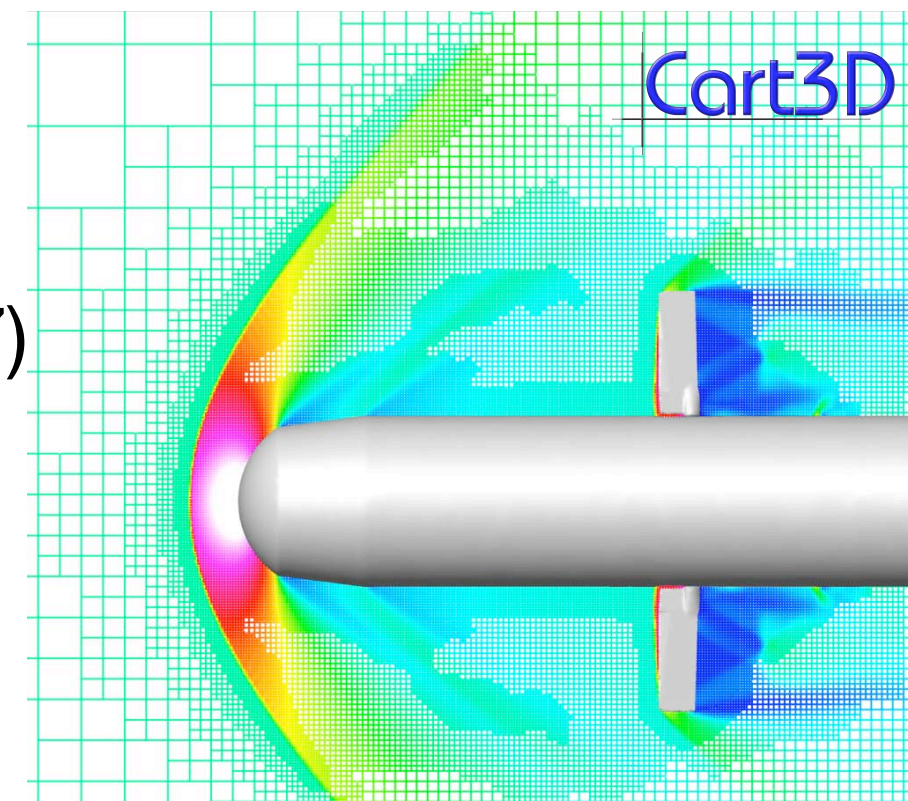
1. Embedded-boundary Cartesian mesh method (1990's)

- Arbitrarily complex domains, efficient and accurate
- Irregularity confined to body intersecting cells



2. Incremental strategy for h-refinement of nested Cartesian meshes (2002)

- Fast local re-meshing of flagged cells
- Guaranteed reliability
- Early work used feature detection and τ -extrapolation



3. Adjoint-weighted residual error estimates (2007)

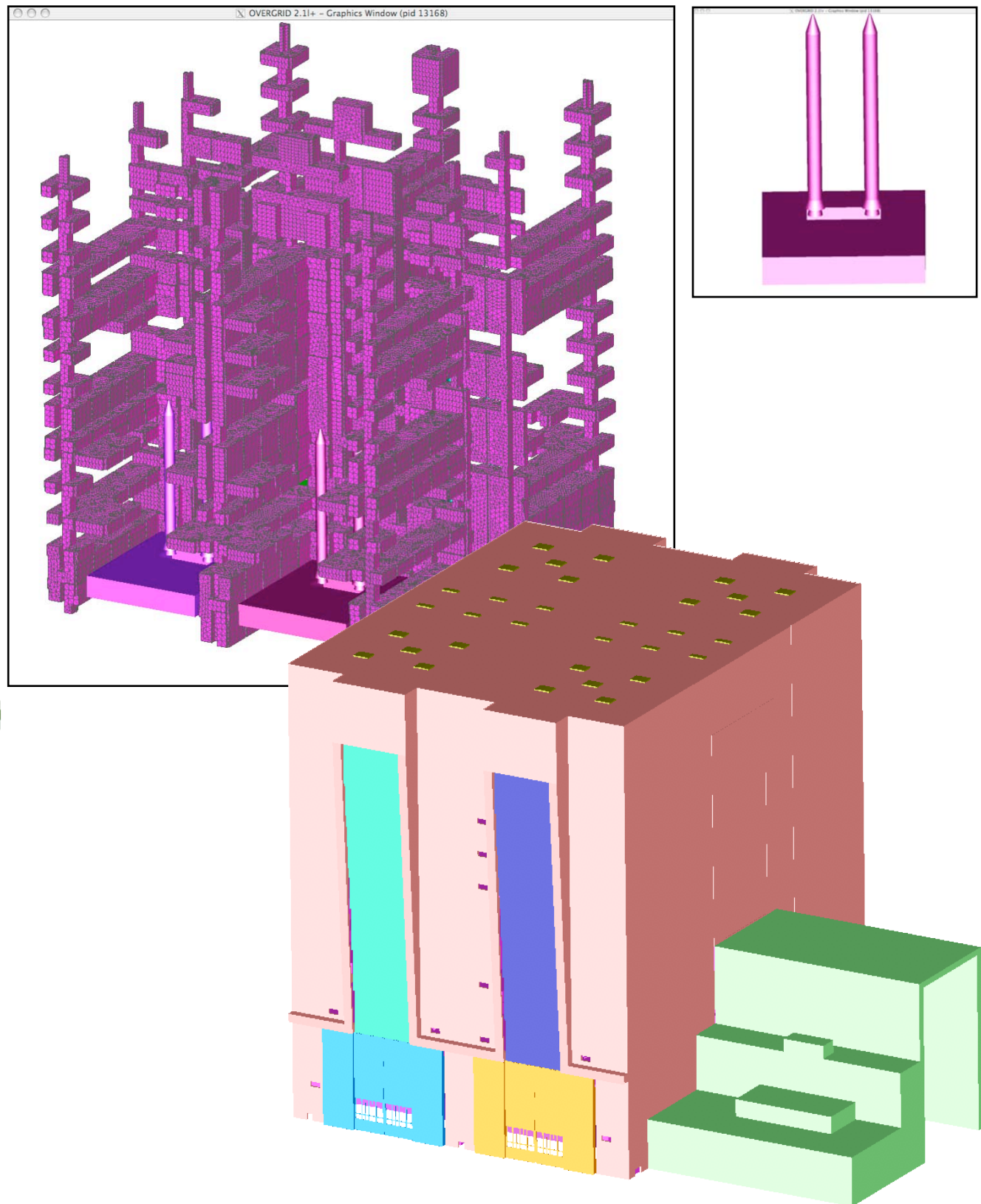
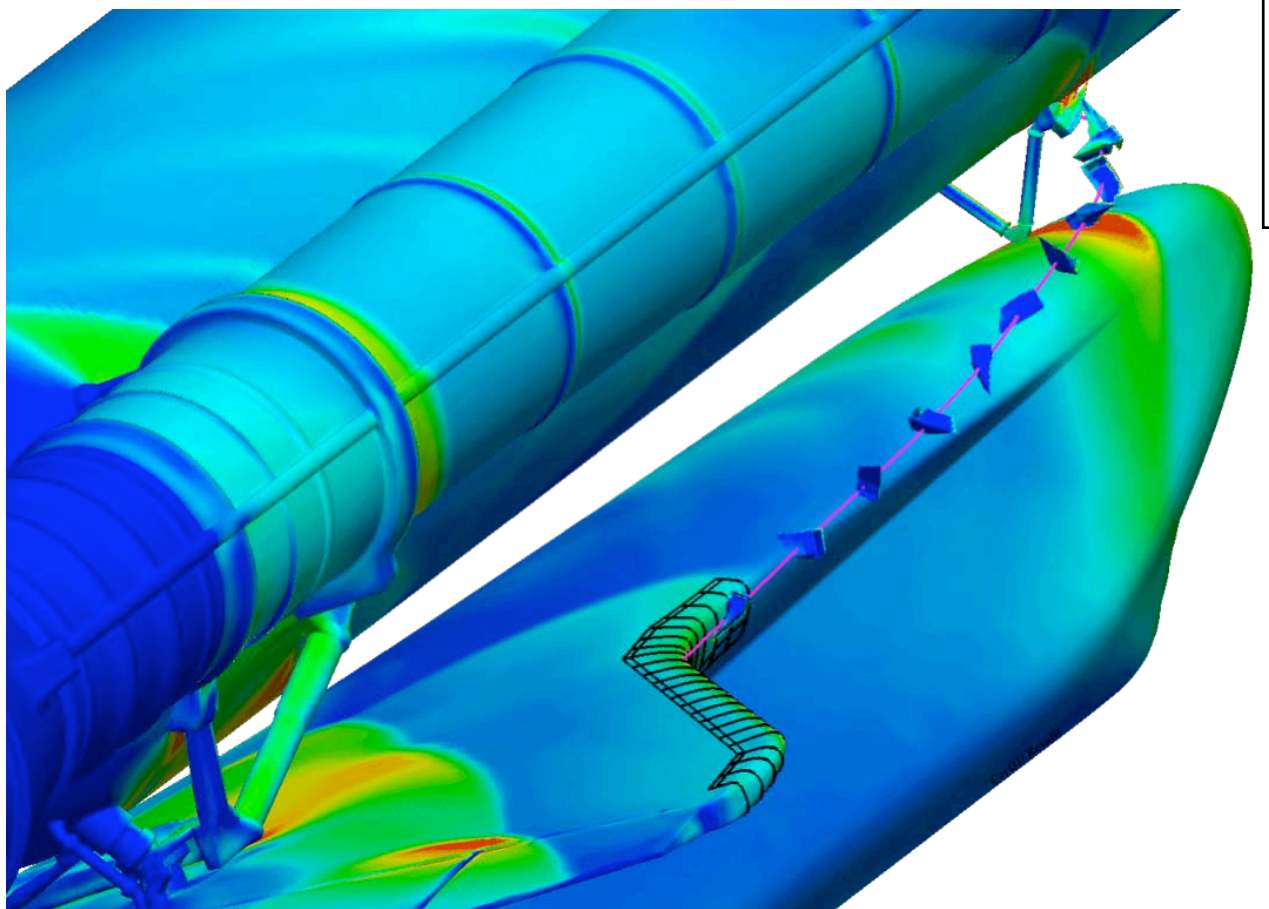
- Mesh enrichment targets output functionals
- Functional error-bound estimates
- Implementation exploits nesting of Cartesian meshes for fast interpolation



Cart3D Overview

Automation and Scalability

1. Surface geometry
2. Volume mesh generator
3. Flow solver

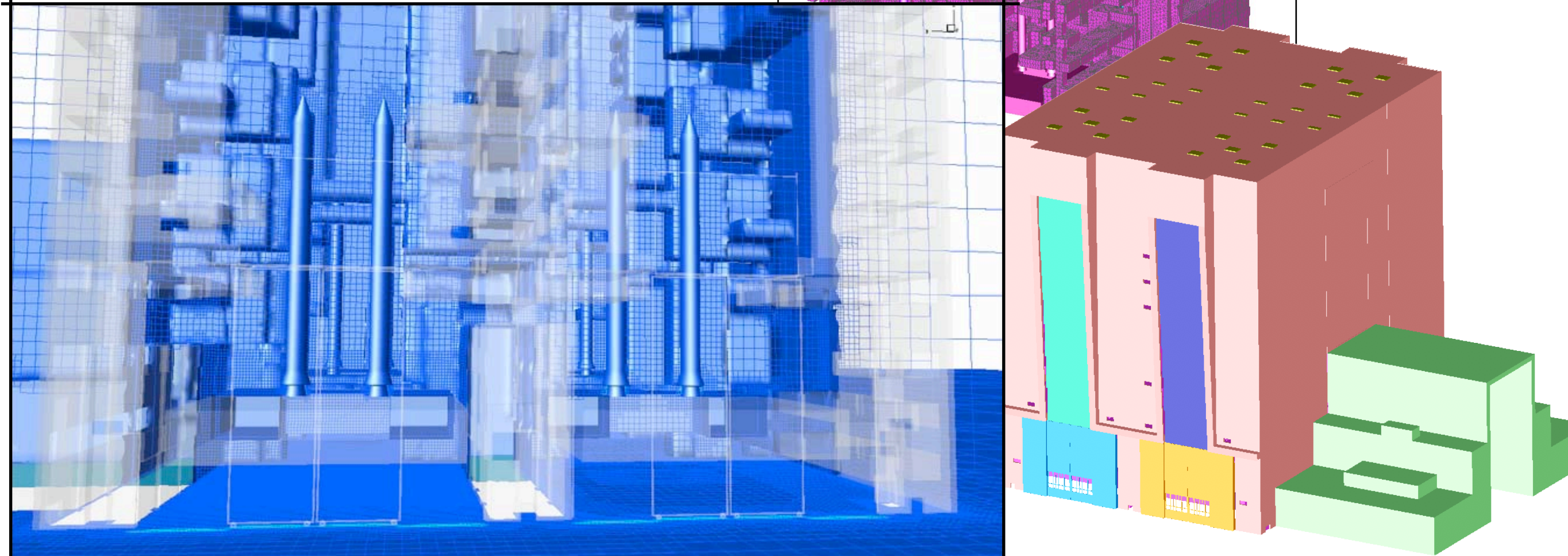
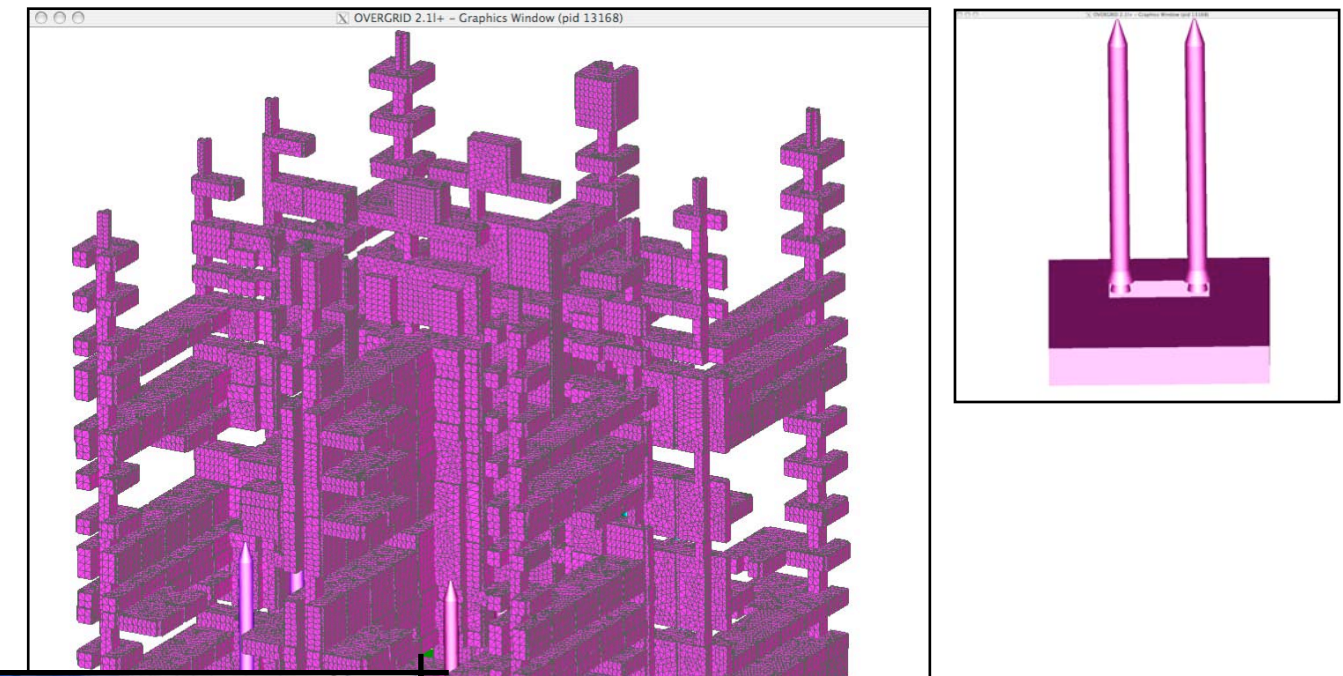




Cart3D Overview

Automation and Scalability

1. Surface geometry
2. Volume mesh generator
3. Flow solver

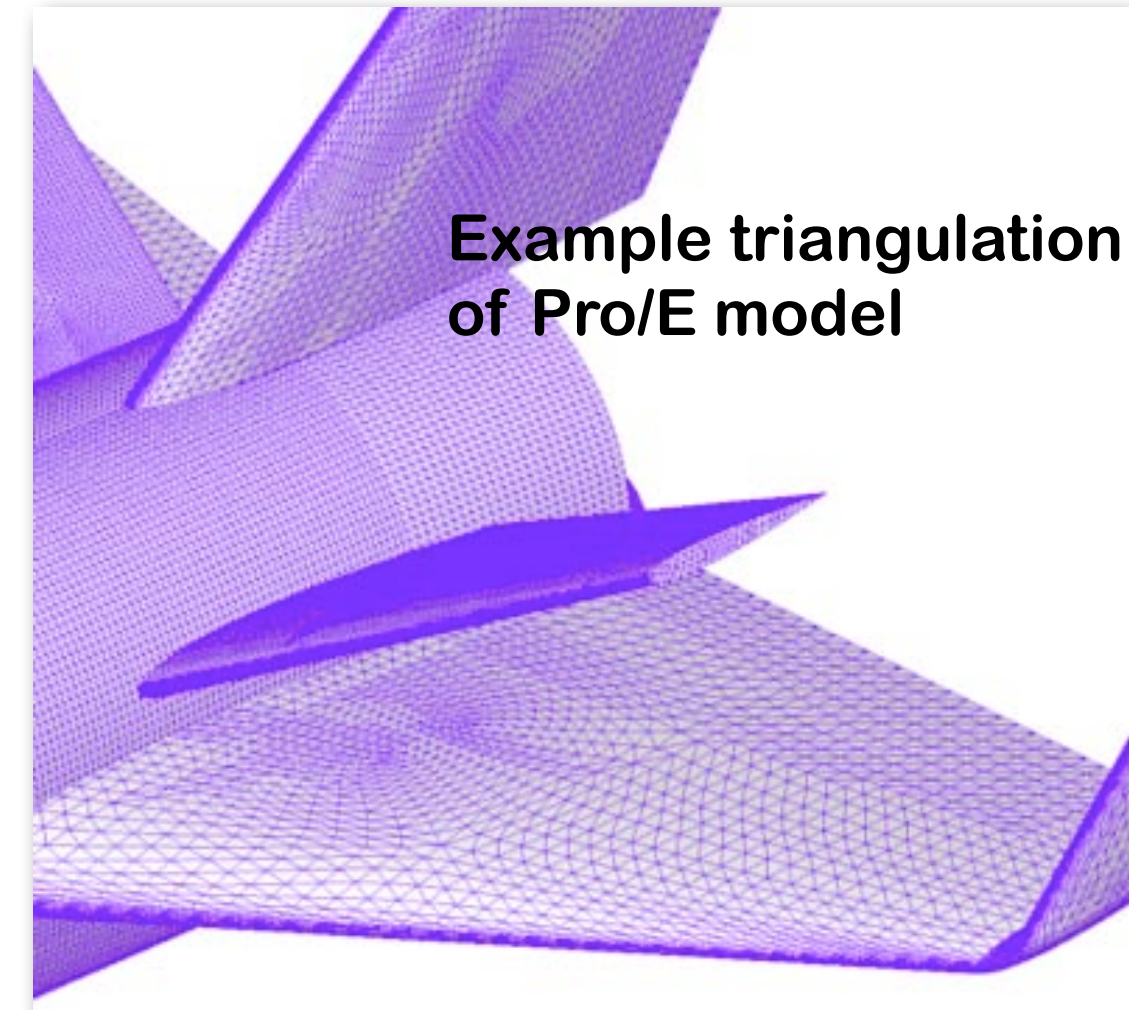
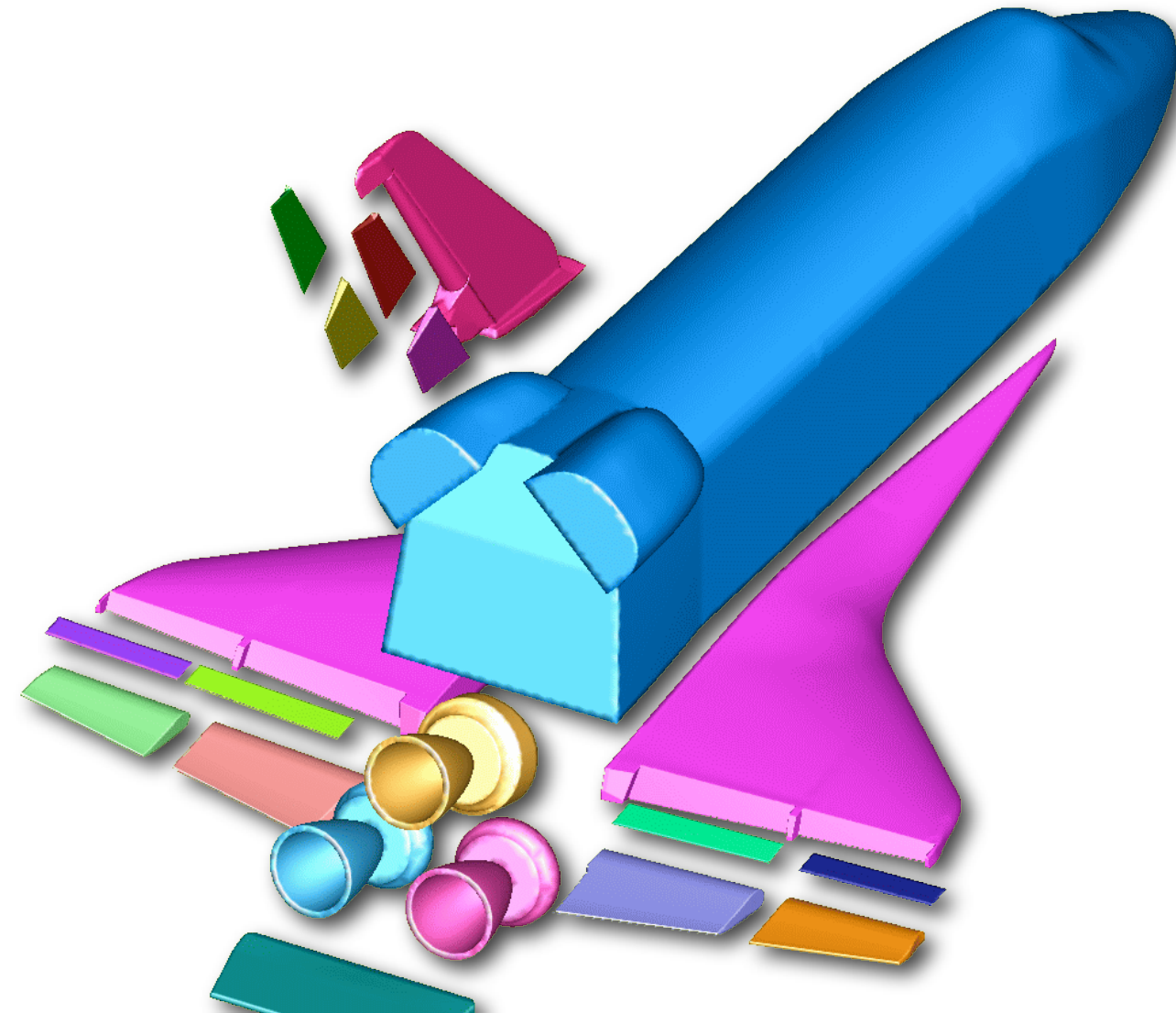




Cart3D

Surface Geometry

- Each solid (part) is an independent component
- “Water-tight” triangulation of individual components
 - Direct interface to native CAD parts and assemblies via CAPRI
- Intersect components to define a wetted-surface



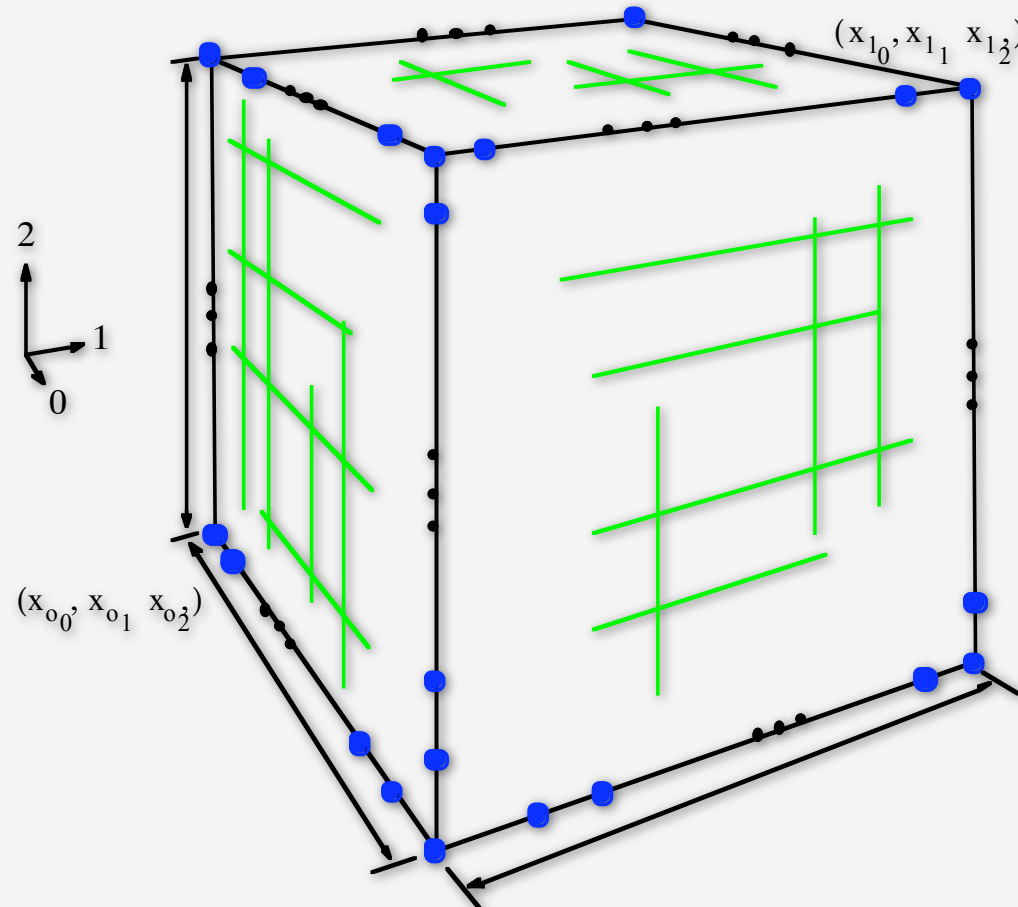
Example triangulation
of Pro/E model



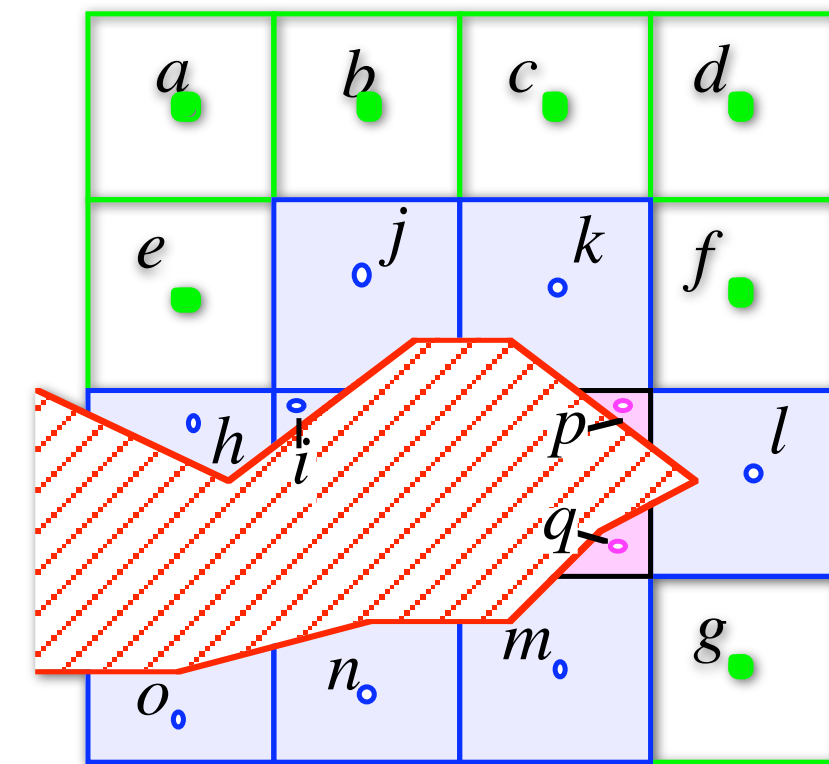
Cart3D

Non-Body-Fitted Cartesian Meshes

Basic Concepts



- All possible meshes fully specified
- Fast and robust



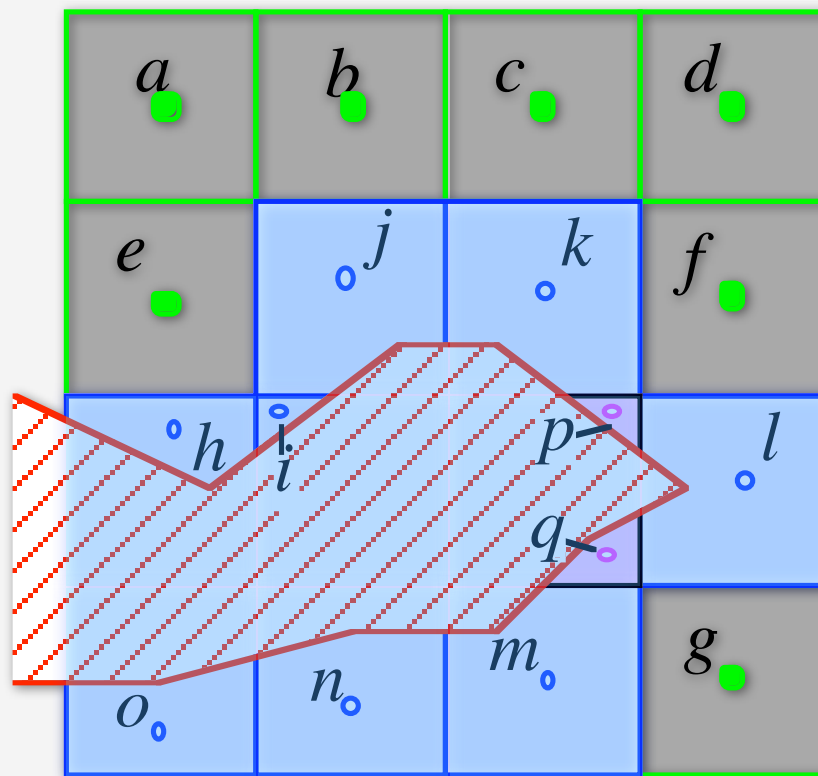
- Only two kinds of cells:
 - Very simple or very complex



Cart3D

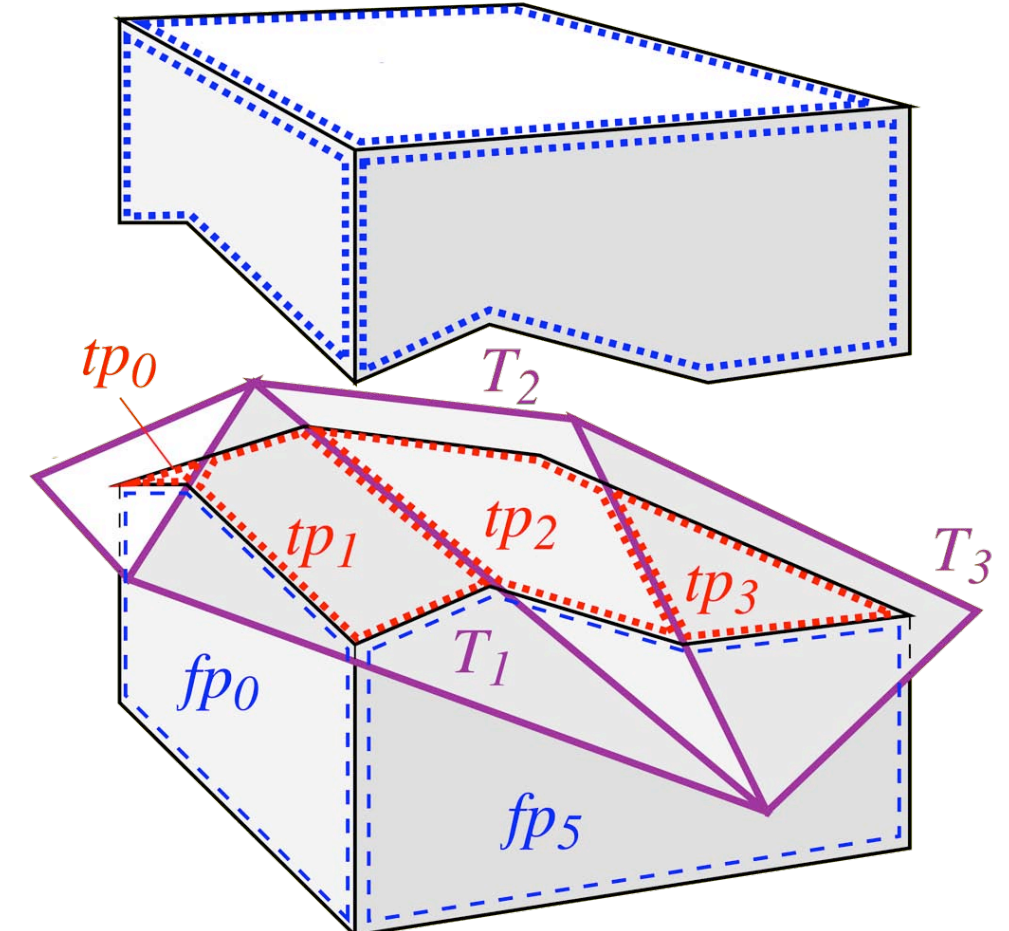
Non-Body-Fitted Cartesian Meshes

Basic Cell Types



- $\mathcal{O}(N^3)$ cells are regular hexahedra
- $\mathcal{O}(N^2)$ Cut-cells are general polyhedra

Cut-cell construction



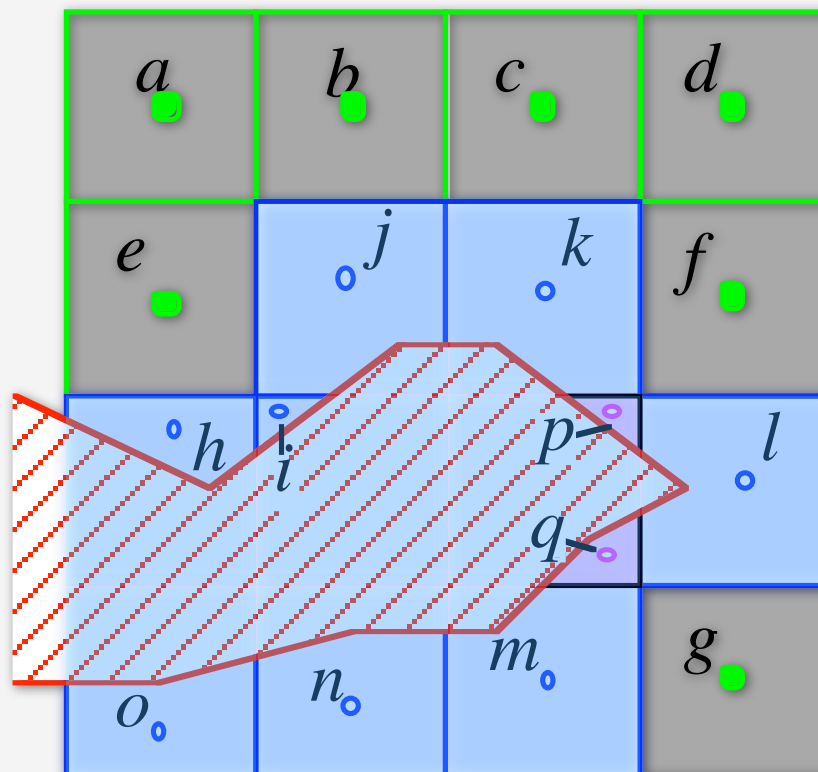
1. Pierce points & triangle polygons
2. Cartesian face areas and centroids
3. Wall normals, cell volumes & centroids



Cart3D

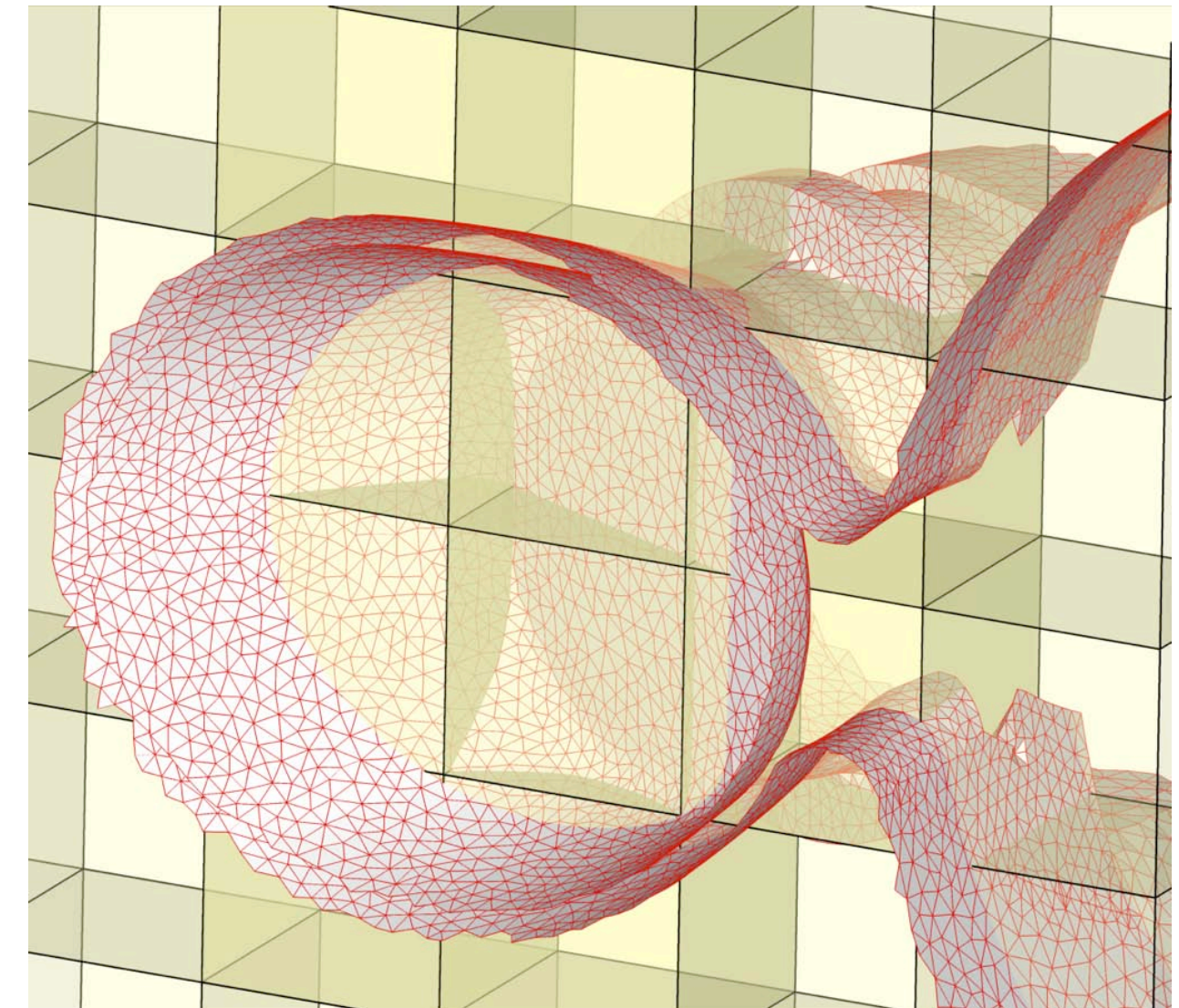
Non-Body-Fitted Cartesian Meshes

Basic Cell Types



- $\mathcal{O}(N^3)$ cells are regular hexahedra
- $\mathcal{O}(N^2)$ Cut-cells are general polyhedra

Cut-cells in practice



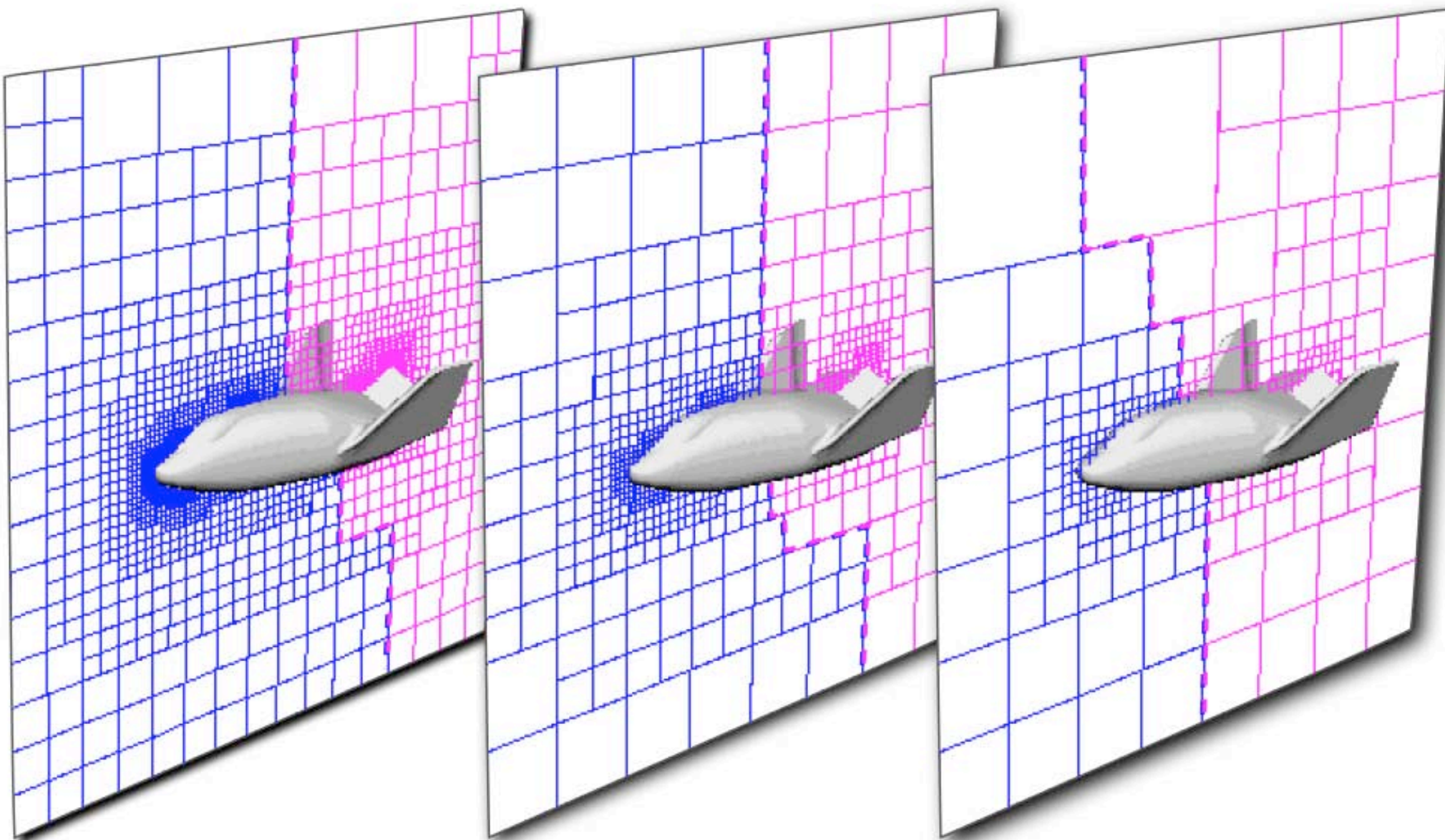
- Robust computational geometry algorithms allow configurations of arbitrary complexity



Cart3D

Steady-State Inviscid Flow Solver

- Second-order accurate spatial discretization; van Leer flux vector splitting
- Runge-Kutta time marching with multigrid acceleration
- Domain decomposition and multigrid coarsening via space-filling curves

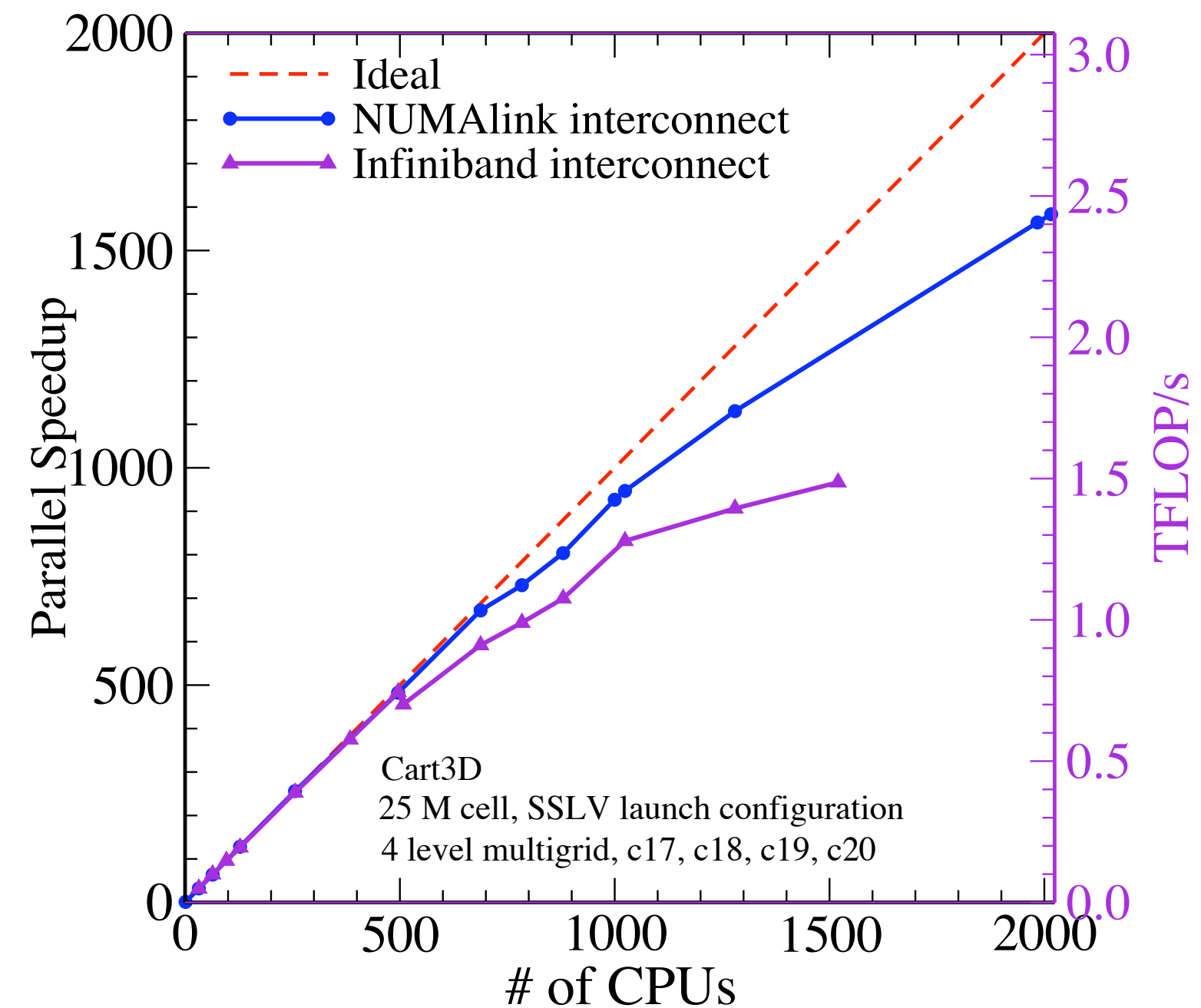
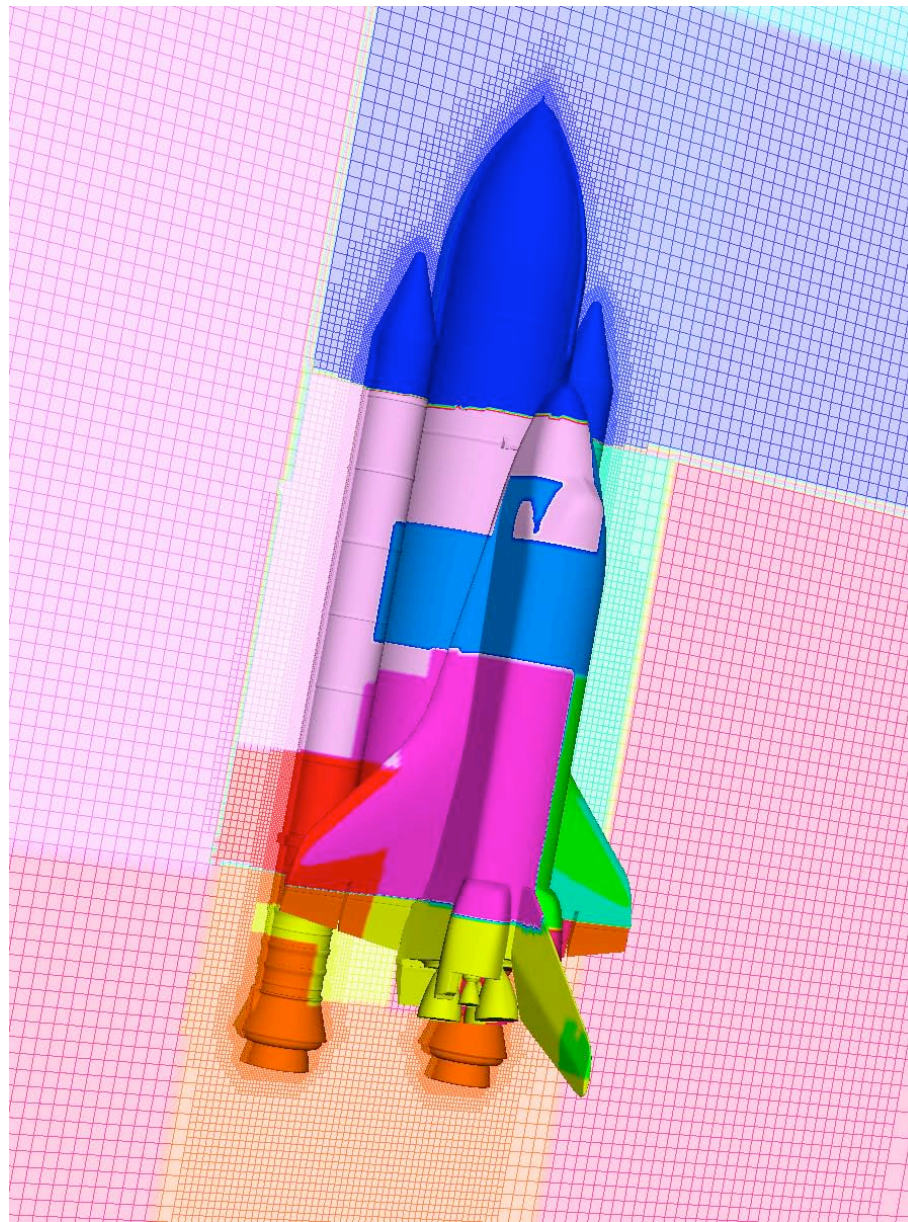




Cart3D

Scalability

- Example computation on NASA's Columbia supercluster

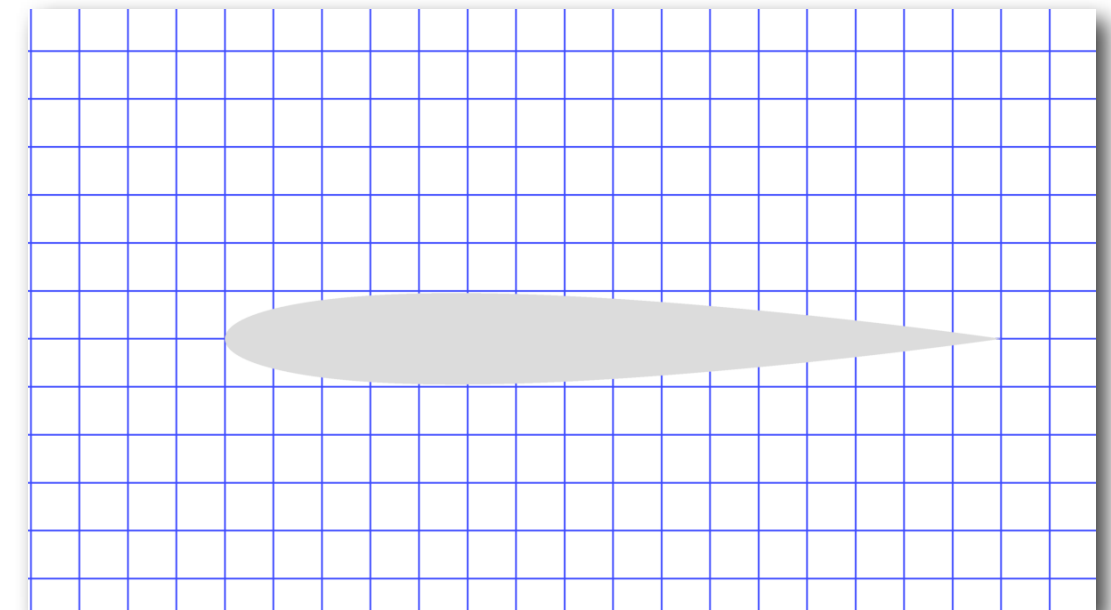
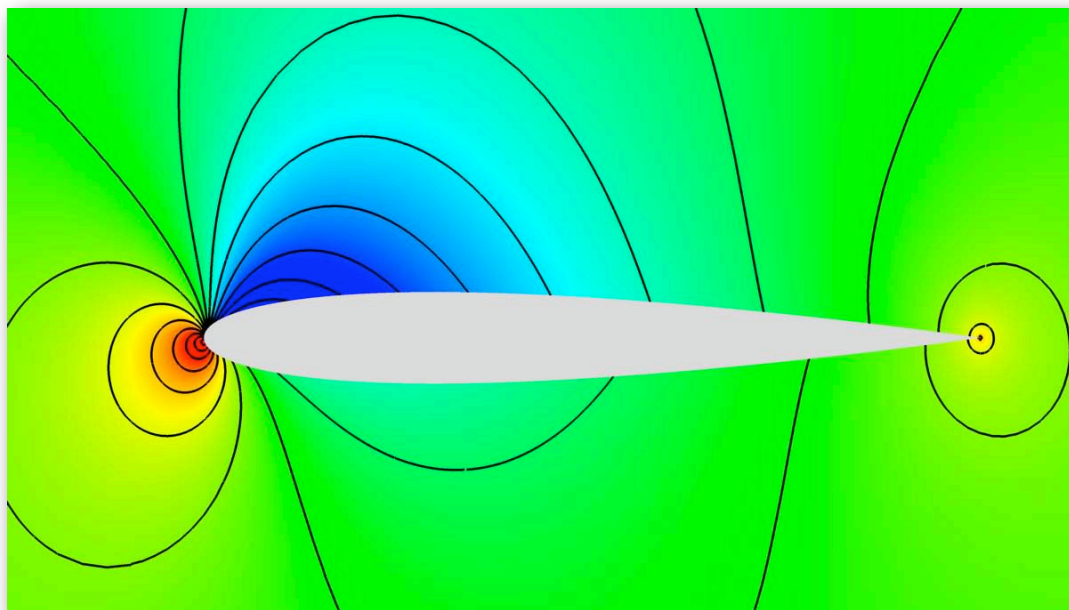




Error Estimation and Mesh Adaptation

Control of Numerical Errors in Flow Simulations

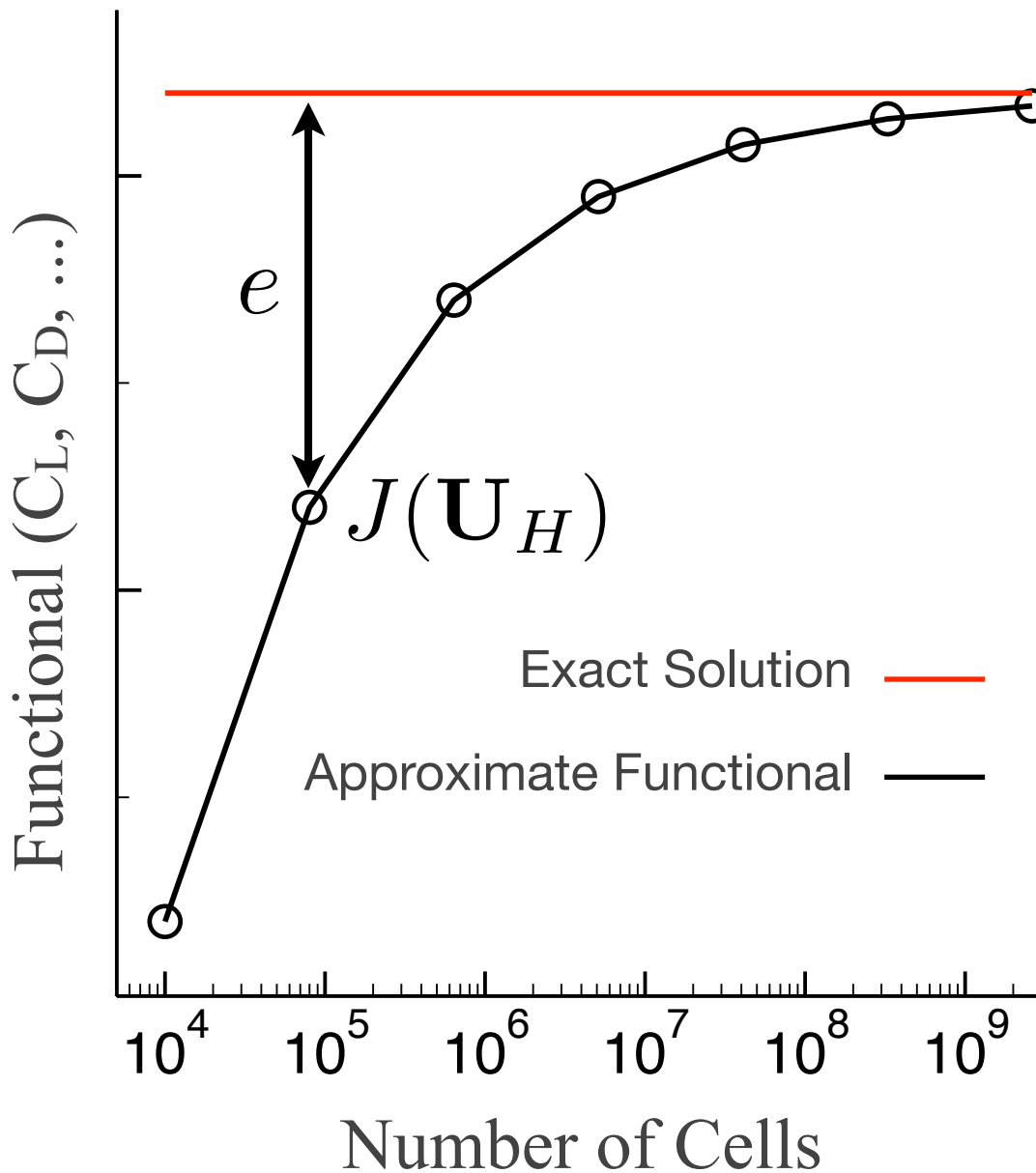
- Consider airfoil in subsonic inviscid flow. Our goal is to compute lift to a specified tolerance
- Where should the mesh be refined? How much?



Remember: our focus is on numerical errors (discretization errors) - the issue of modeling errors, i.e., how well do the solutions approximate experimental and flight data, is not addressed directly



Numerical Error Uniform Mesh Refinement



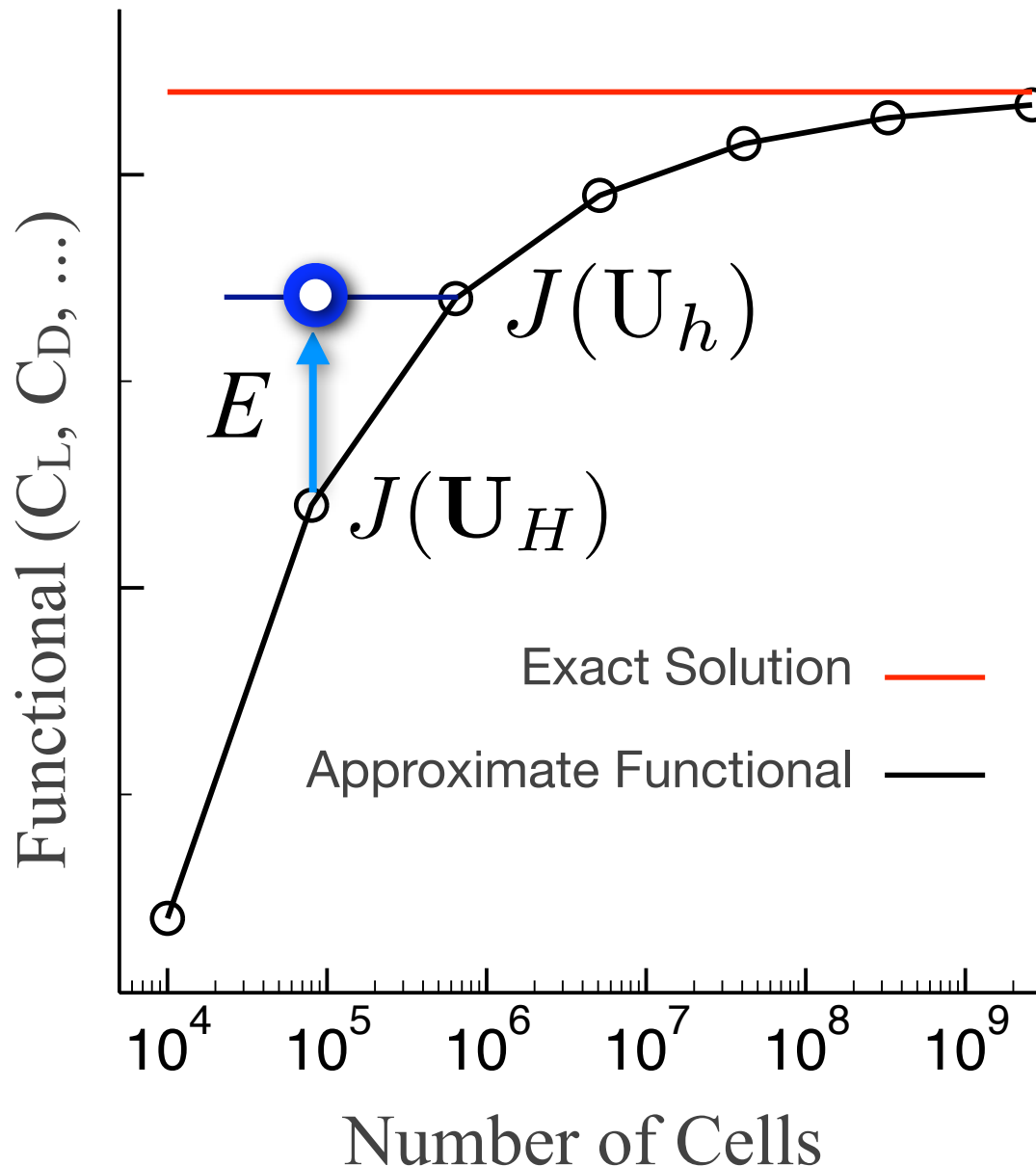
Exact Solution: \mathcal{J}

- Numerical solution on a mesh with cell-size H gives approximate functional:
$$J(\mathbf{U}_H)$$
- Error in functional:
$$e = |\mathcal{J} - J(\mathbf{U}_H)|$$
- Goal is to estimate error as a function of the approximate flow solution:

$$e = f(\mathbf{U}_H)$$



Discrete Estimate of Numerical Error



- Consider simpler problem of computing relative error:

$$E = |J(\mathbf{U}_h) - J(\mathbf{U}_H)|$$

- We will use an adjoint solution on mesh H to estimate

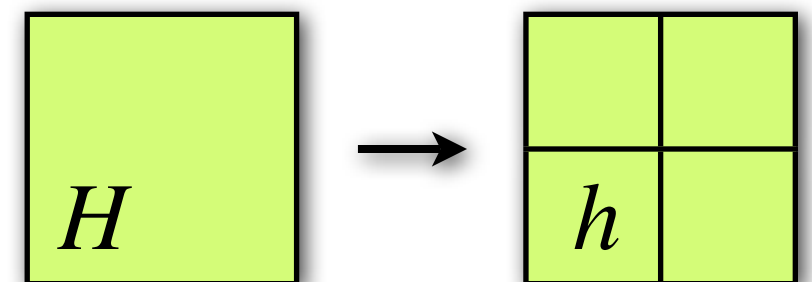
$$E = f(\mathbf{U}_H, \psi_h)$$



Adjoint Error Estimates

- Consider a functional $J(\mathbf{U}_H)$ computed from the solution of Euler equations discretized on an affordable mesh with cell-size H :

$$R(\mathbf{U}_H) = 0$$



- In addition, consider an embedded mesh with cell-size h obtained via uniform refinement of the baseline mesh
- We seek to compute the error relative to the embedded mesh without solving the problem on the fine mesh

$$e_h = |J(\mathbf{U}_h) - J(\mathbf{U}_h^H)|$$



- Estimate of functional on embedded mesh is obtained from Taylor series expansion of functional and residual equations about the coarse mesh solution

$$J(\mathbf{U}_h) \approx J(\mathbf{U}_h^H) + \frac{\partial J(\mathbf{U}_h^H)}{\partial \mathbf{U}_h} (\mathbf{U}_h - \mathbf{U}_h^H)$$

$$\mathbf{R}(\mathbf{U}_h) = 0 \approx \mathbf{R}(\mathbf{U}_h^H) + \frac{\partial \mathbf{R}(\mathbf{U}_h^H)}{\partial \mathbf{U}_h} (\mathbf{U}_h - \mathbf{U}_h^H)$$

- These equations are combined to give

$$J(\mathbf{U}_h) \approx J(\mathbf{U}_h^H) - \psi_h^T \mathbf{R}(\mathbf{U}_h^H)$$

where ψ satisfies the adjoint equation

$$\left[\frac{\partial \mathbf{R}(\mathbf{U}_h^H)}{\partial \mathbf{U}_h} \right]^T \psi_h = \frac{\partial J(\mathbf{U}_h^H)}{\partial \mathbf{U}_h}^T$$



Adjoint Correction and Error Bound

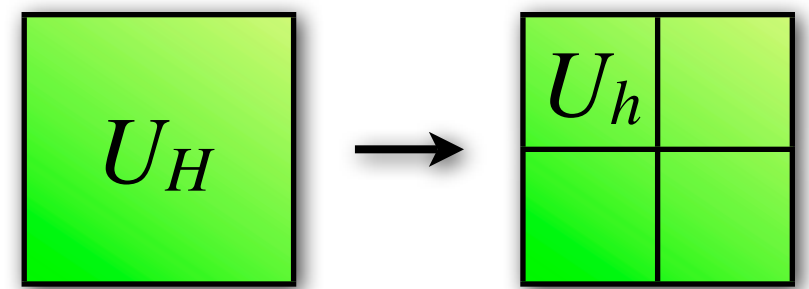
- Since the adjoint solution is not known on the embedded mesh, we use an approximate solution from the coarse mesh to obtain

$$J(\mathbf{U}_h) \approx J(\mathbf{U}_h^H) - (\psi_h^H)^T \mathbf{R}(\mathbf{U}_h^H) - (\psi_h - \psi_h^H)^T \mathbf{R}(\mathbf{U}_h^H)$$

Adjoint Correction

Remaining Error

- Use piecewise quadratic (Q), linear (L) and constant (C) reconstruction operators to lift solutions from coarse mesh to embedded mesh
- How do we interpret adjoint solutions? And how do we use the adjoint correction and remaining error terms?

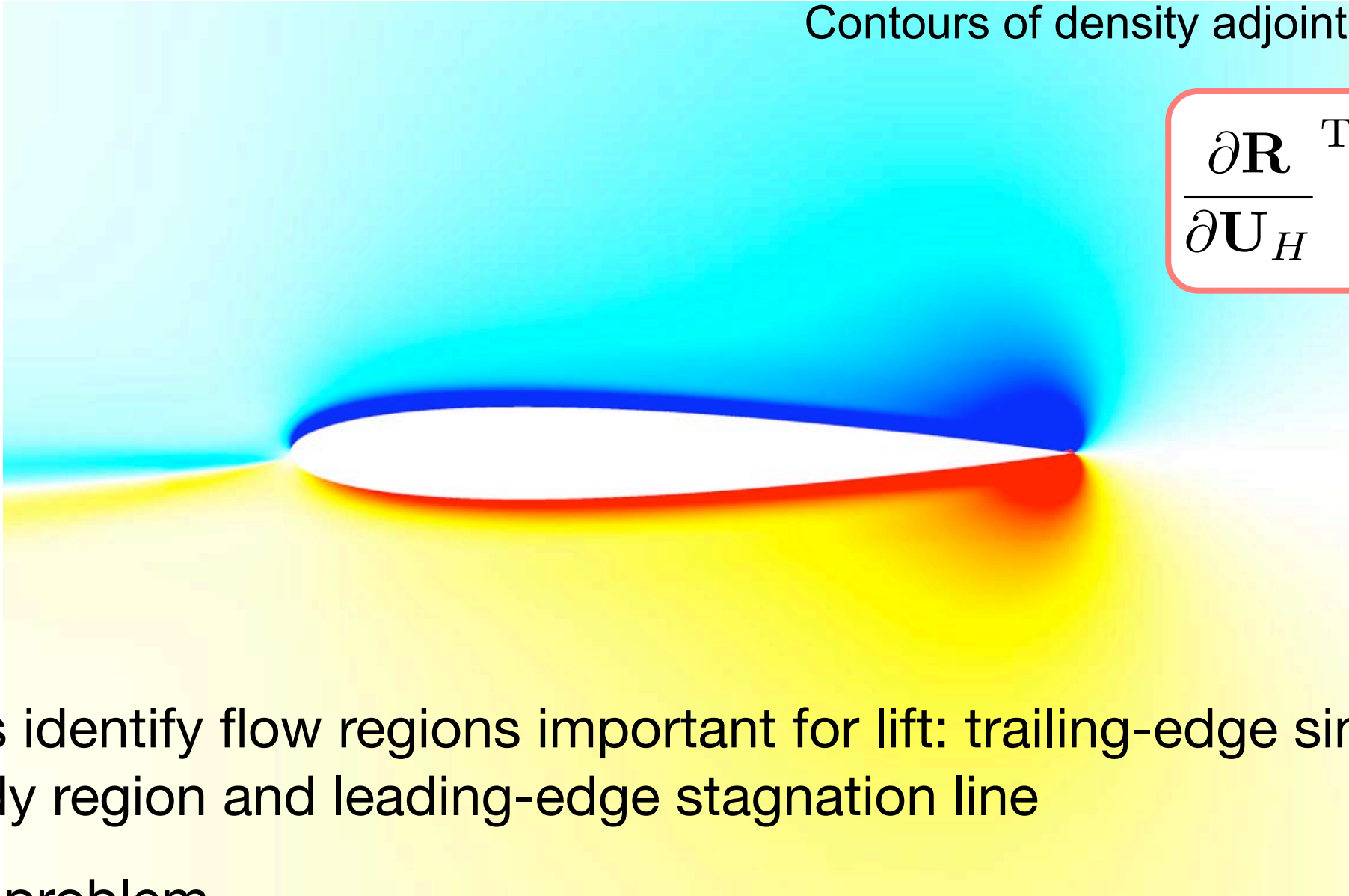




Example Adjoint Solution for Lift

Contours of density adjoint

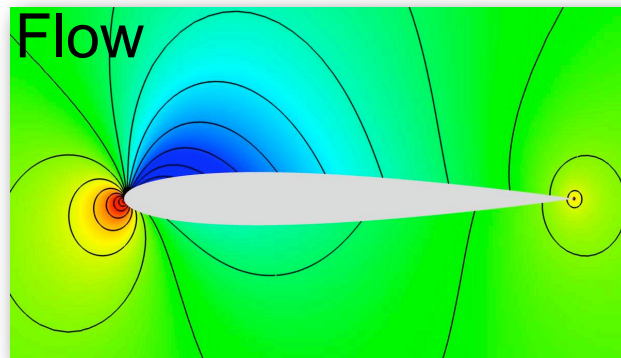
$$\frac{\partial \mathbf{R}}{\partial \mathbf{U}_H}^T \psi_H = \frac{\partial J}{\partial \mathbf{U}_H}^T$$



- Adjoint identify flow regions important for lift: trailing-edge singularity, near-body region and leading-edge stagnation line
- Control problem
 - Optimal shape design: adjust design variables to control the flow and improve performance
 - Error analysis: adjust mesh refinement to control discretization errors

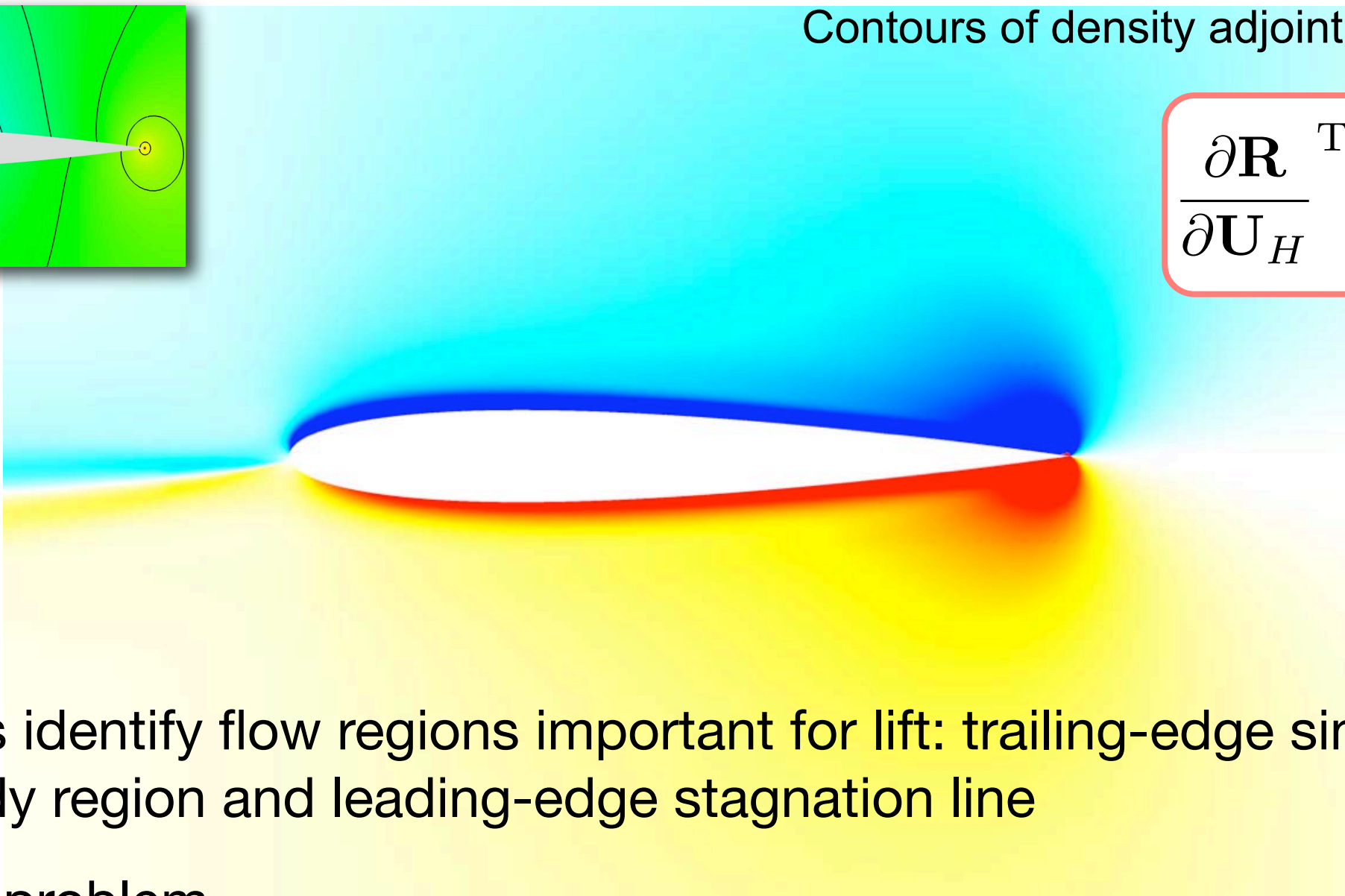


Example Adjoint Solution for Lift



Contours of density adjoint

$$\frac{\partial \mathbf{R}}{\partial \mathbf{U}_H}^T \psi_H = \frac{\partial J}{\partial \mathbf{U}_H}^T$$

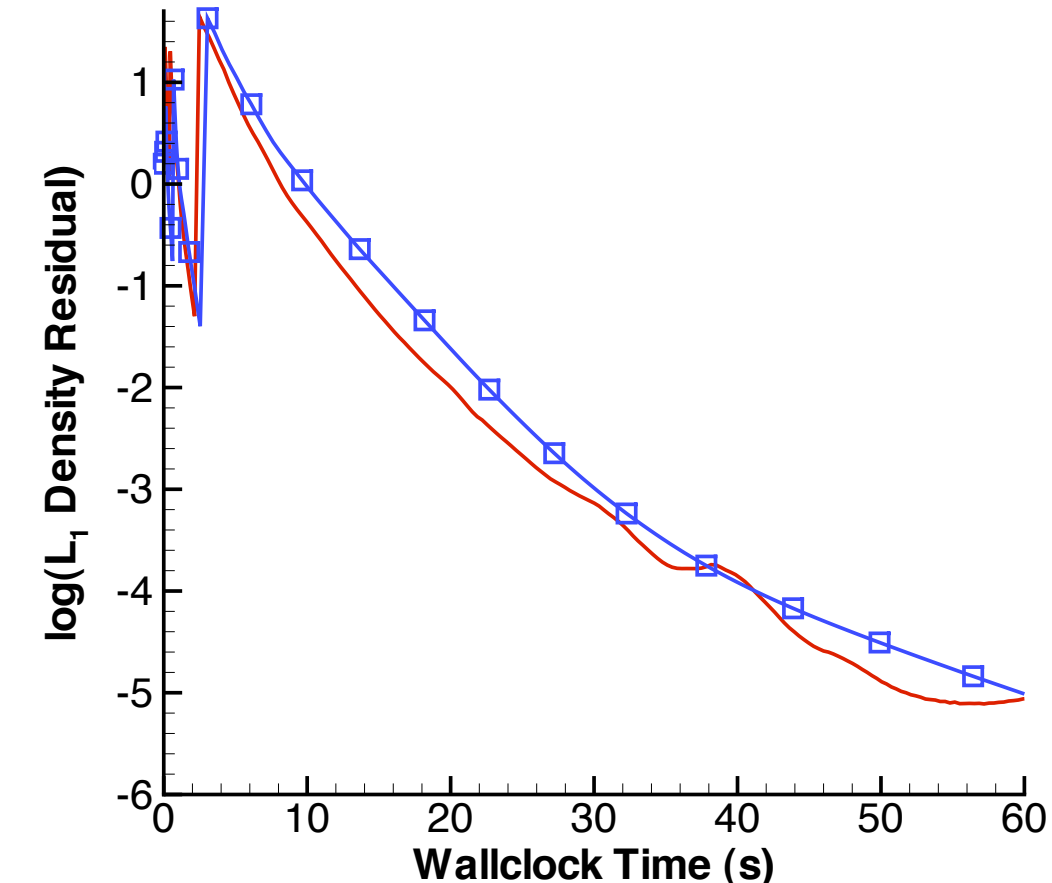
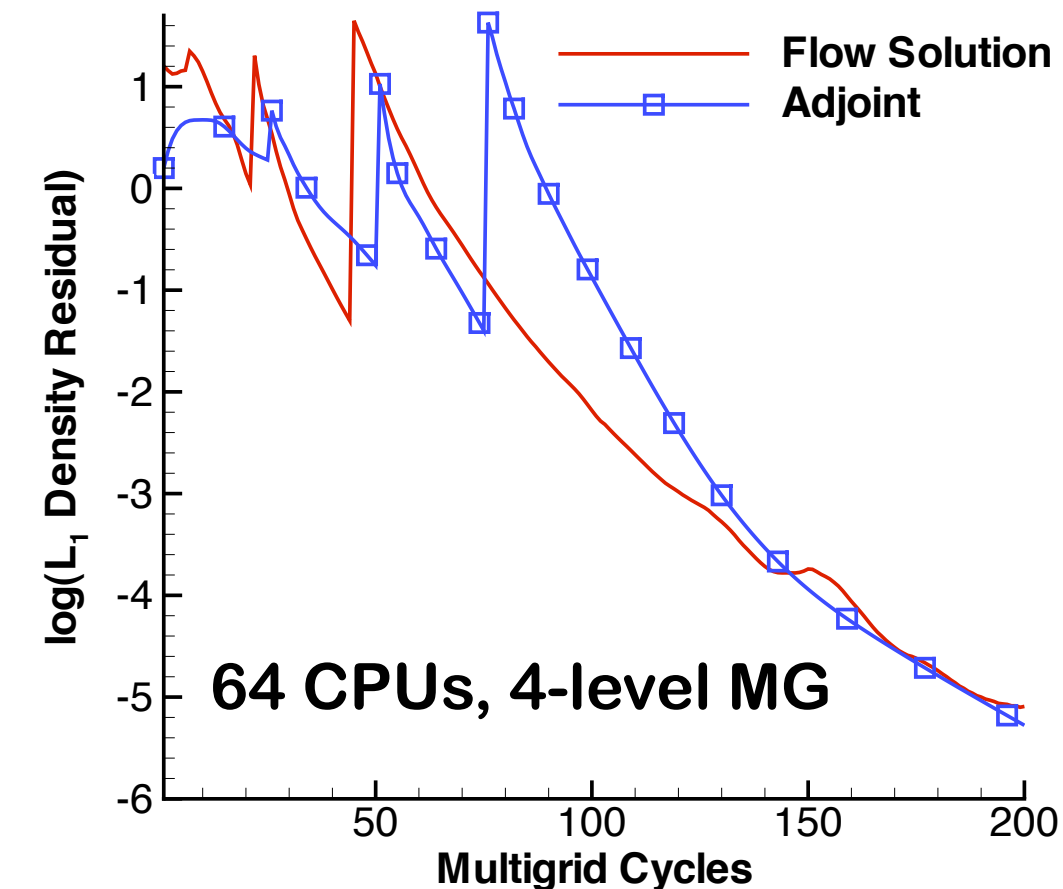


- Adjoint solutions identify flow regions important for lift: trailing-edge singularity, near-body region and leading-edge stagnation line
- Control problem
 - Optimal shape design: adjust design variables to control the flow and improve performance
 - Error analysis: adjust mesh refinement to control discretization errors



Adjoint Implementation

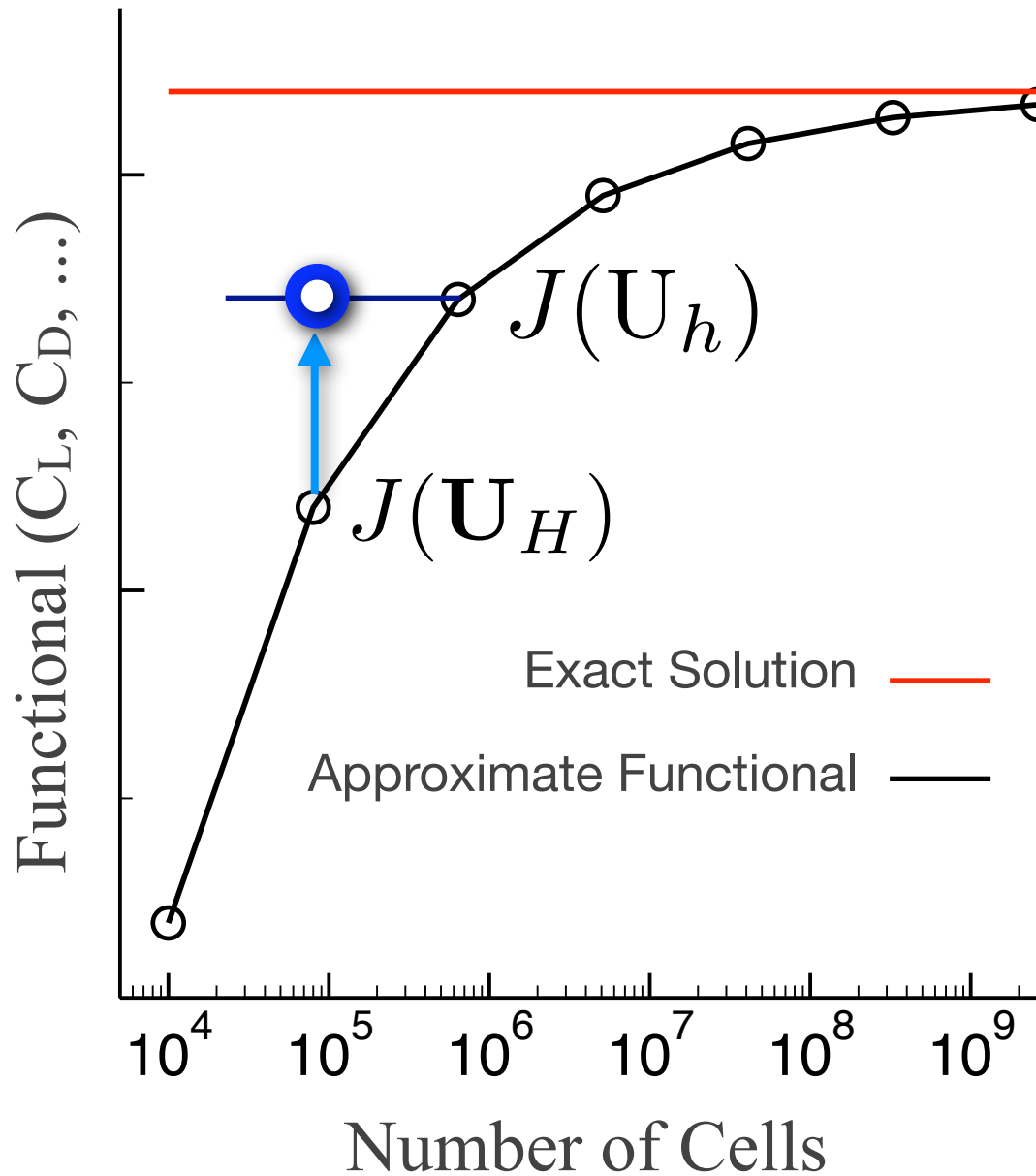
- Exact linearization of flow solver
 - Except for limiters (assumed constant)
- Duality preserving approach
 - Adopt RK5 time marching with multigrid and domain decomposition schemes of the flow solver
 - Minor modifications in gradient updates in MG restriction to reduce wall-clock time
- In practice, convergence of adjoint multigrid is not as robust as flow solver
 - Positivity preserving prolongation operator from flow solver cannot be used directly in the adjoint solver



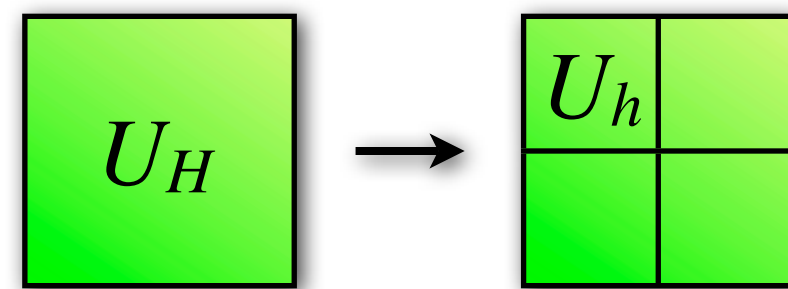


Adjoint Correction

$$J(\mathbf{U}_h) \approx J(\mathbf{U}_h^H) - (\psi_h^H)^T \mathbf{R}(\mathbf{U}_h^H) - (\psi_h - \psi_h^H)^T \mathbf{R}(\mathbf{U}_h^H)$$



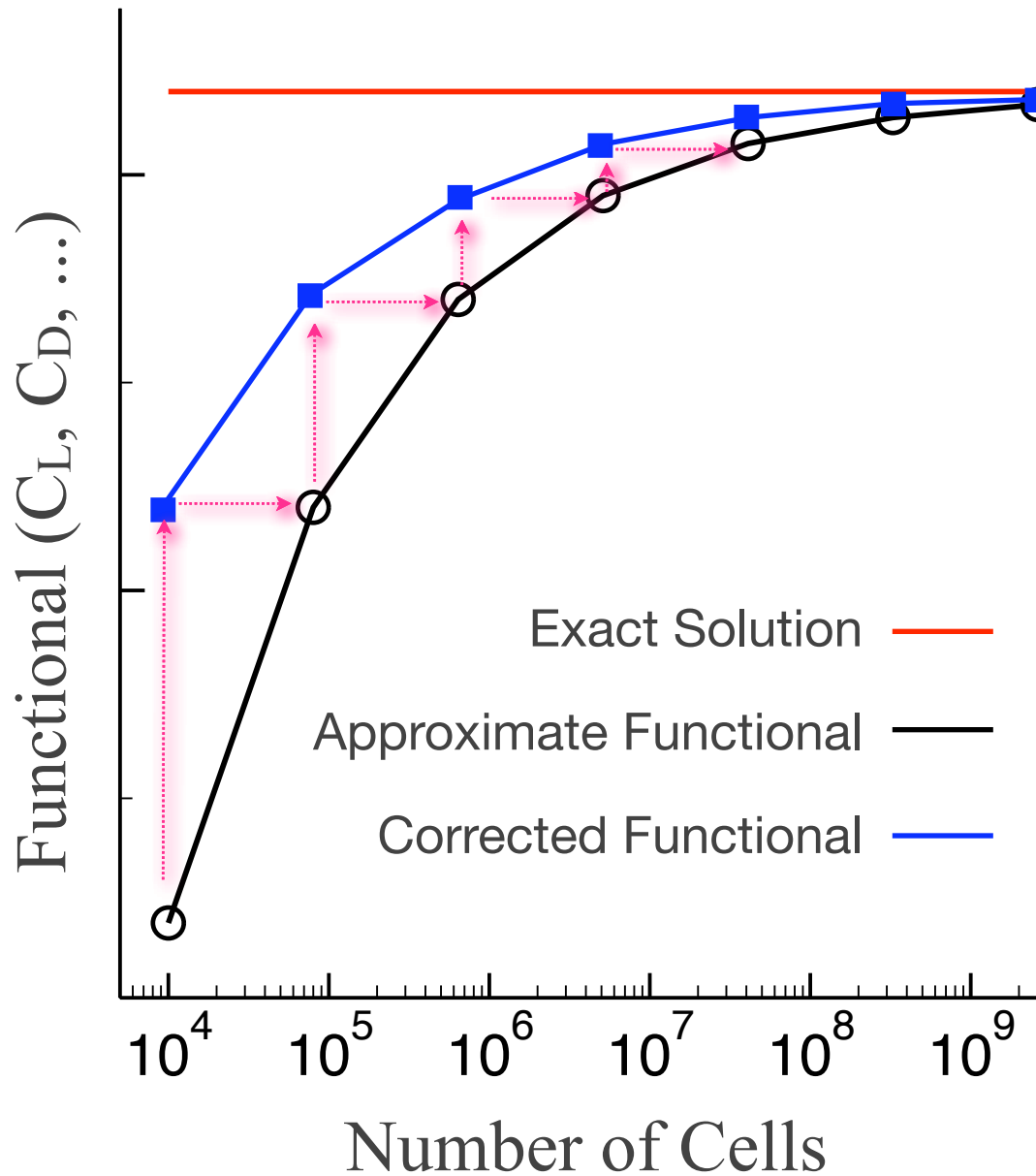
- Predict functional on a fine mesh with cell-size h from a coarse mesh solution with cell size H



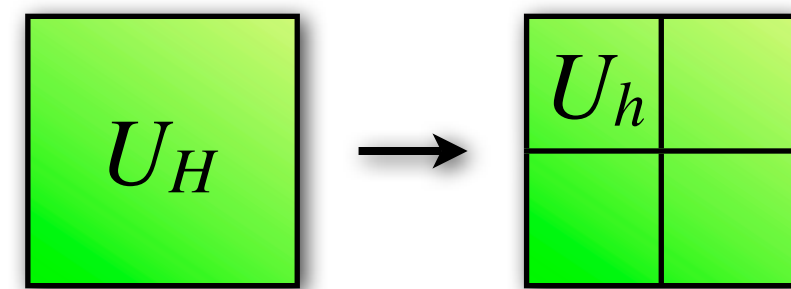


Adjoint Correction

$$J(\mathbf{U}_h) \approx J(\mathbf{U}_h^H) - (\psi_h^H)^T \mathbf{R}(\mathbf{U}_h^H) - (\psi_h - \psi_h^H)^T \mathbf{R}(\mathbf{U}_h^H)$$



- Predict functional on a fine mesh with cell-size h from a coarse mesh solution with cell size H





Error Bound Estimate

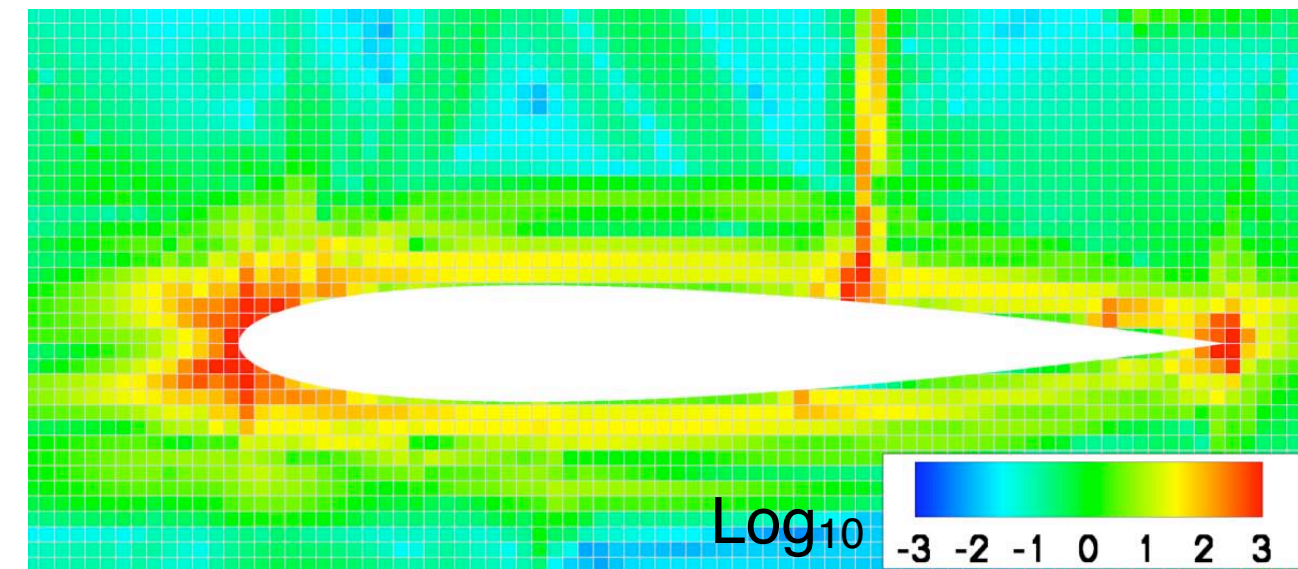
$$J(\mathbf{U}_h) \approx J(\mathbf{U}_h^H) - (\psi_h^H)^T \mathbf{R}(\mathbf{U}_h^H) - (\psi_h - \psi_h^H)^T \mathbf{R}(\mathbf{U}_h^H)$$

- Bound on remaining error in each coarse cell k

$$e_k = \sum \left| (\psi_L - \psi_C)^T \mathbf{R}(U_L) \right|_k$$

- Net functional error $E = \sum_{k=0}^N e_k$

- Given a user specified tolerance TOL , termination criterion is satisfied when $E < TOL$

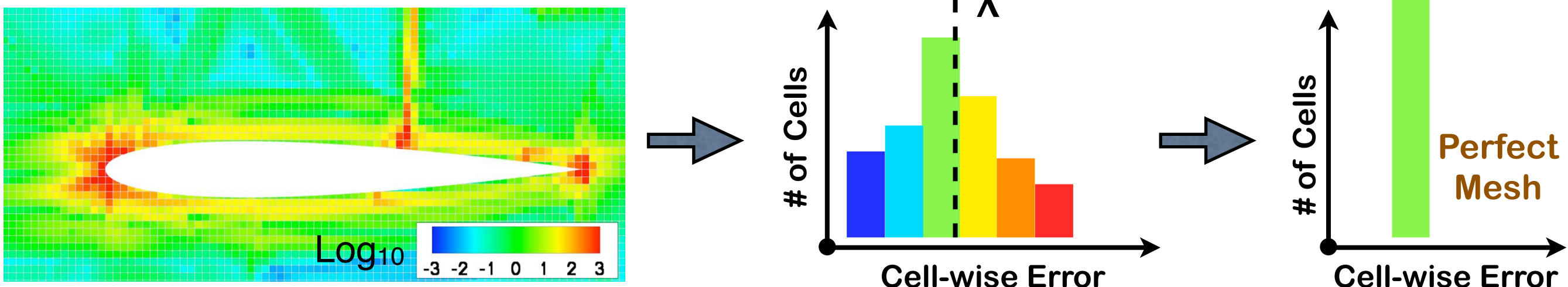




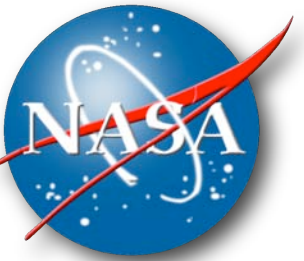
Refinement Parameter

- Define maximum allowable error level in each coarse cell via equidistribution: $t = \text{TOL} / N$
- Refinement parameter in each cell is given by $r_k = \frac{e_k}{t}$
- Refine cells for which $r_k > \lambda$ where $\lambda \geq 1$ is a global threshold factor

Error Histograms



How do you choose λ at each adaptation cycle to minimize simulation cost? ... see AIAA 2008-0725



Results

Focus on applications

Part A. Classic examples

1. Typical Launch Abort Vehicle database
2. Parametric studies of Launch Vehicles
3. Transport Aircraft
4. Quiet Supersonic Cruise

Part B. Most recent (preliminary) work on cases with jets

1. Axial Flow Jet
2. Nozzle-Guide-Vane Missile
3. Launch Abort Vehicle with Abort Control Motor Jets



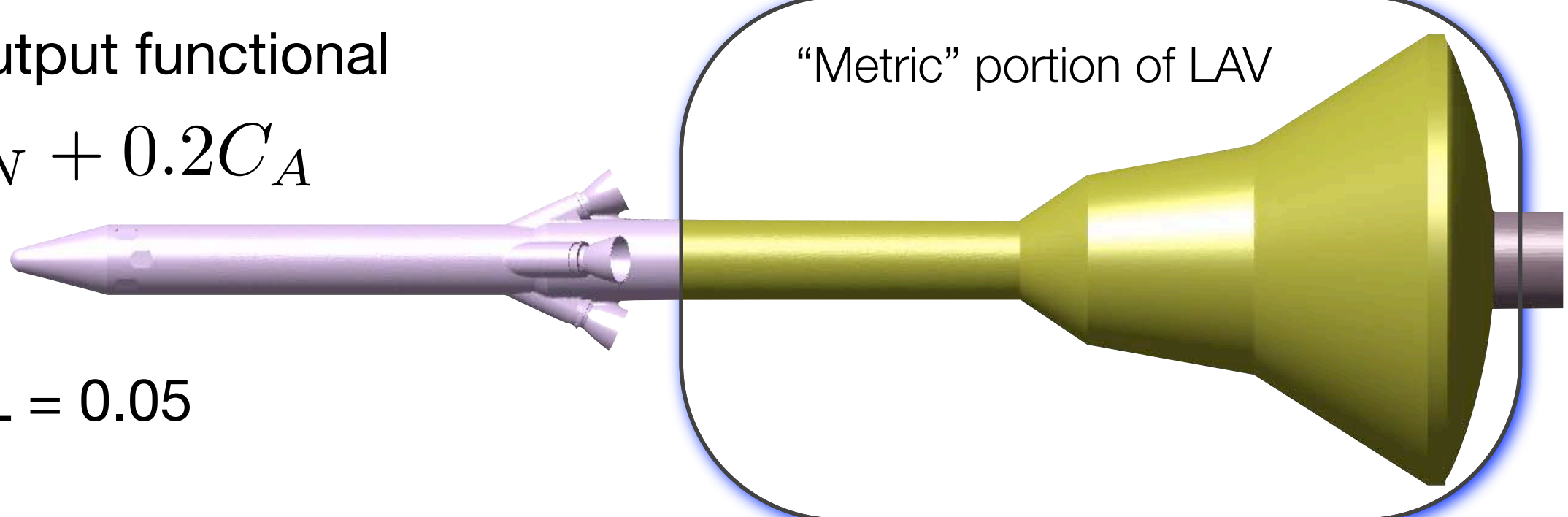
Launch Abort Vehicle (LAV)

- Complex geometry
- Perform aerodynamic analysis for range of operating conditions
 - $M_\infty = 0.5, 1.1, 1.3$
 - $\alpha = -25^\circ, -20^\circ, -12^\circ, -8^\circ, -4^\circ, -2^\circ, 0^\circ, 2^\circ, 4^\circ, 6^\circ$
- Goal is to construct an aerodynamic database that satisfies a uniform error tolerance without user supervision

Selected output functional

$$J = C_N + 0.2C_A$$

TOL = 0.05





Launch Abort Vehicle (LAV)

- Complex geometry
- Perform aerodynamic analysis for range of operating conditions

→ $M_\infty = 0.5, 1.1, 1.3$

→ $\alpha = -25^\circ, -20^\circ, -12^\circ$

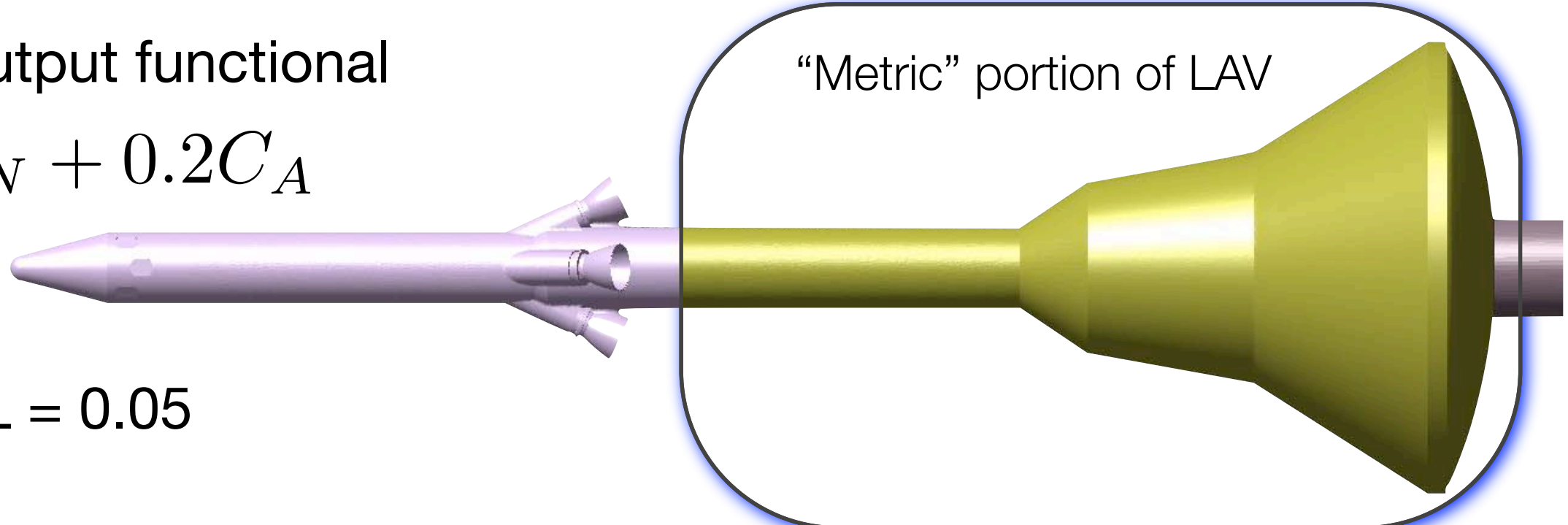
Examine a typical case
and discuss local error estimates
on uniform meshes

- Goal is to construct an aerodynamic database that satisfies a uniform error tolerance without user supervision

Selected output functional

$$J = C_N + 0.2C_A$$

TOL = 0.05

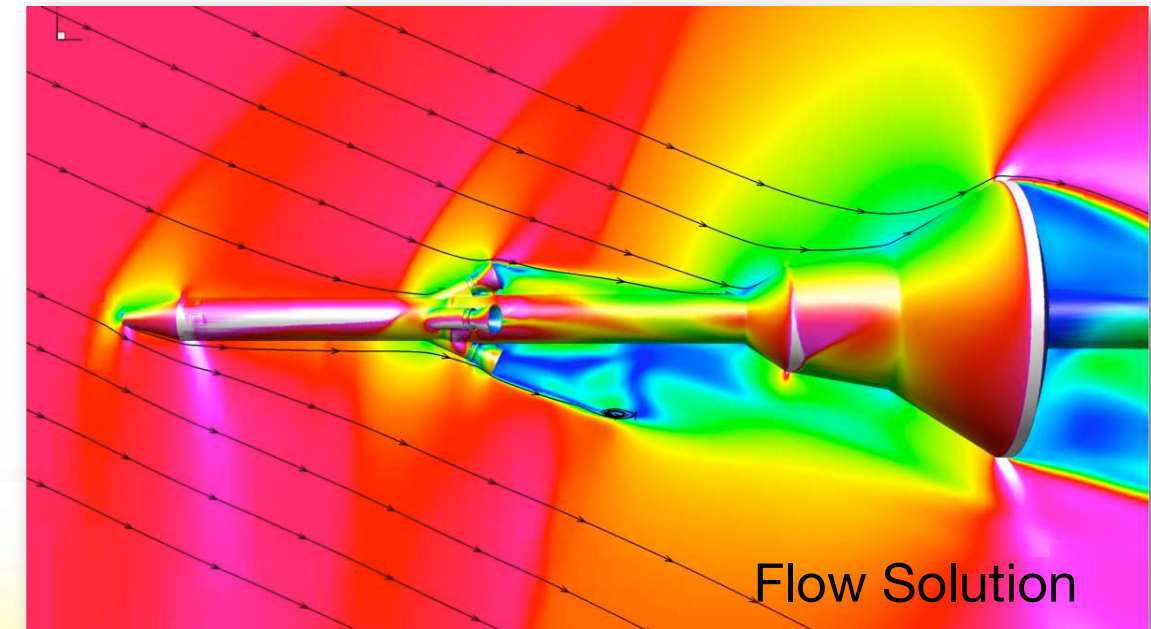
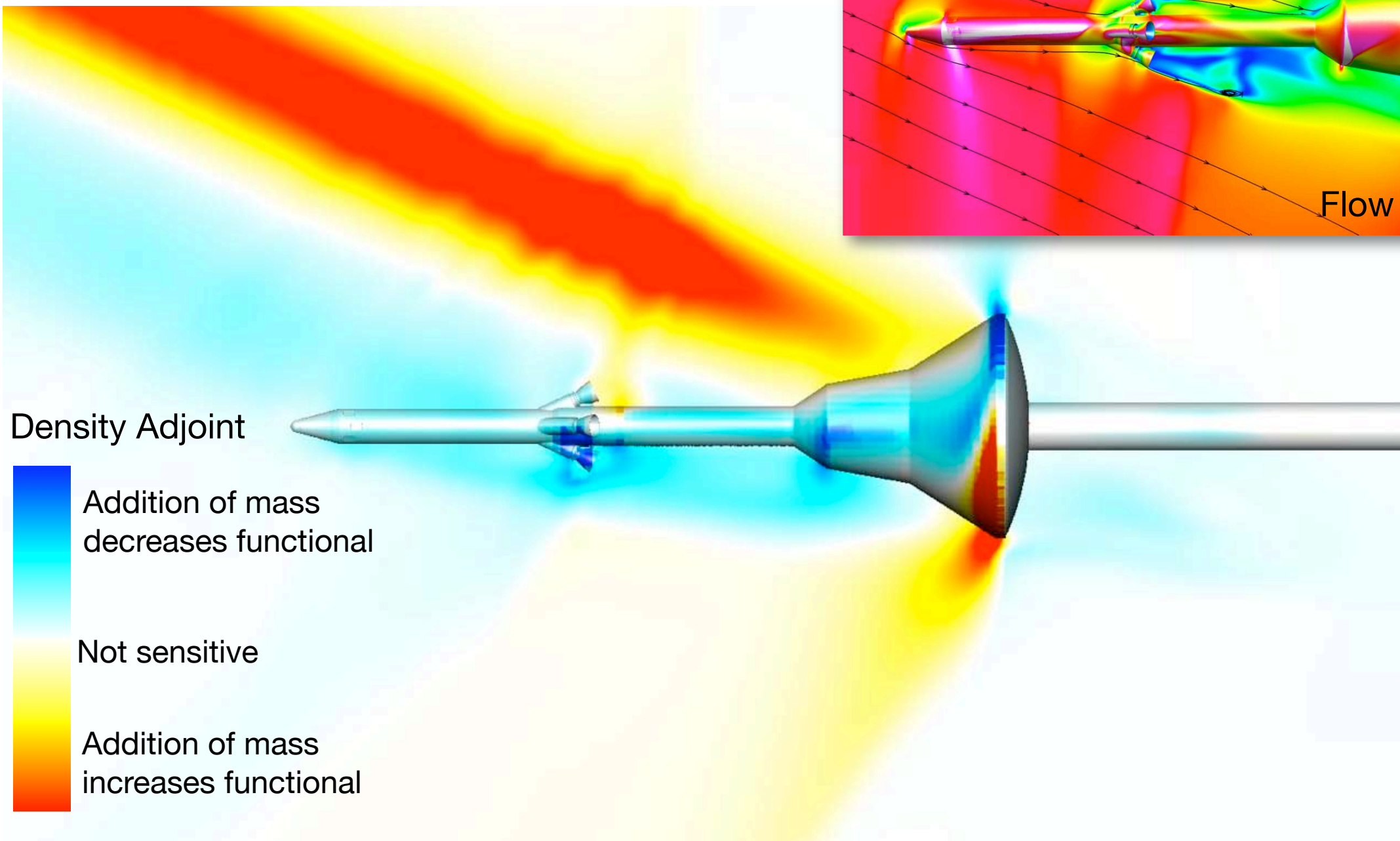




Adjoint Solution

$M_\infty = 1.1, \alpha = -25^\circ$

$$J = C_N + 0.2C_A$$

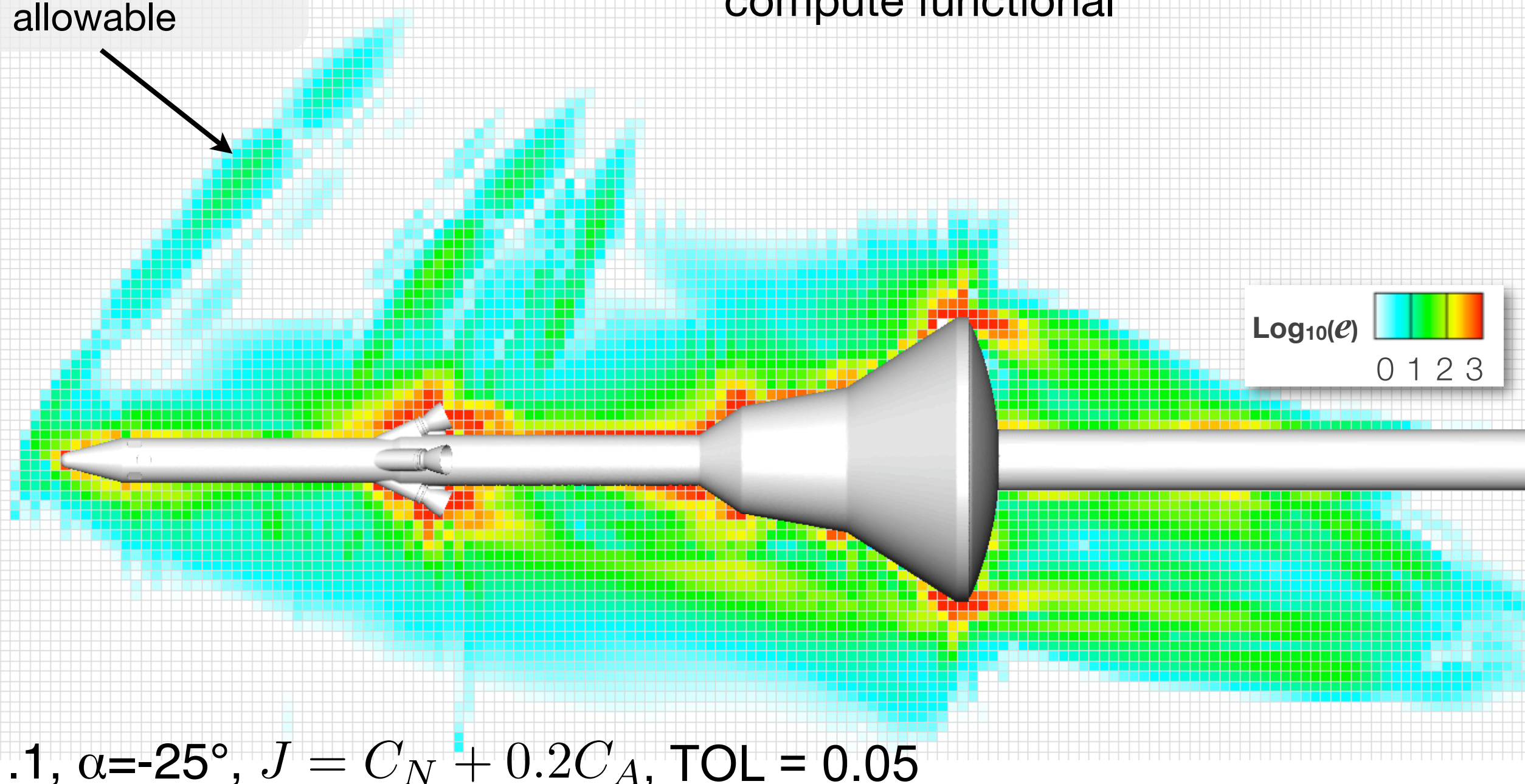


Flow Solution



Local Error Estimates

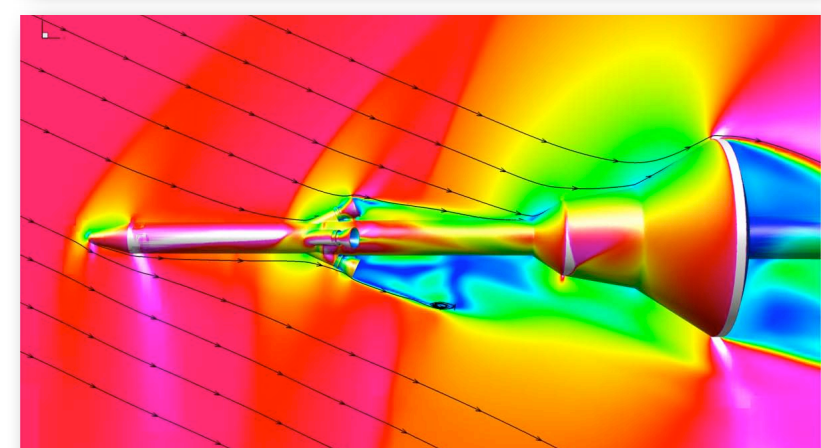
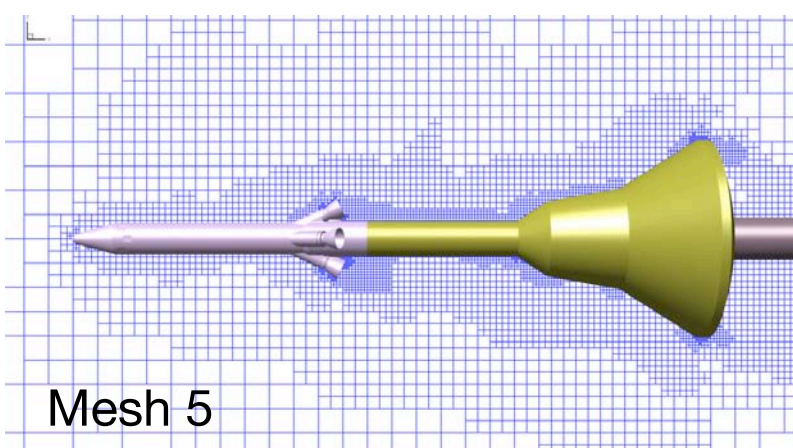
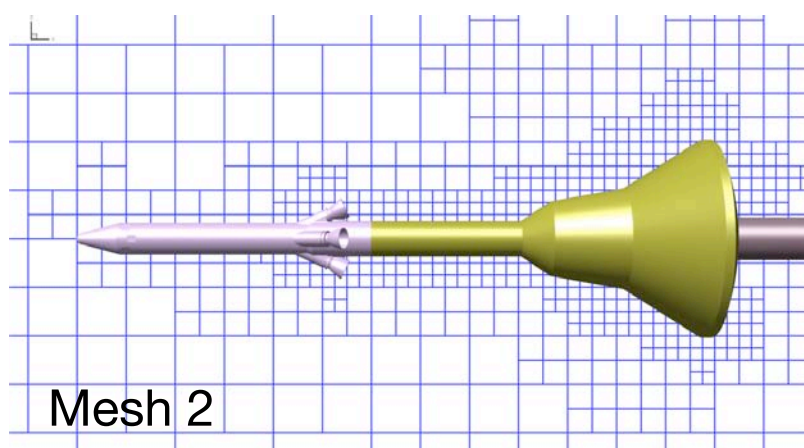
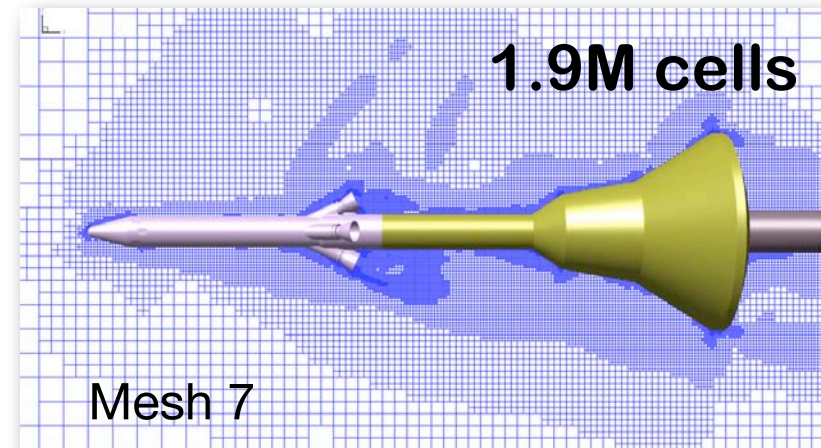
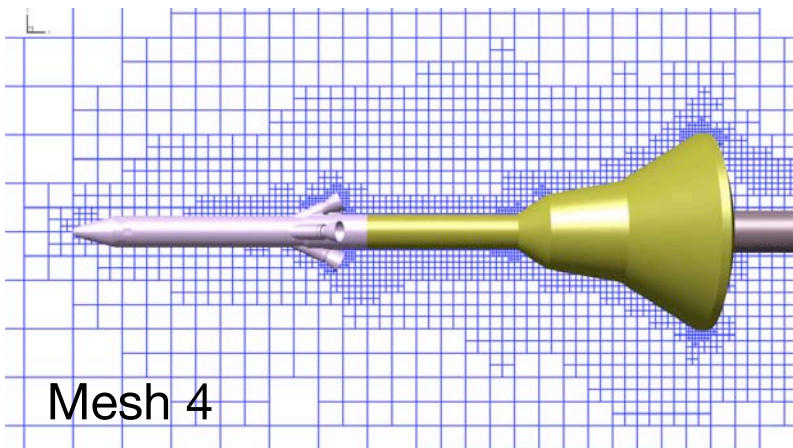
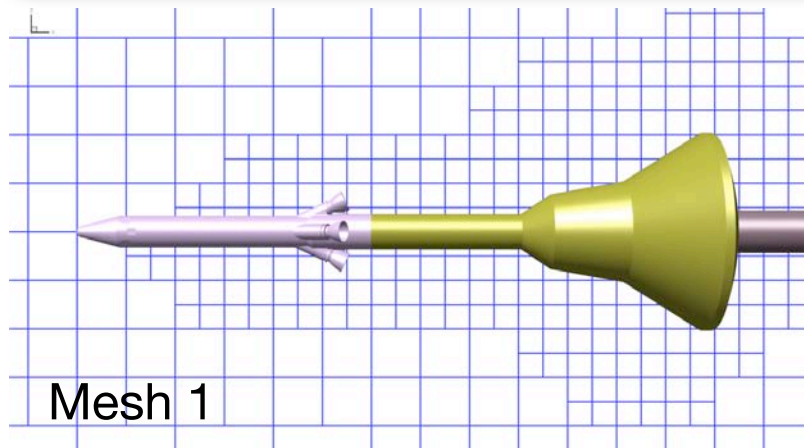
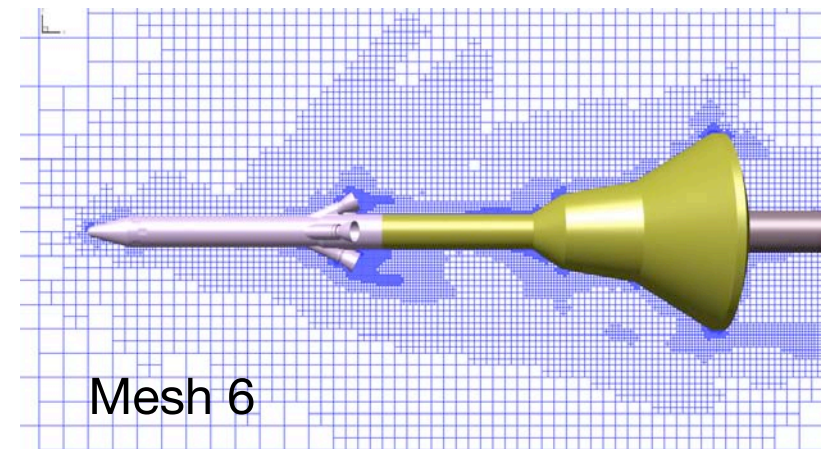
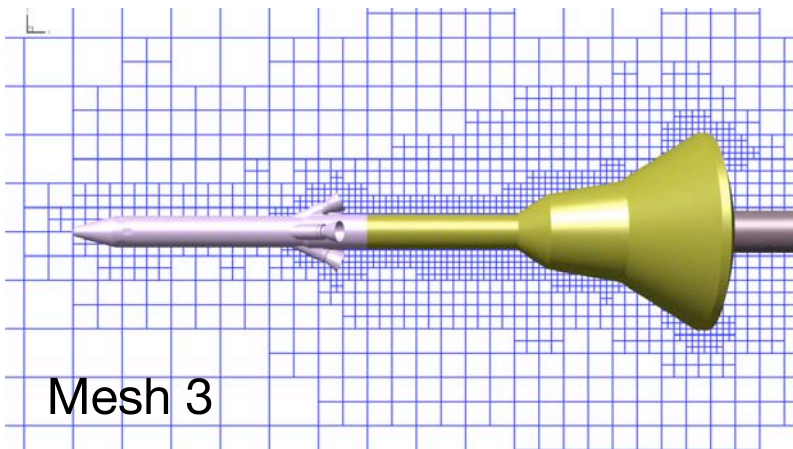
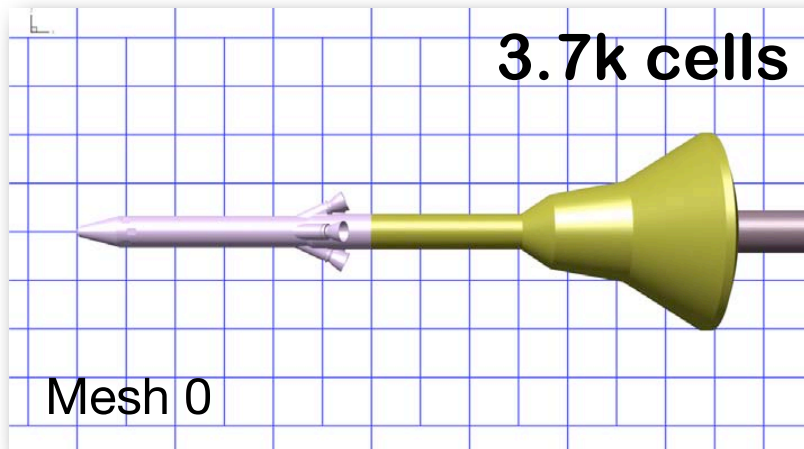
Adapt any cell that contributes more error to the functional than is allowable





Example Mesh Evolution

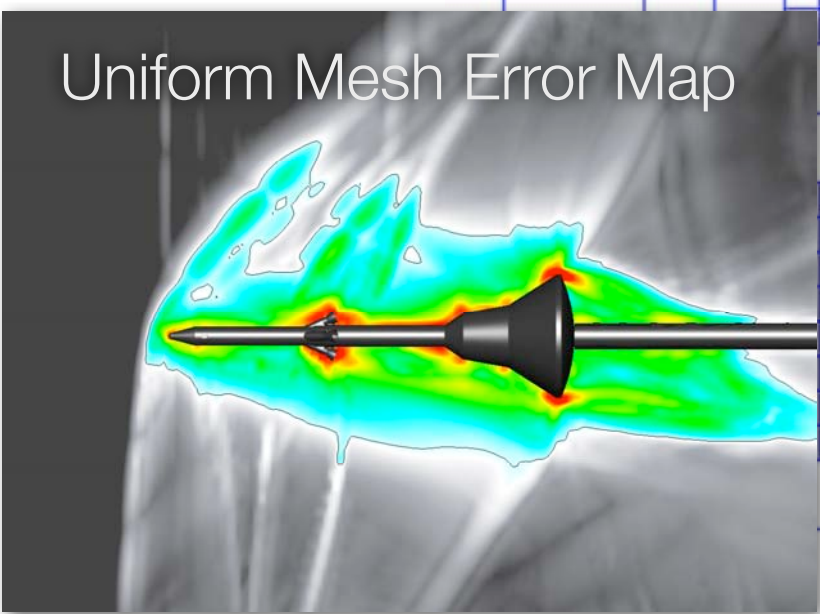
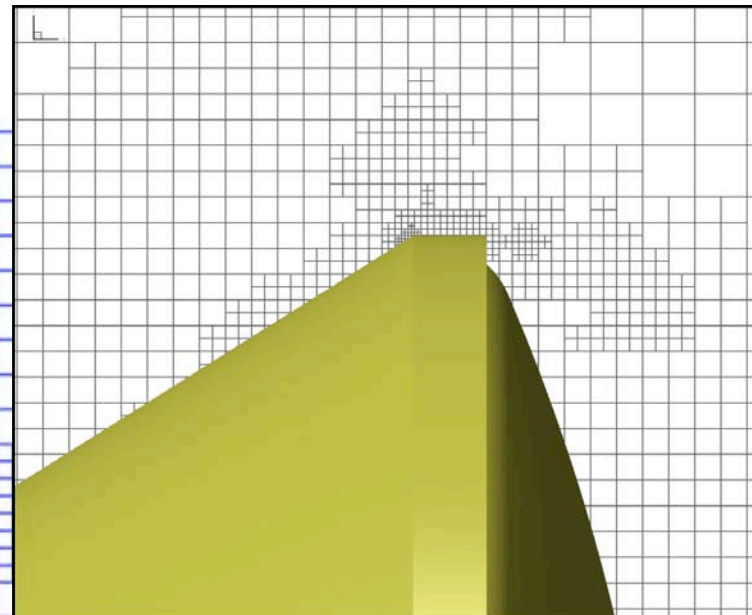
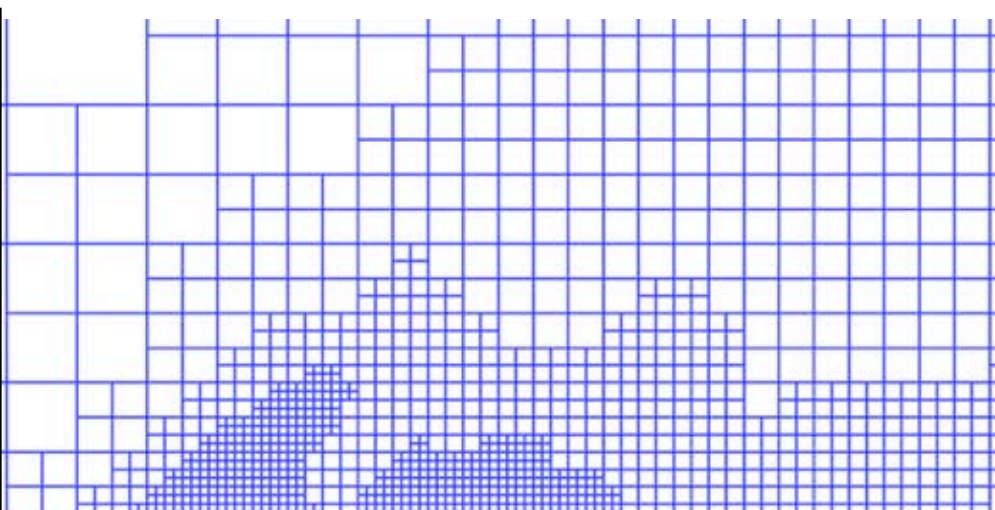
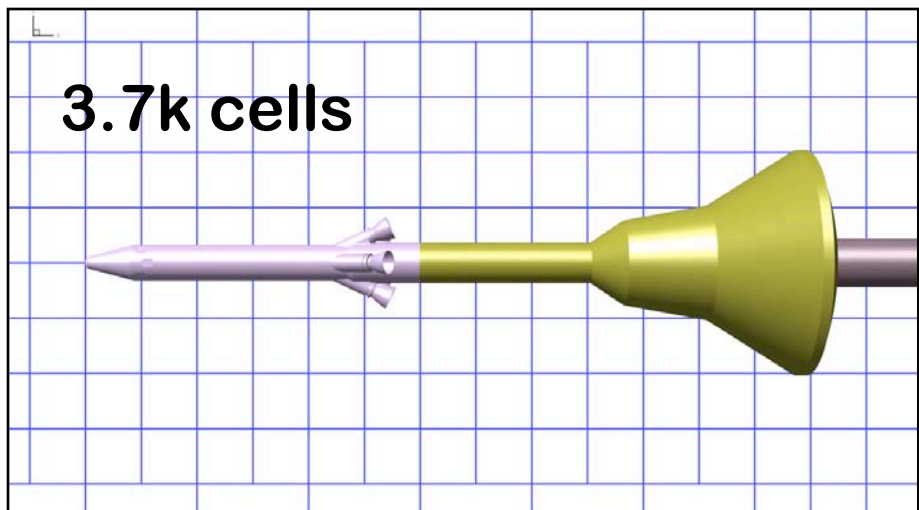
$M_\infty=1.1, \alpha=-25^\circ$





Example Mesh Evolution

$M_\infty=1.1, \alpha=-25^\circ, J = C_N + 0.2C_A$

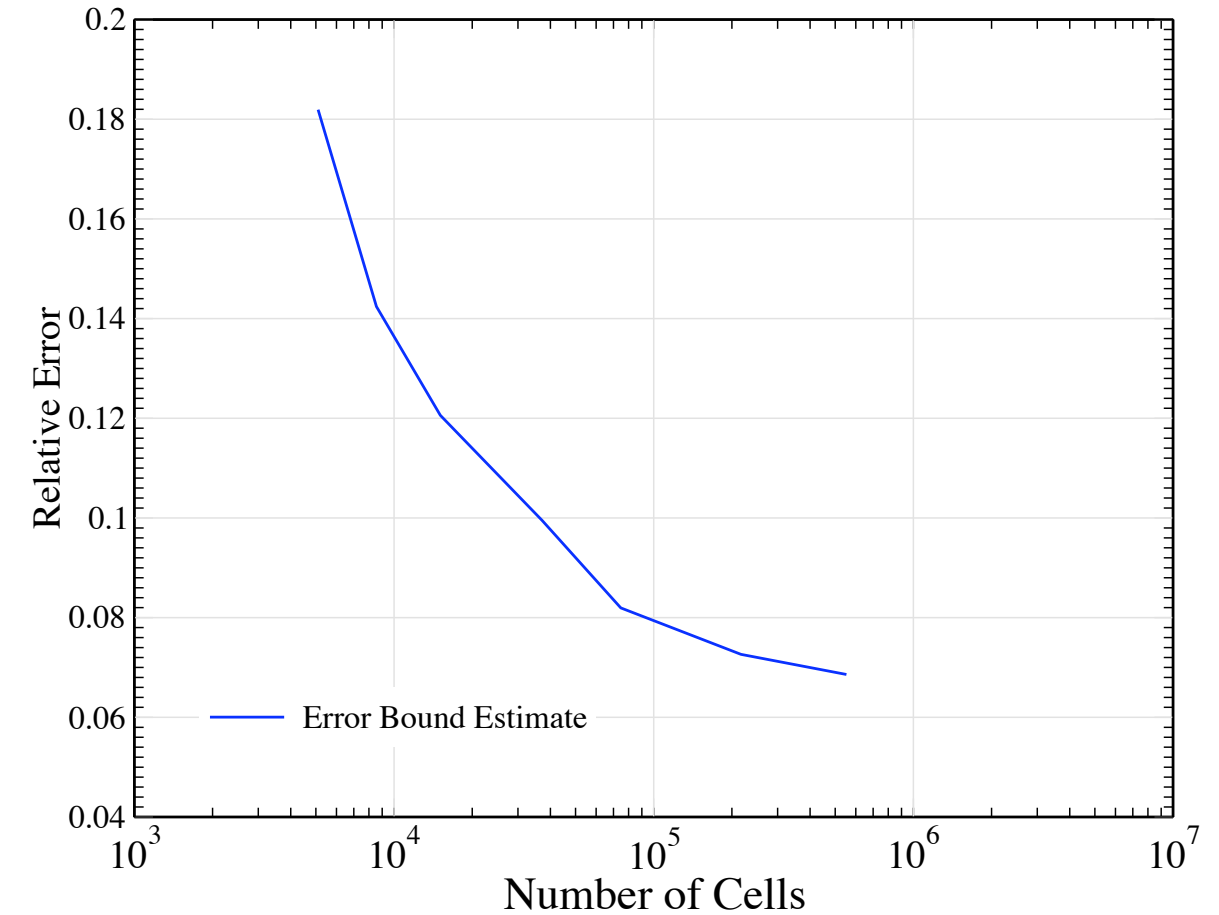
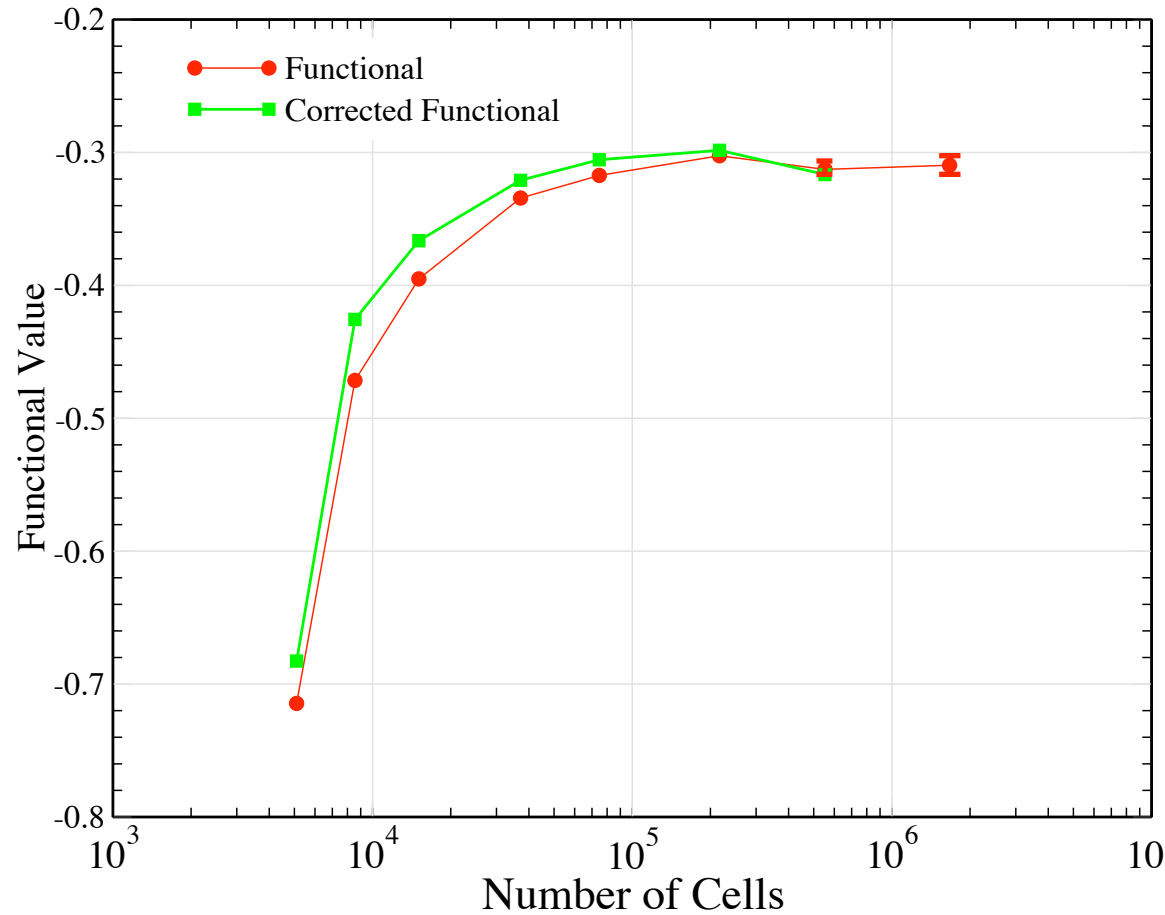


- Final mesh contains 1.9M cells
- Wall-clock time: 30 mins on 16 CPUs



Functional Convergence

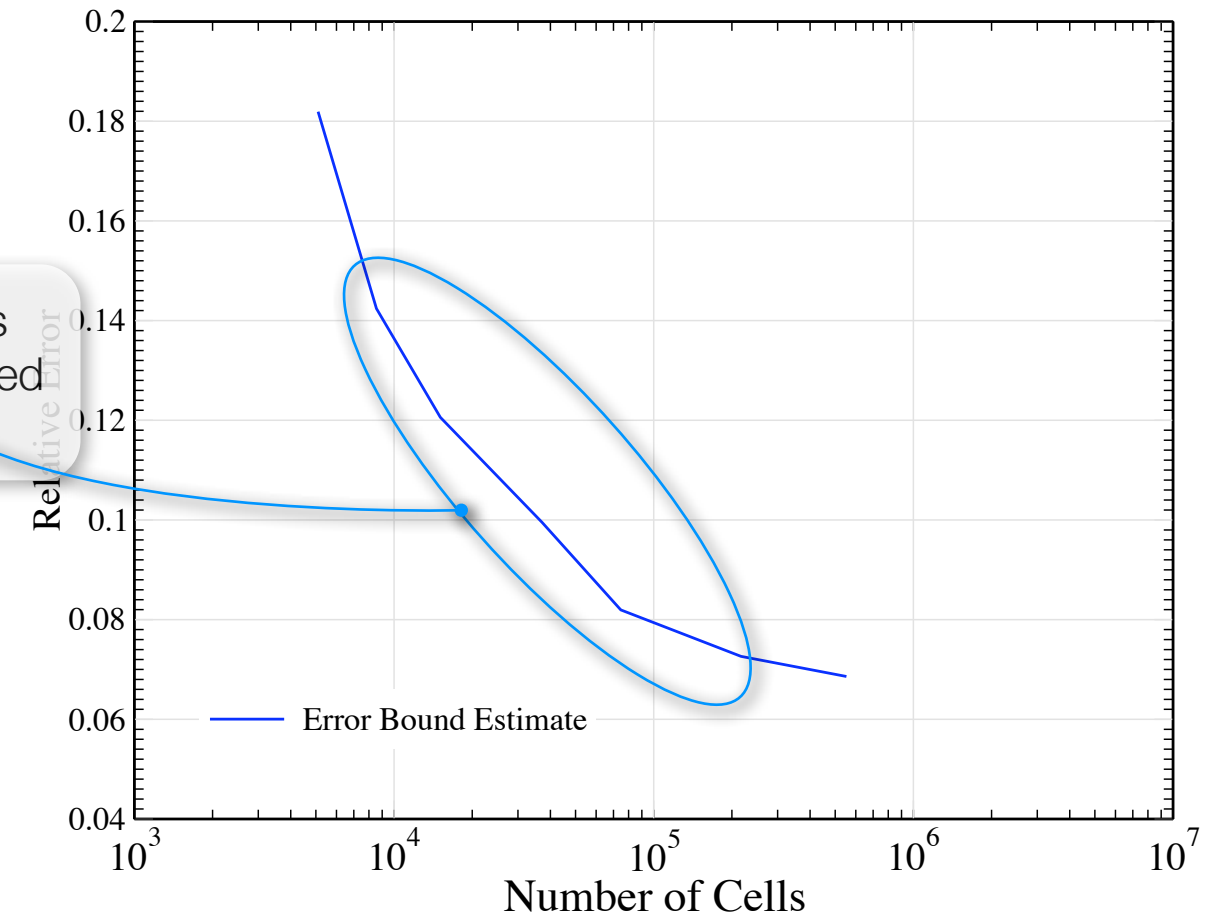
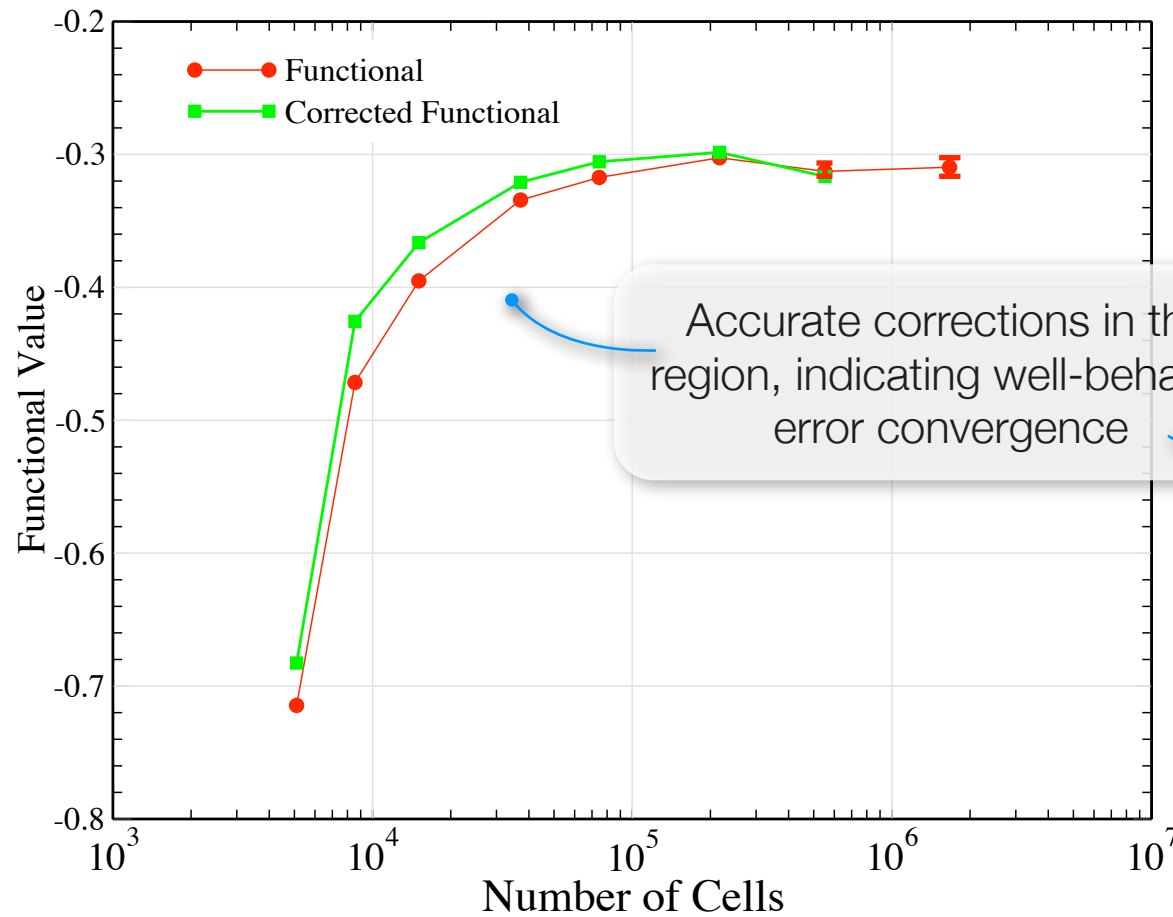
$M_\infty = 1.1, \alpha = -25^\circ, J = C_N + 0.2C_A, \text{TOL} = 0.05$





Functional Convergence

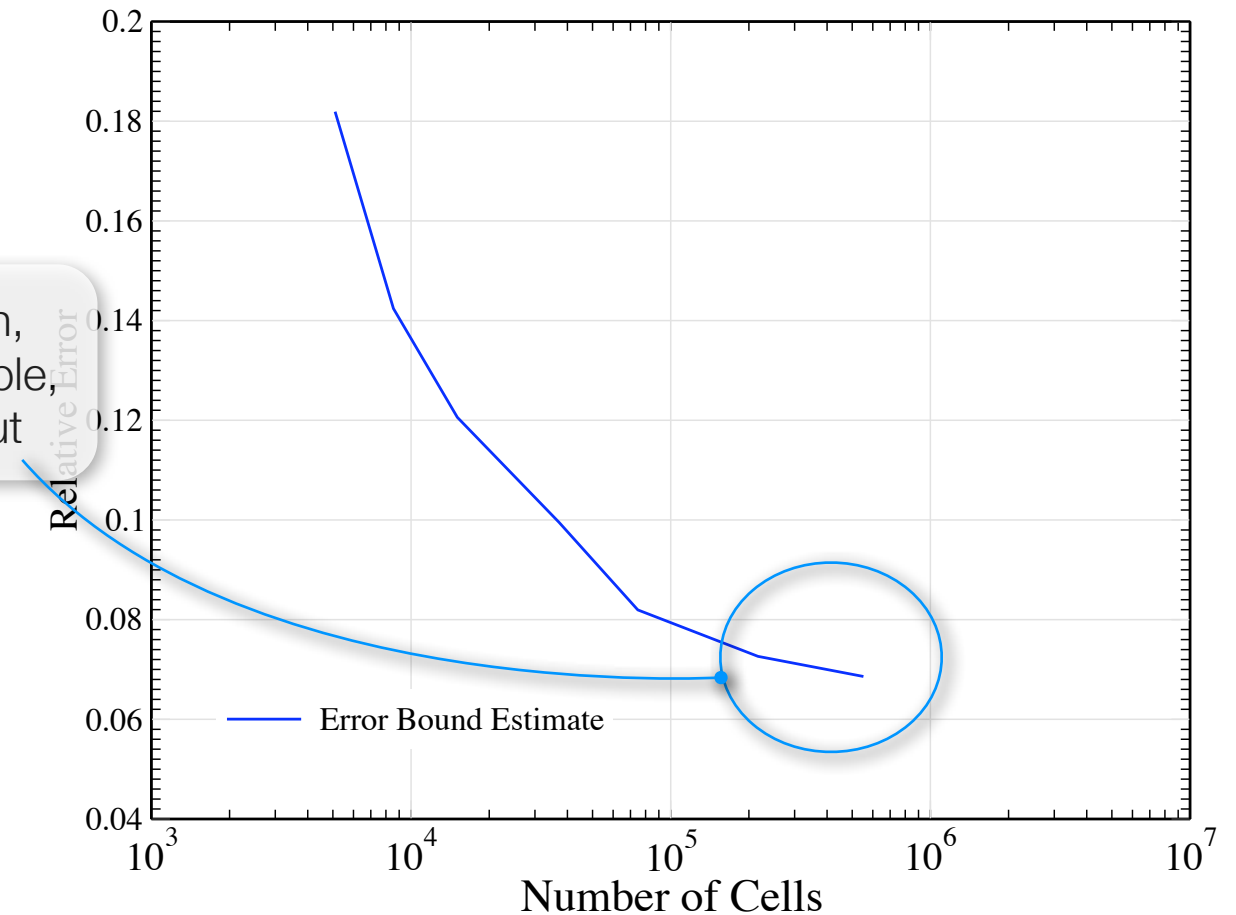
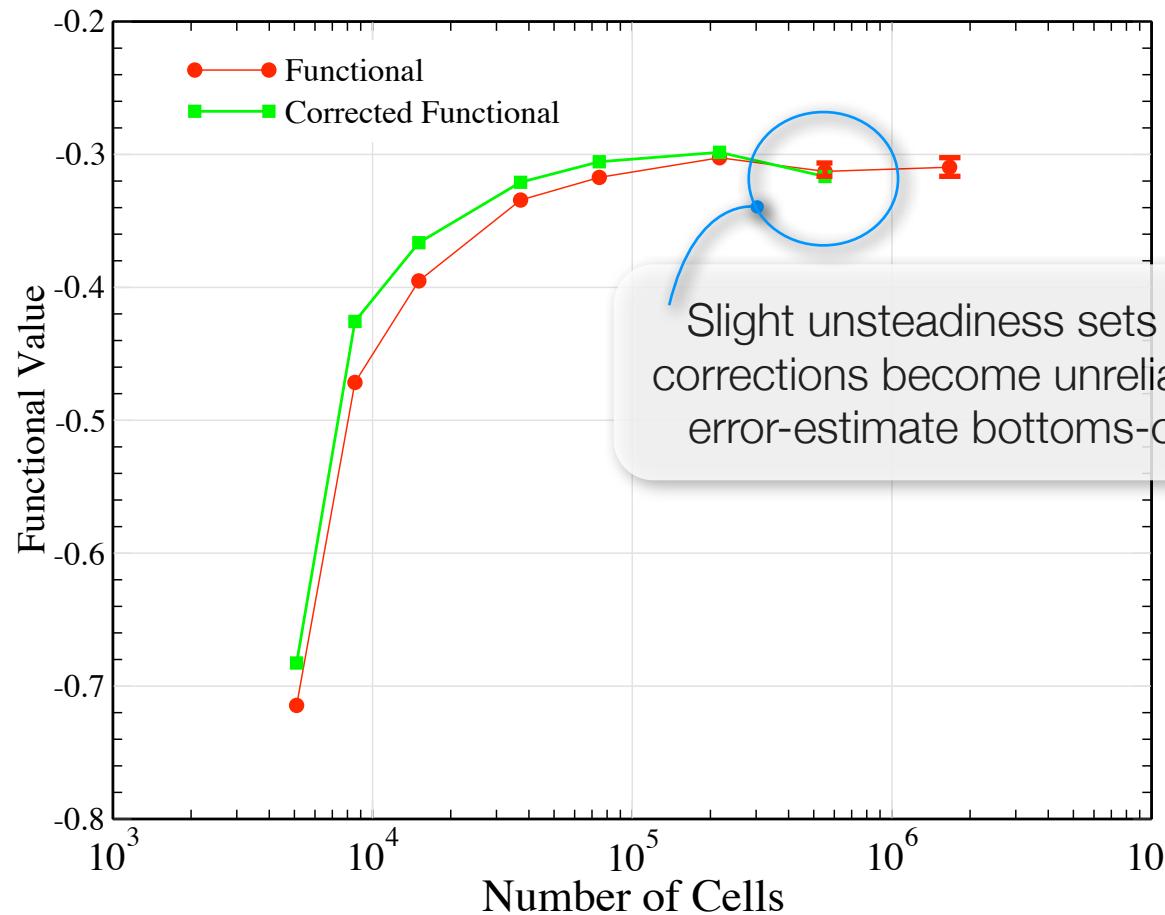
$M_\infty = 1.1, \alpha = -25^\circ, J = C_N + 0.2C_A, \text{TOL} = 0.05$





Functional Convergence

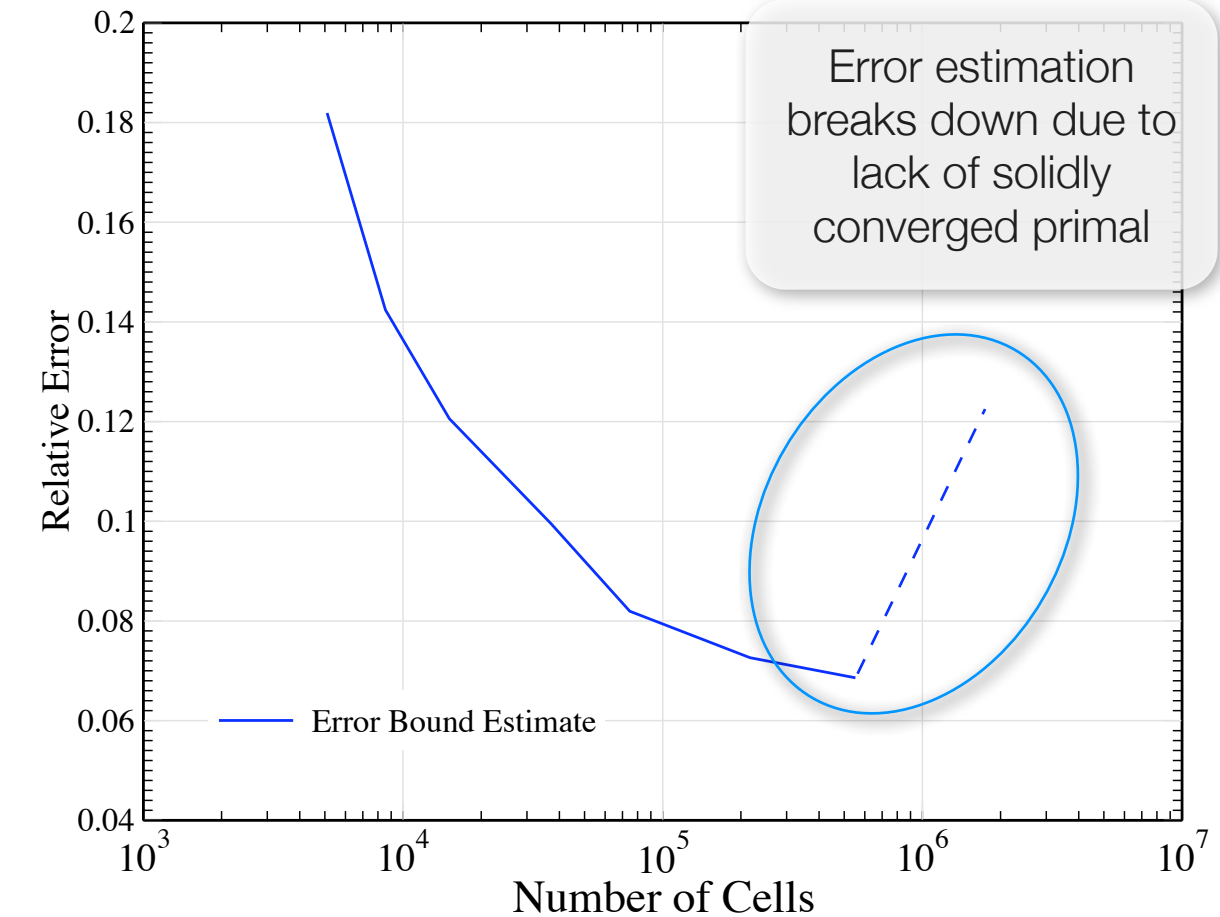
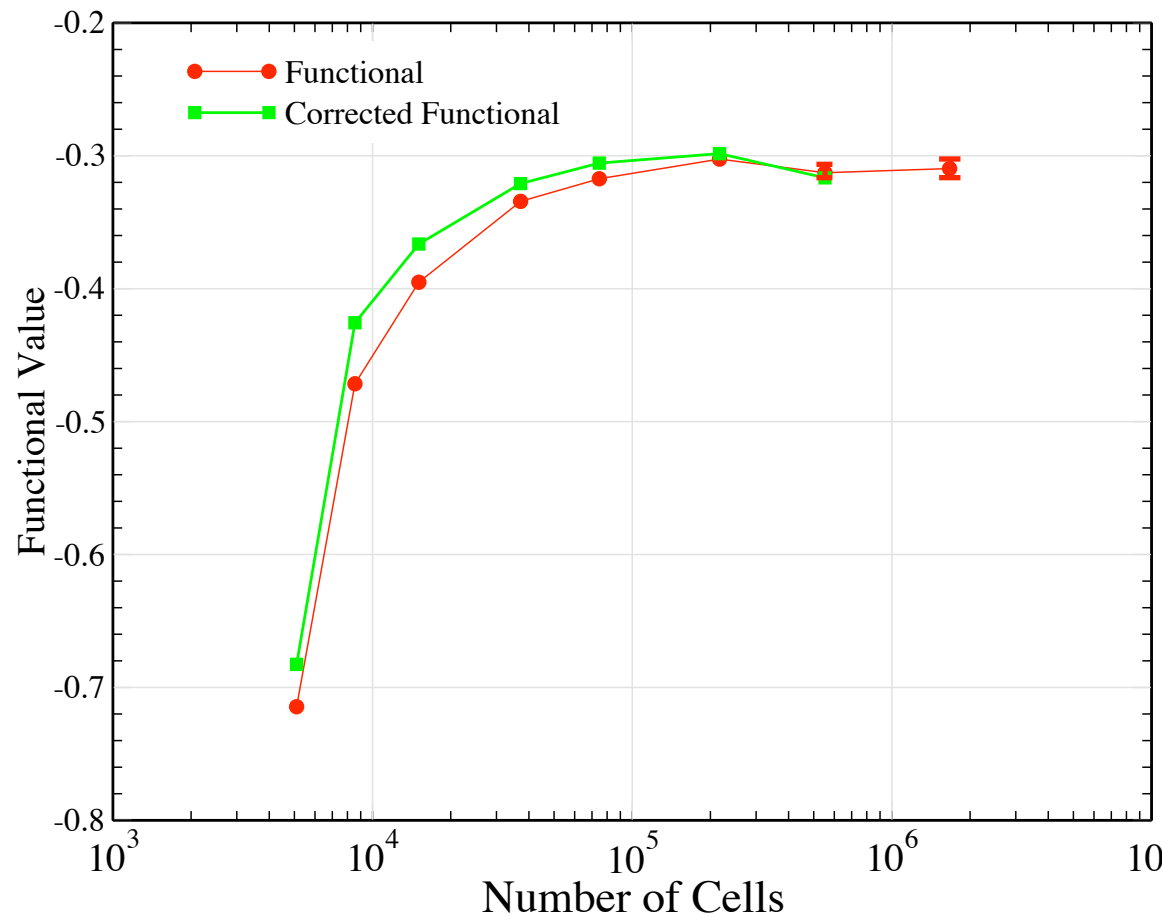
$M_\infty=1.1, \alpha=-25^\circ, J = C_N + 0.2C_A, \text{TOL} = 0.05$





Functional Convergence

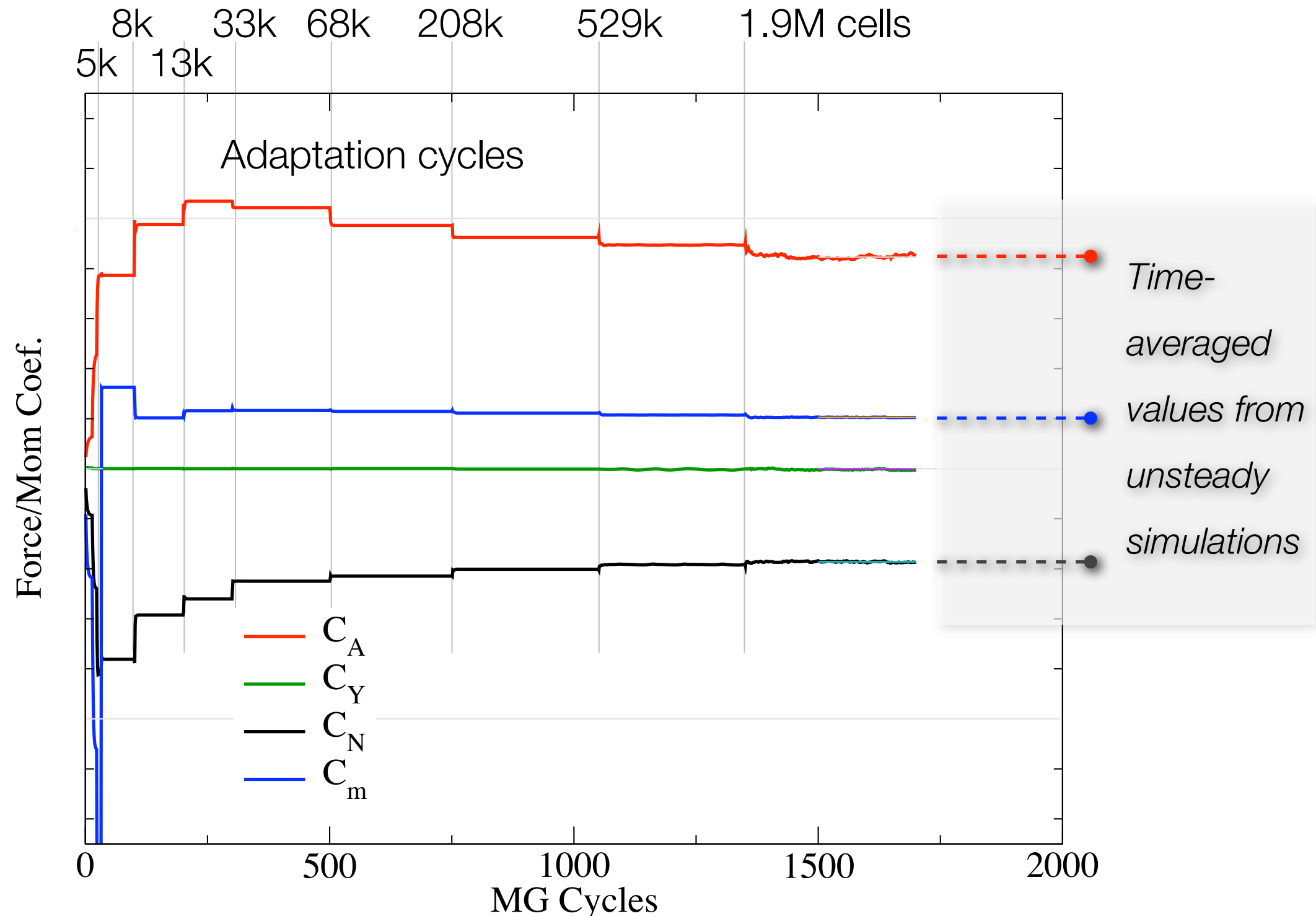
$M_\infty=1.1$, $\alpha=-25^\circ$, $J = C_N + 0.2C_A$, TOL = 0.05



- Convergence of functional, correction and error-bound estimate provides insight into onset of “unsteadiness” (noise due to incomplete convergence)



Functional Convergence

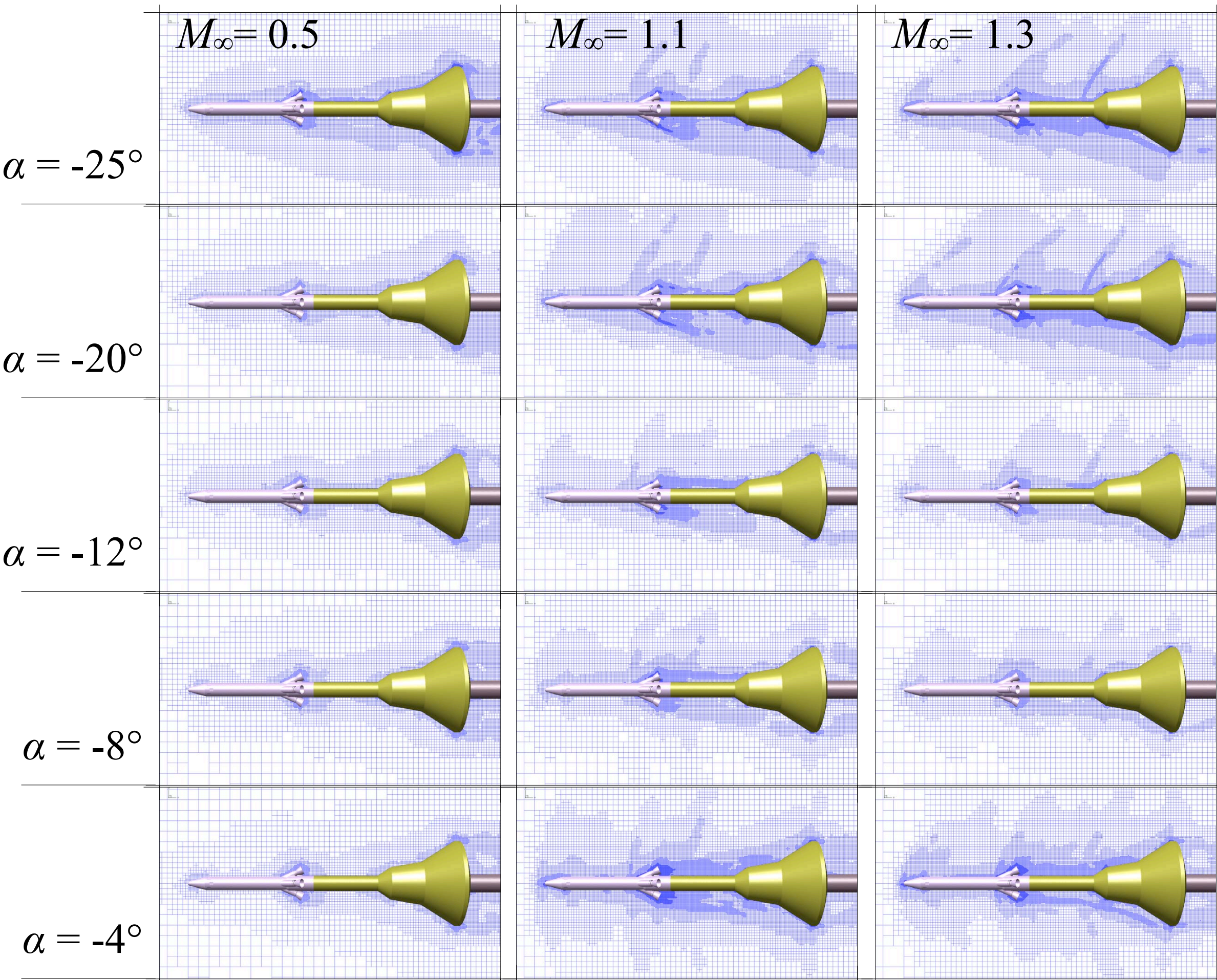


$M_\infty = 1.1, \alpha = -25^\circ, J = C_N + 0.2C_A, TOL = 0.05$



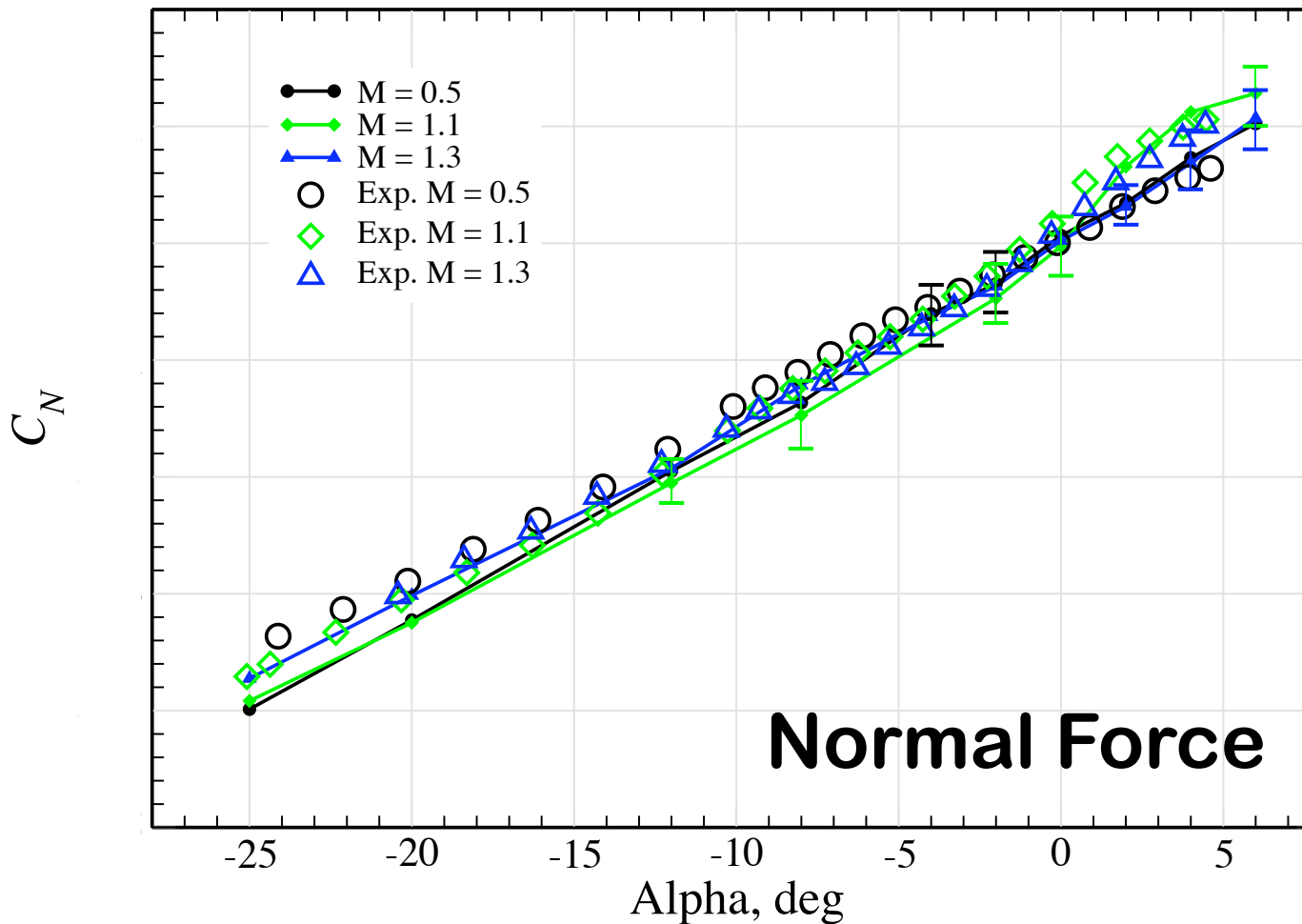
← Mach Numbers →

↑ Angles of Attack ↓

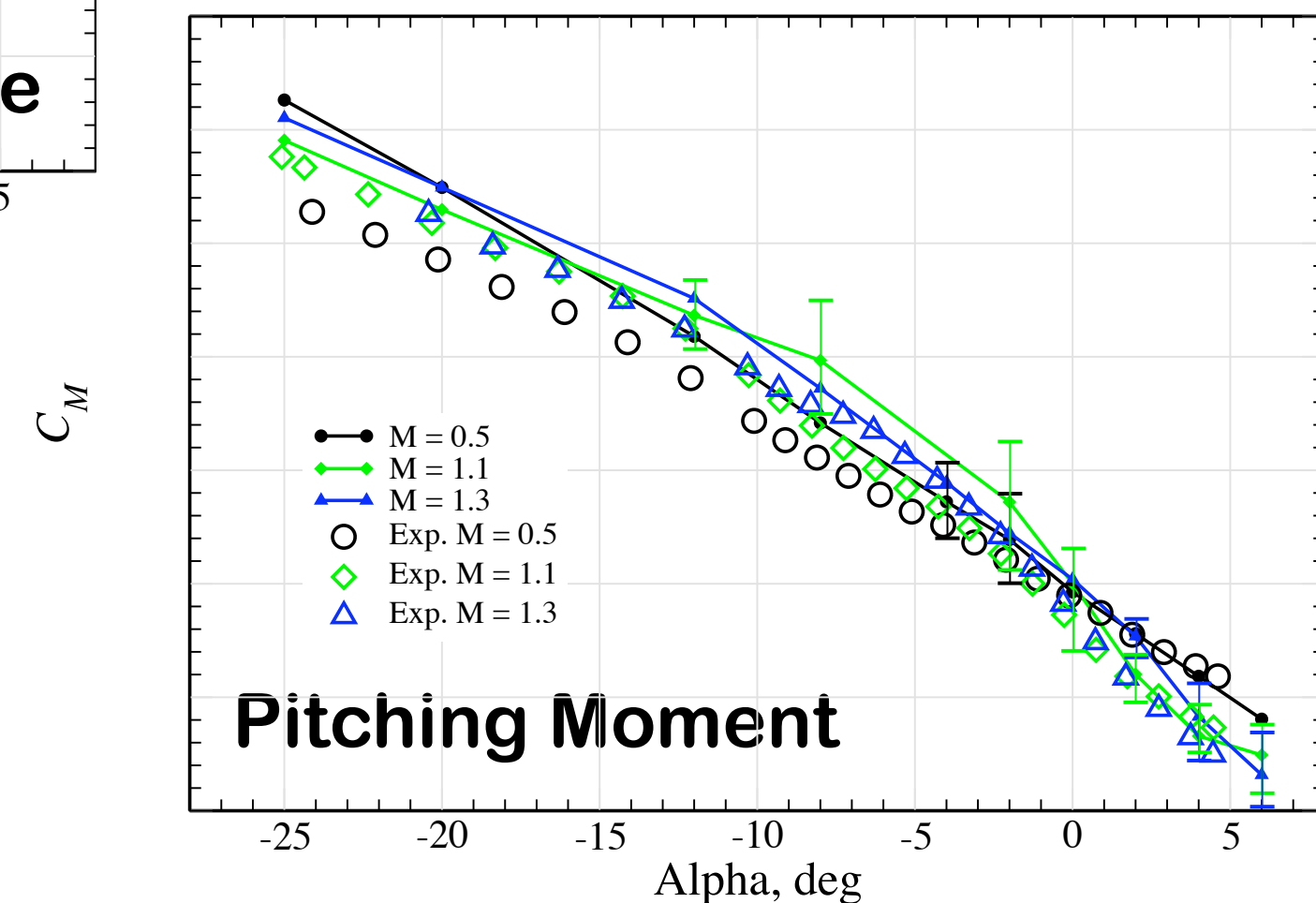




Comparison with Experiment



- Run matrix involved 30 cases
- General agreement with experimental values for normal and axial forces, and pitching moment

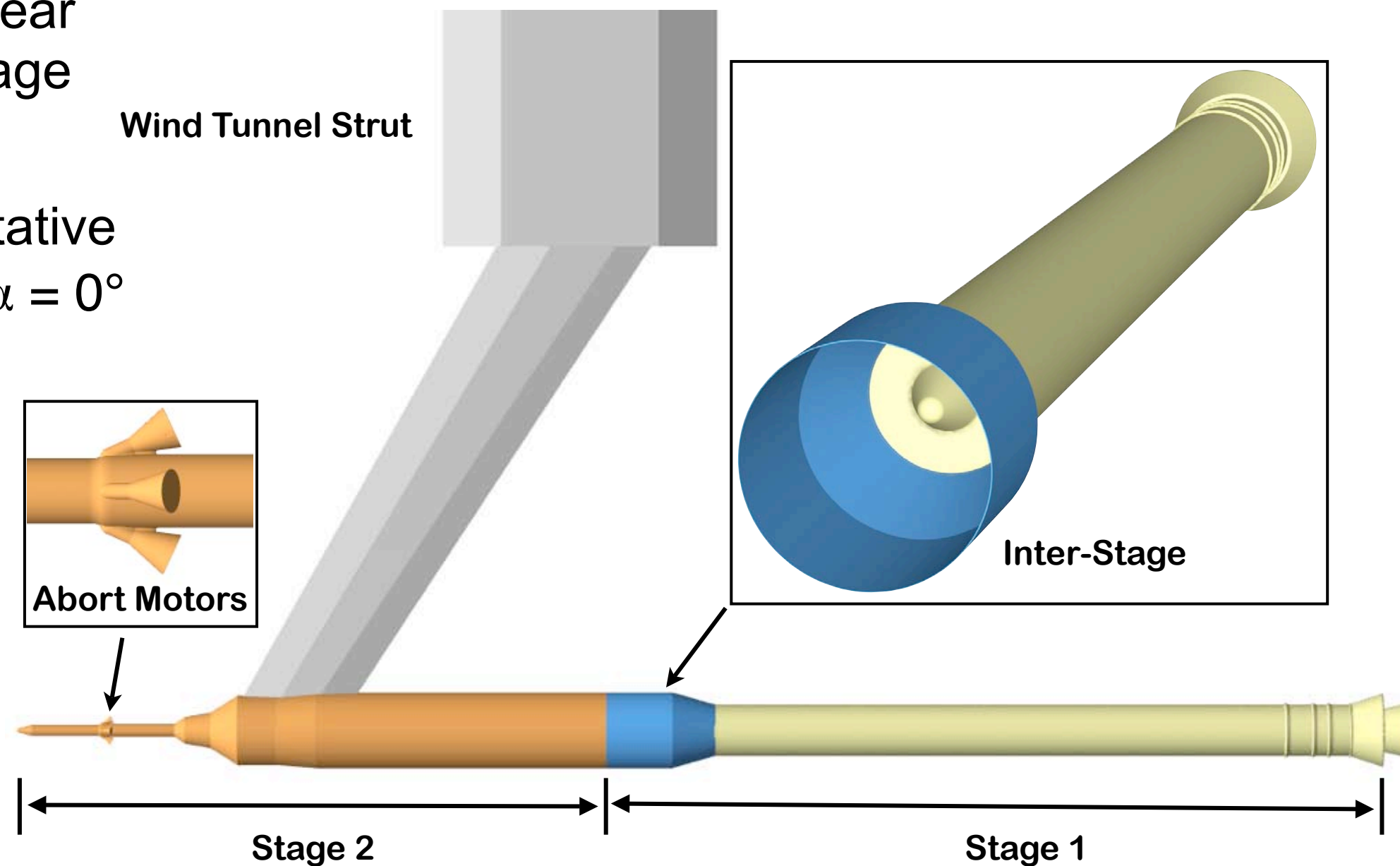


- Error bars indicate level of noise in functional due to incomplete flow convergence
- Indication of where unsteady analysis is required



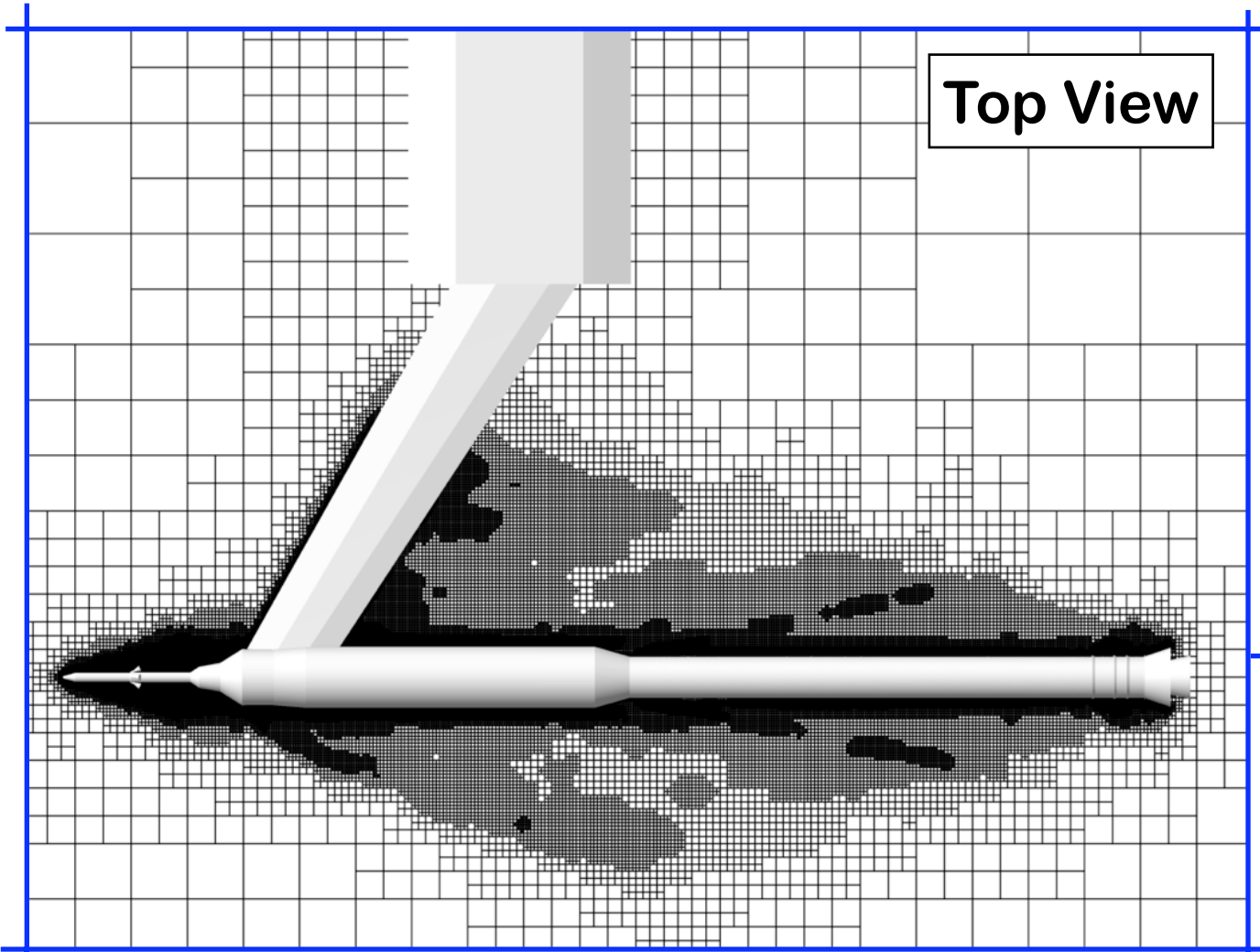
Launch-Vehicle Stage Separation

- Parametric study of aerodynamic performance for various separation distances and strut interference effects
- Roughly 25 configurations at two angles of attack with fixed Mach number
- Functional is a linear combination of Stage 1 and 2 drag
- Present representative case at $M_\infty = 4.5$, $\alpha = 0^\circ$
- Decreasing Threshold: $\lambda = 16, \dots, 1$
- Uniform error tolerance of 0.1

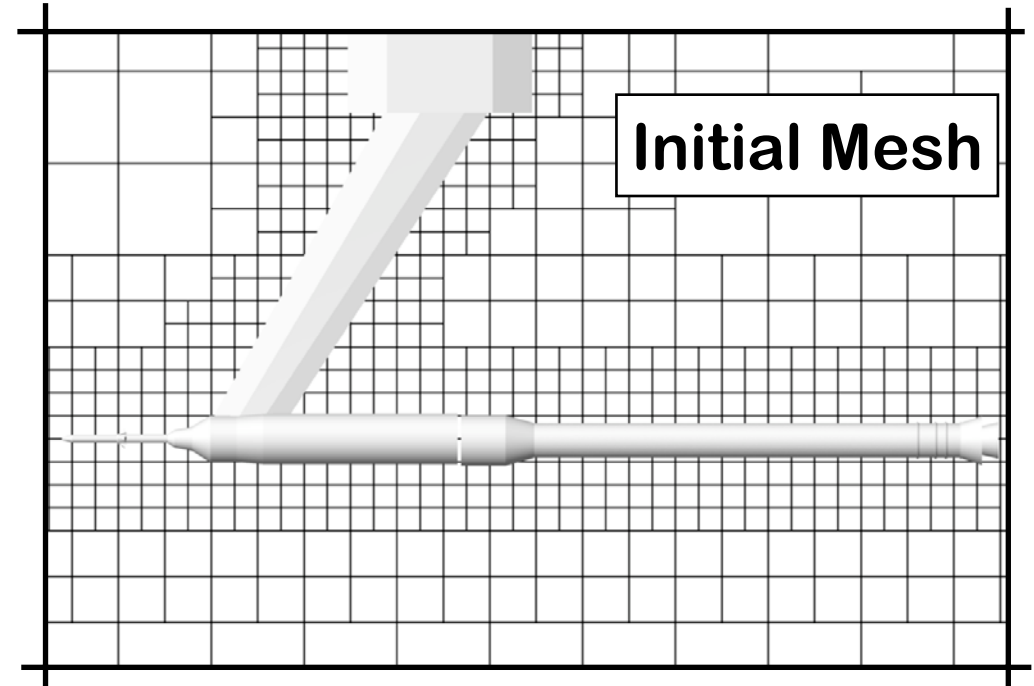




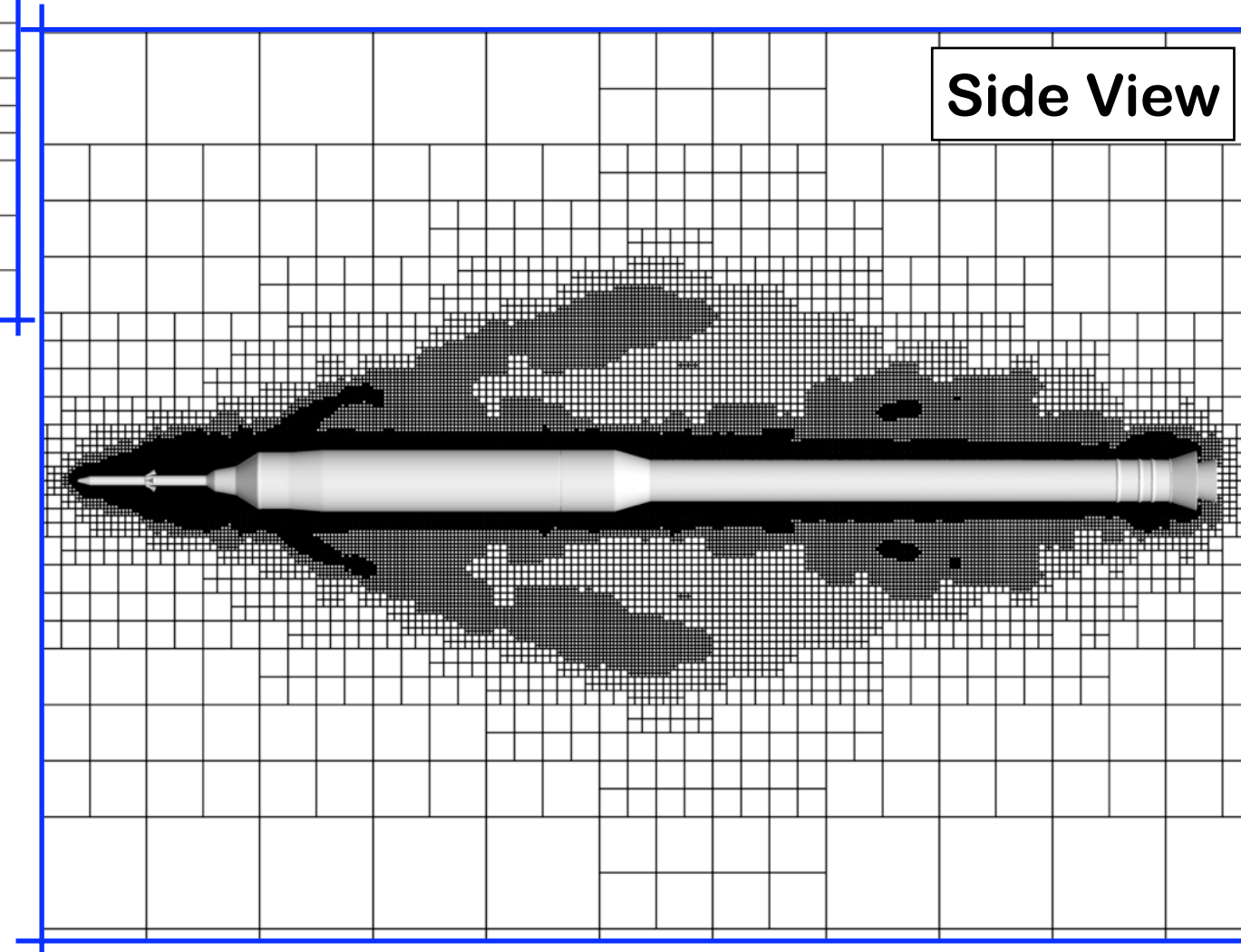
Near-Body Mesh Views



Top View



Initial Mesh



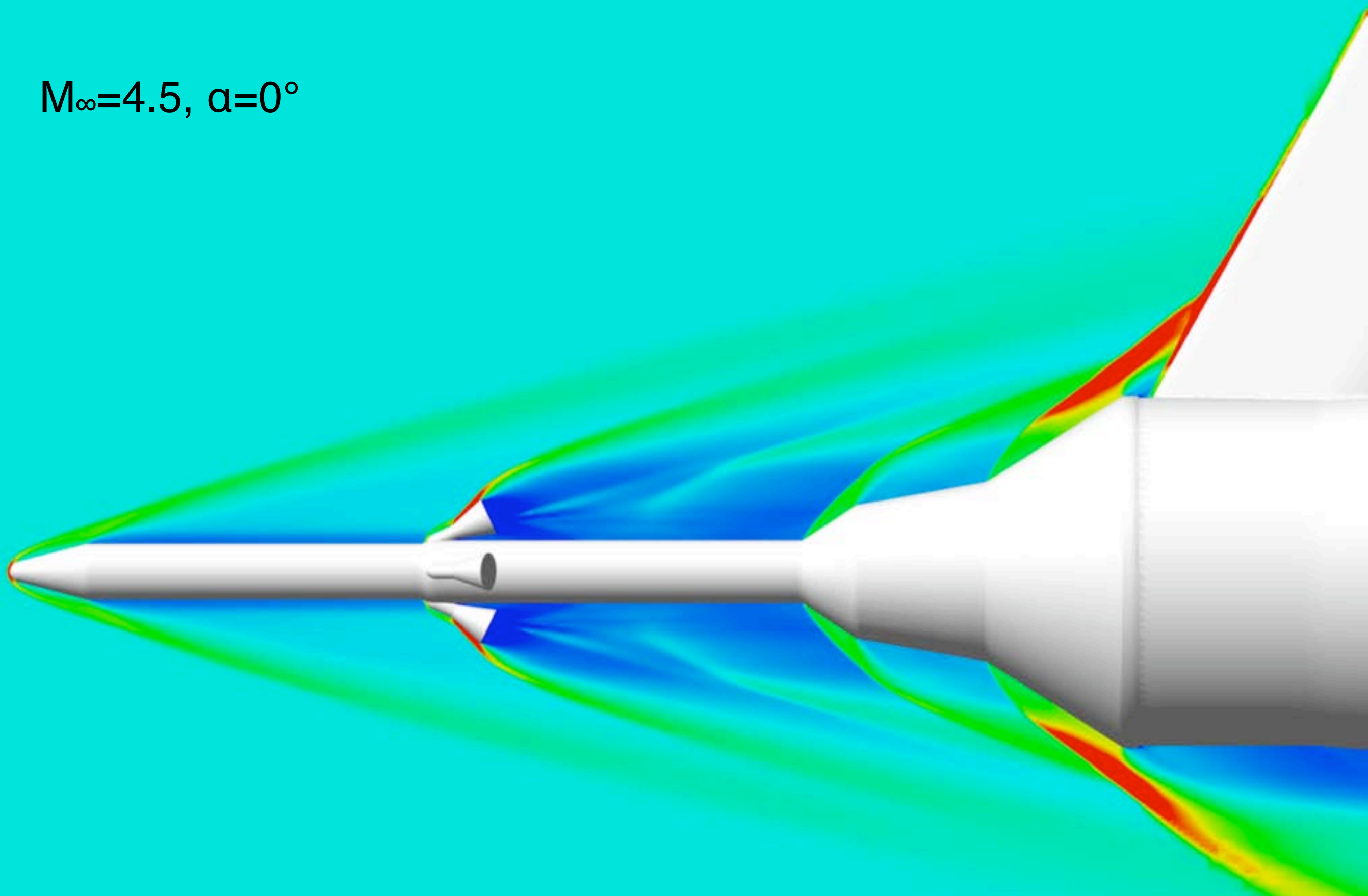
Side View

- Initial mesh contains only 13k cells
- Final meshes contain between 8M to 20M cells



Pressure Contours

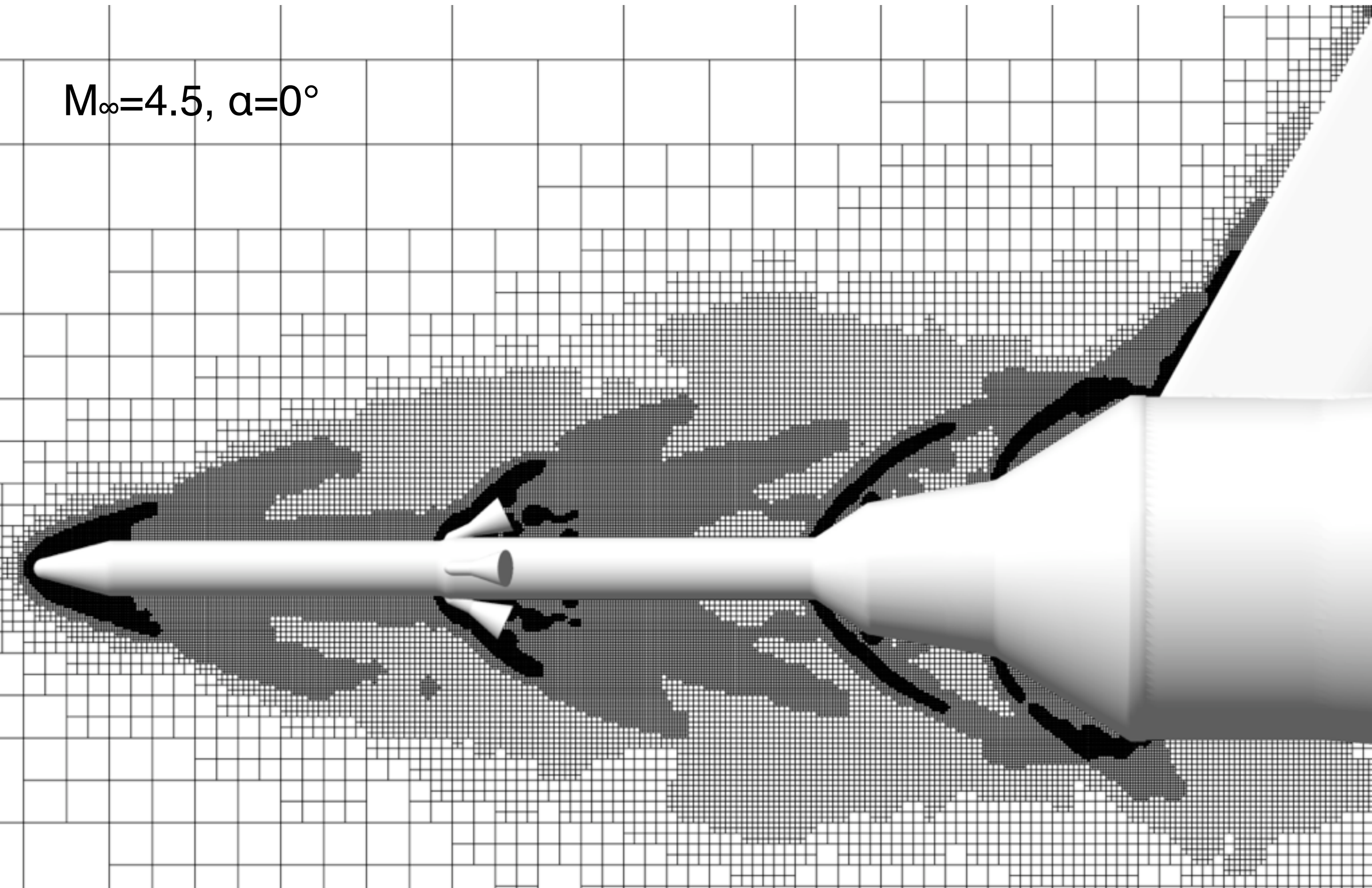
$M_\infty=4.5, \alpha=0^\circ$

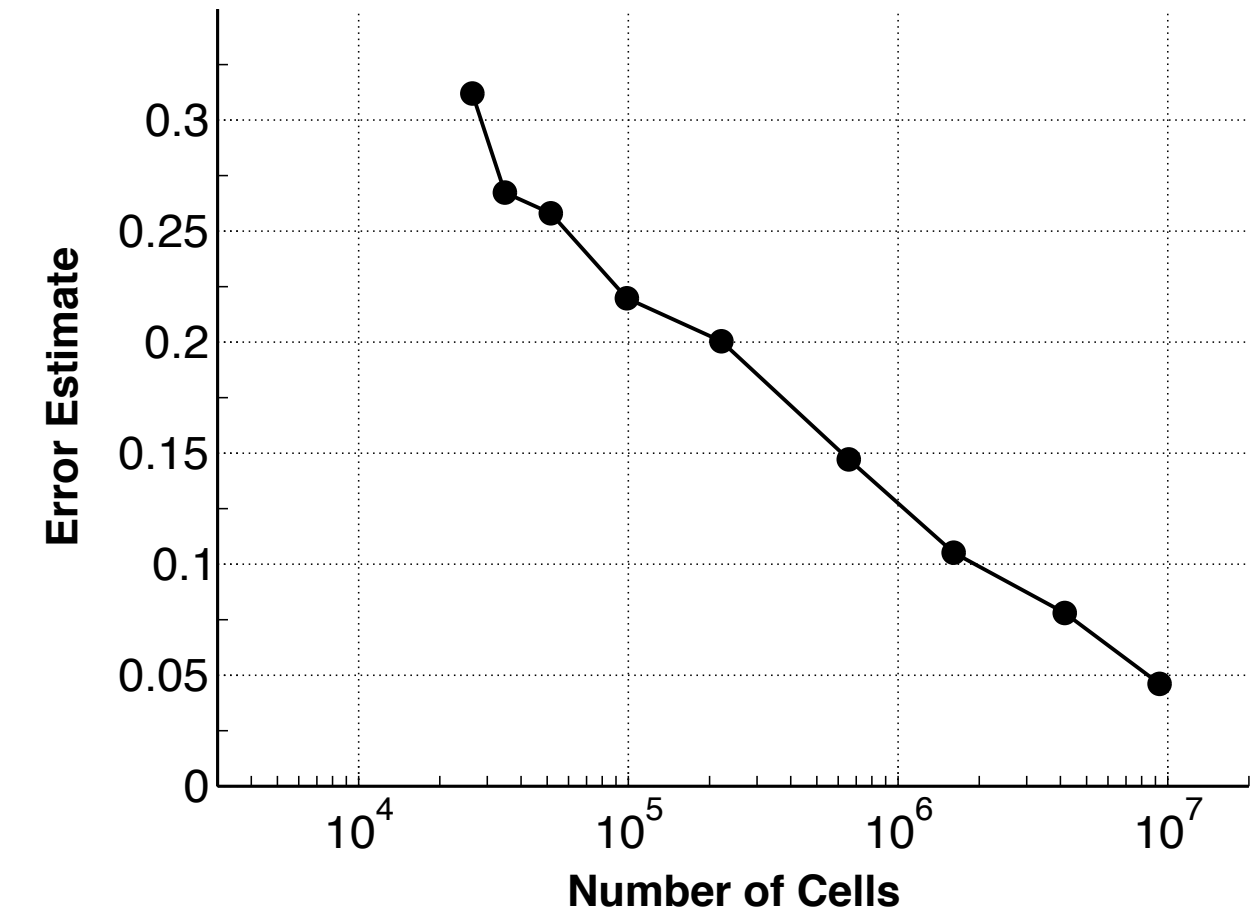
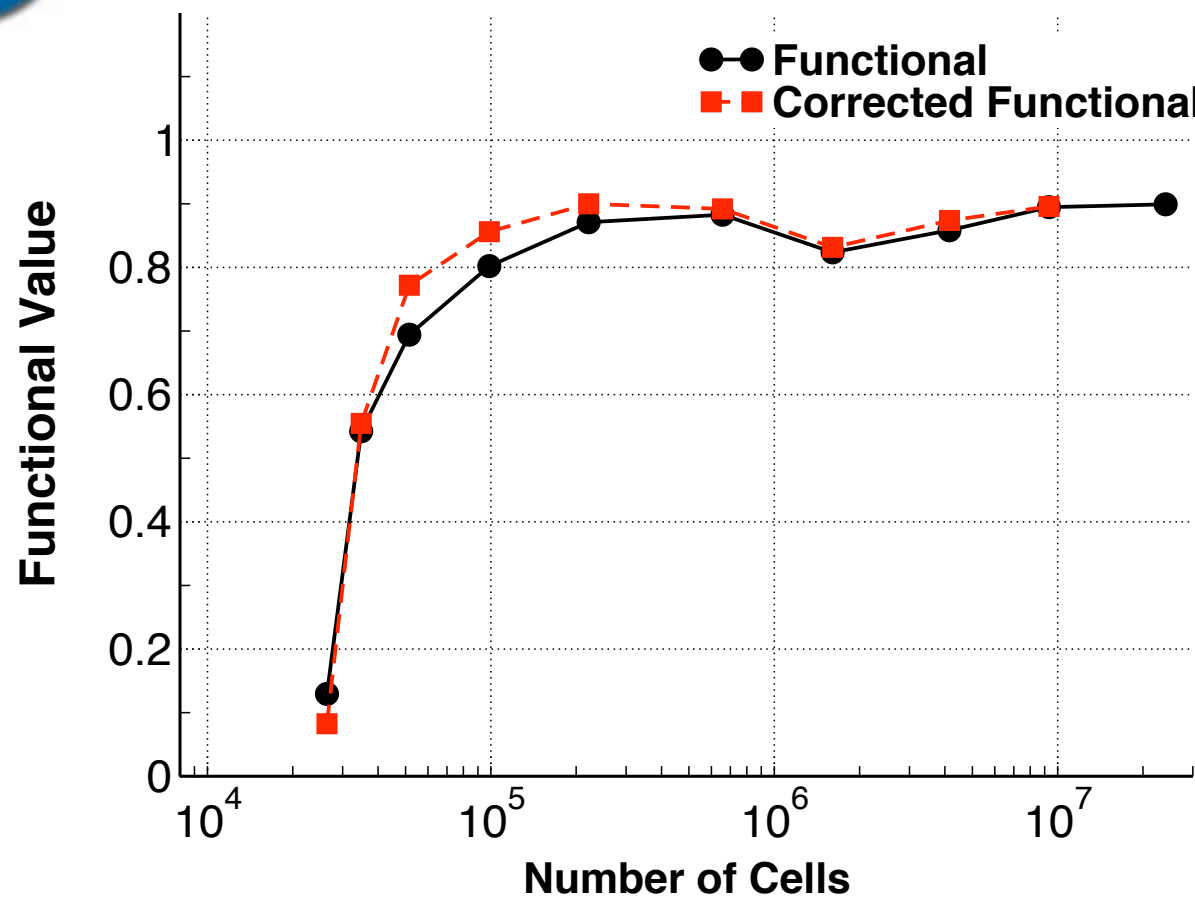




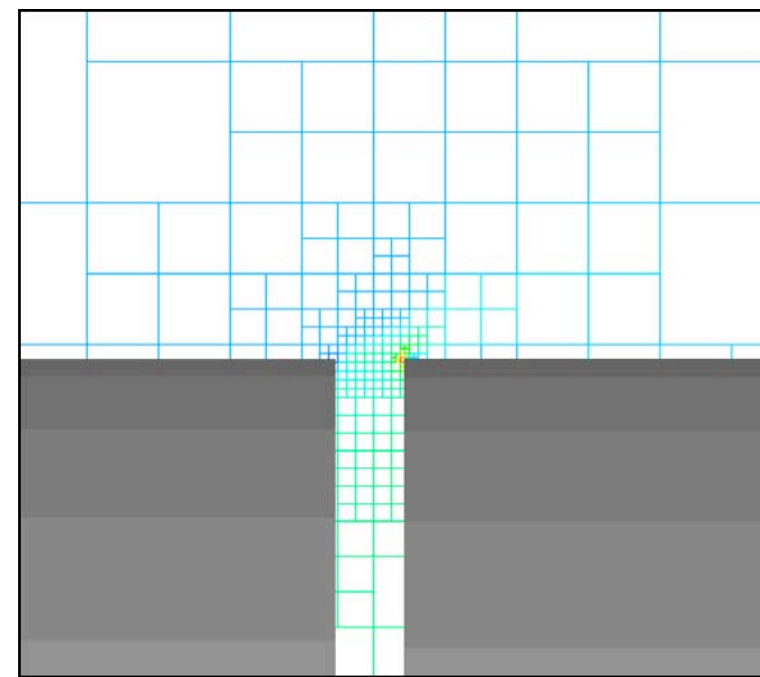
Pressure Contours

$M_\infty = 4.5, \alpha = 0^\circ$

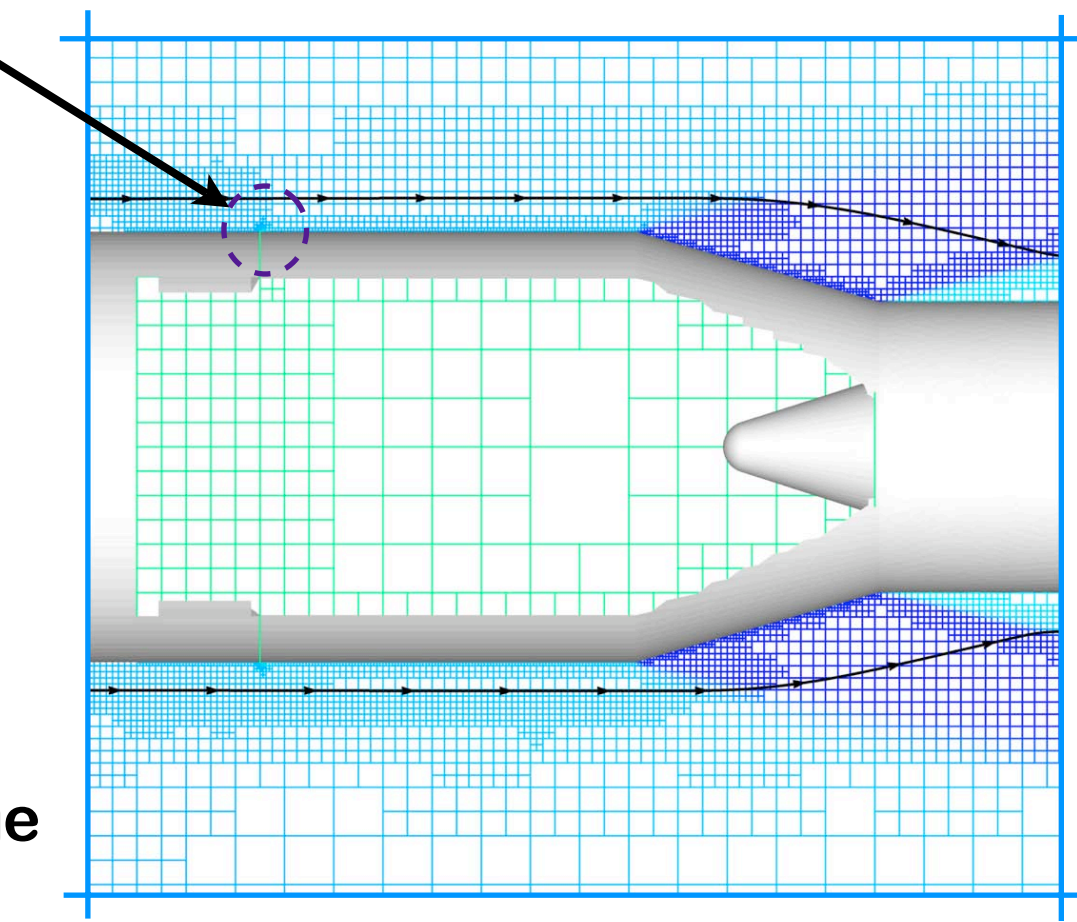




- Minimal refinement of inter-stage region
- Gap is highly refined
- Overall, excellent convergence of functional and error estimate



Cutaway view of inter-stage

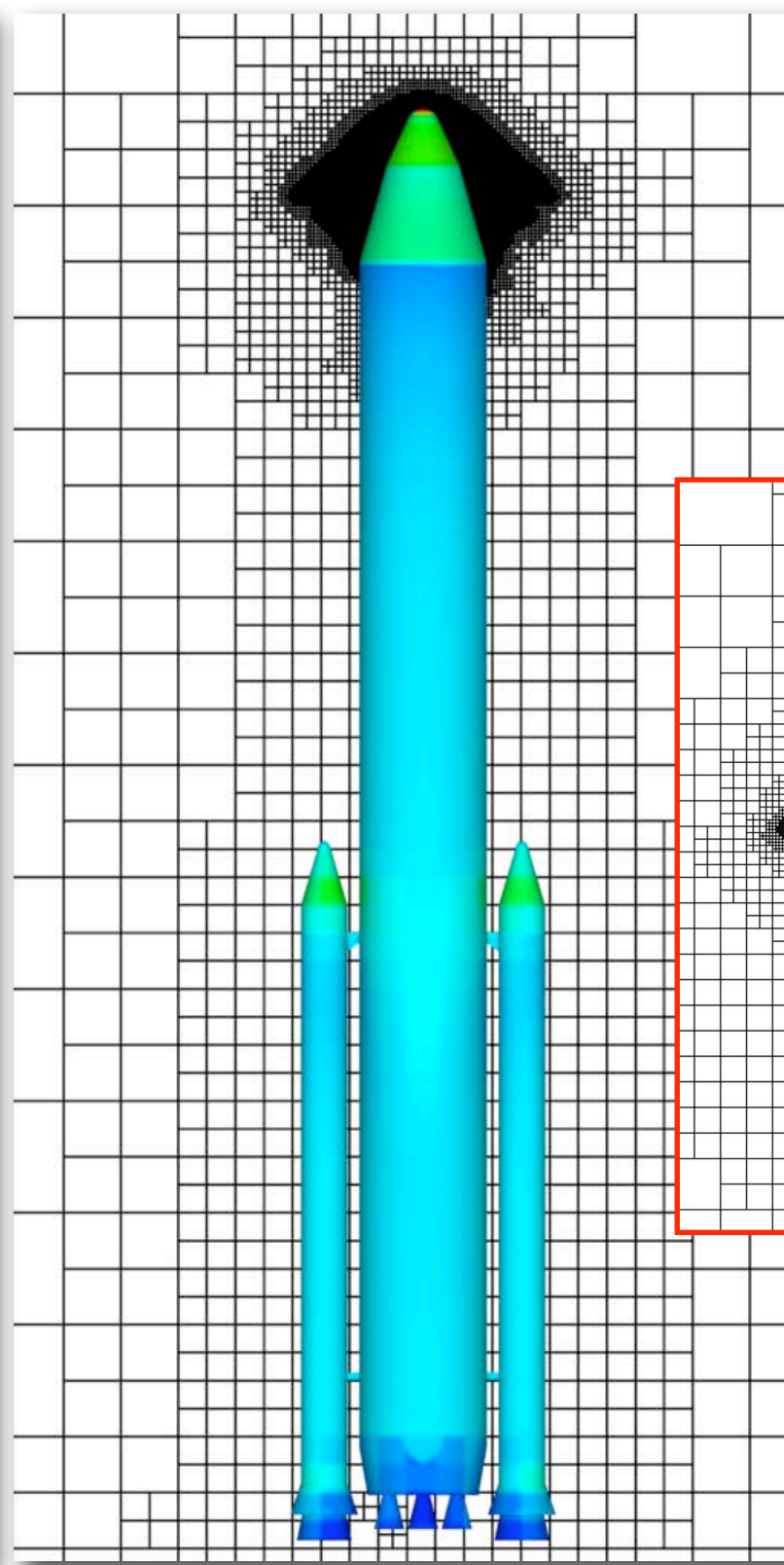
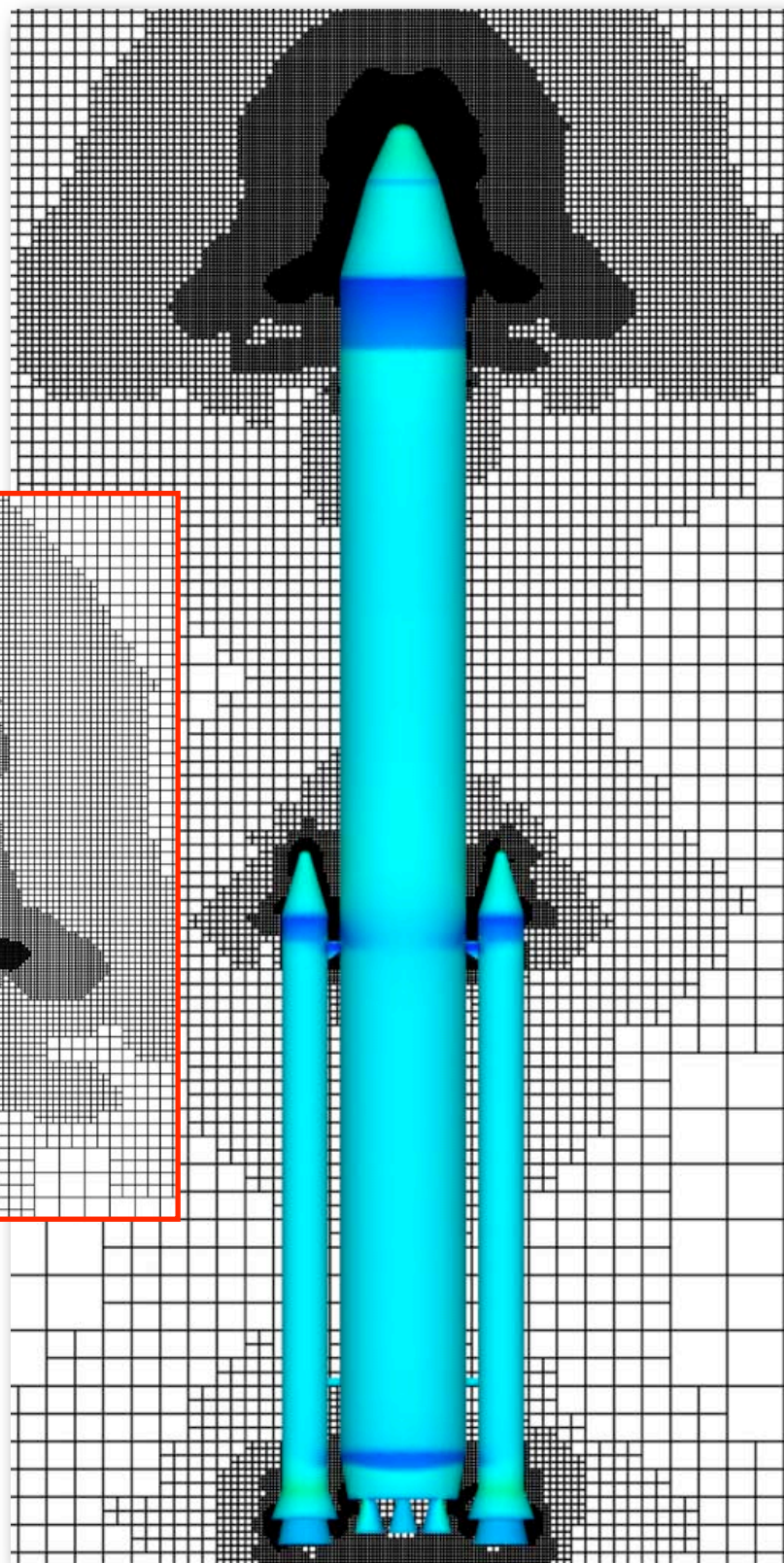


Launch Vehicle

Functional: Axial force on nose fairing



Transonic
Flow

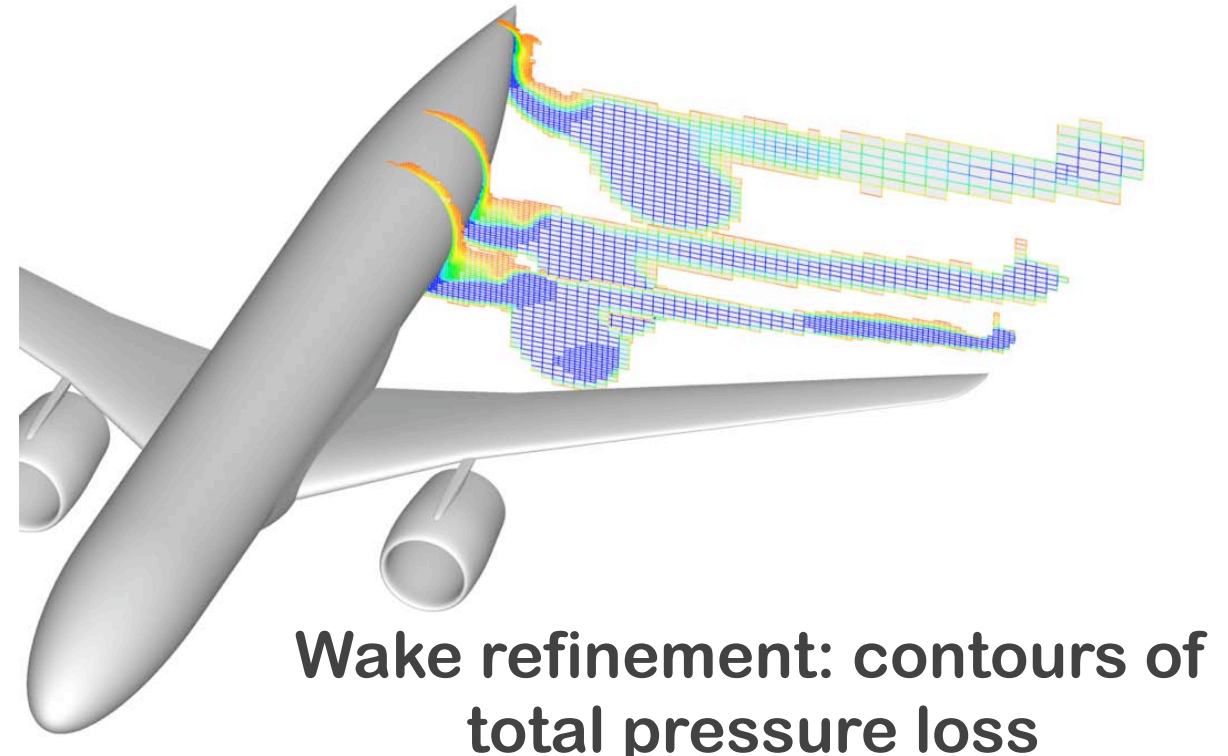
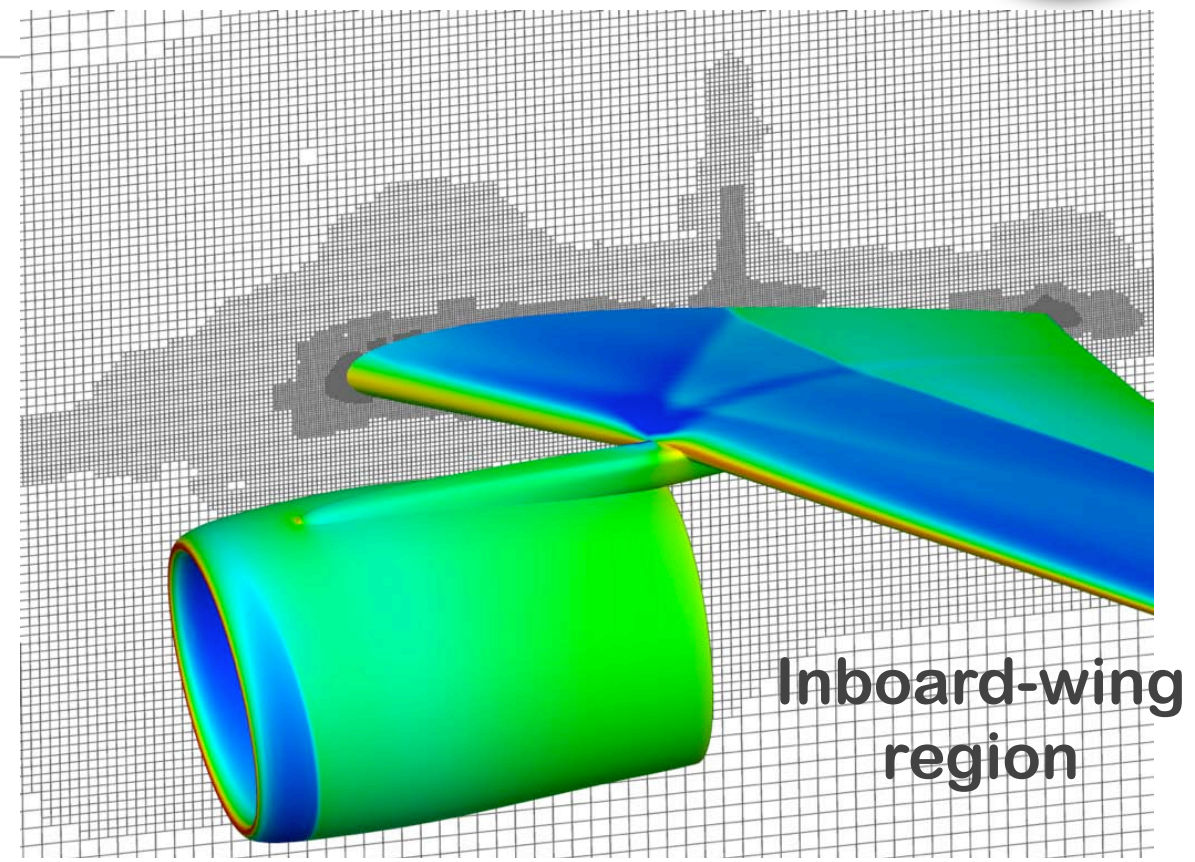
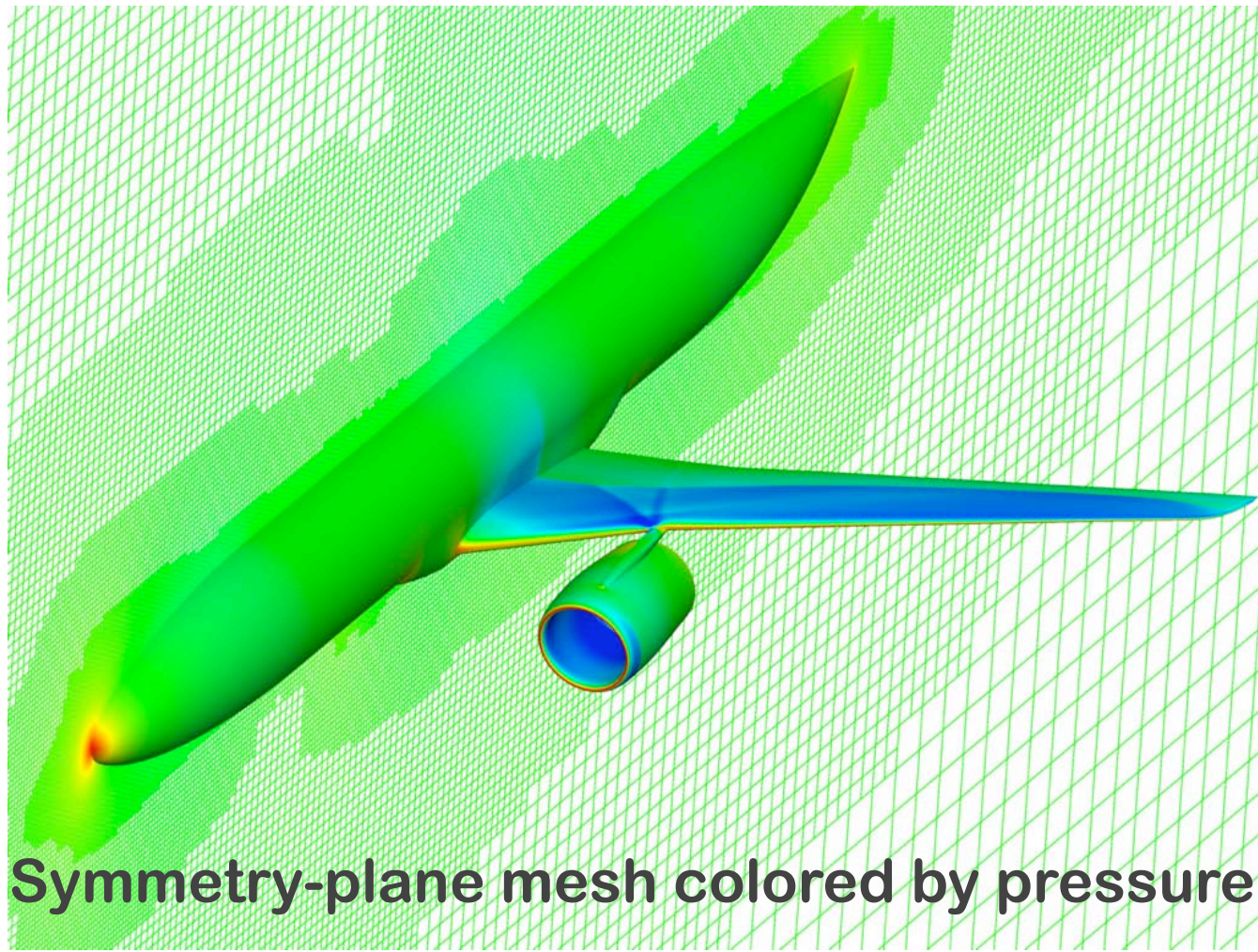


Supersonic
Flow

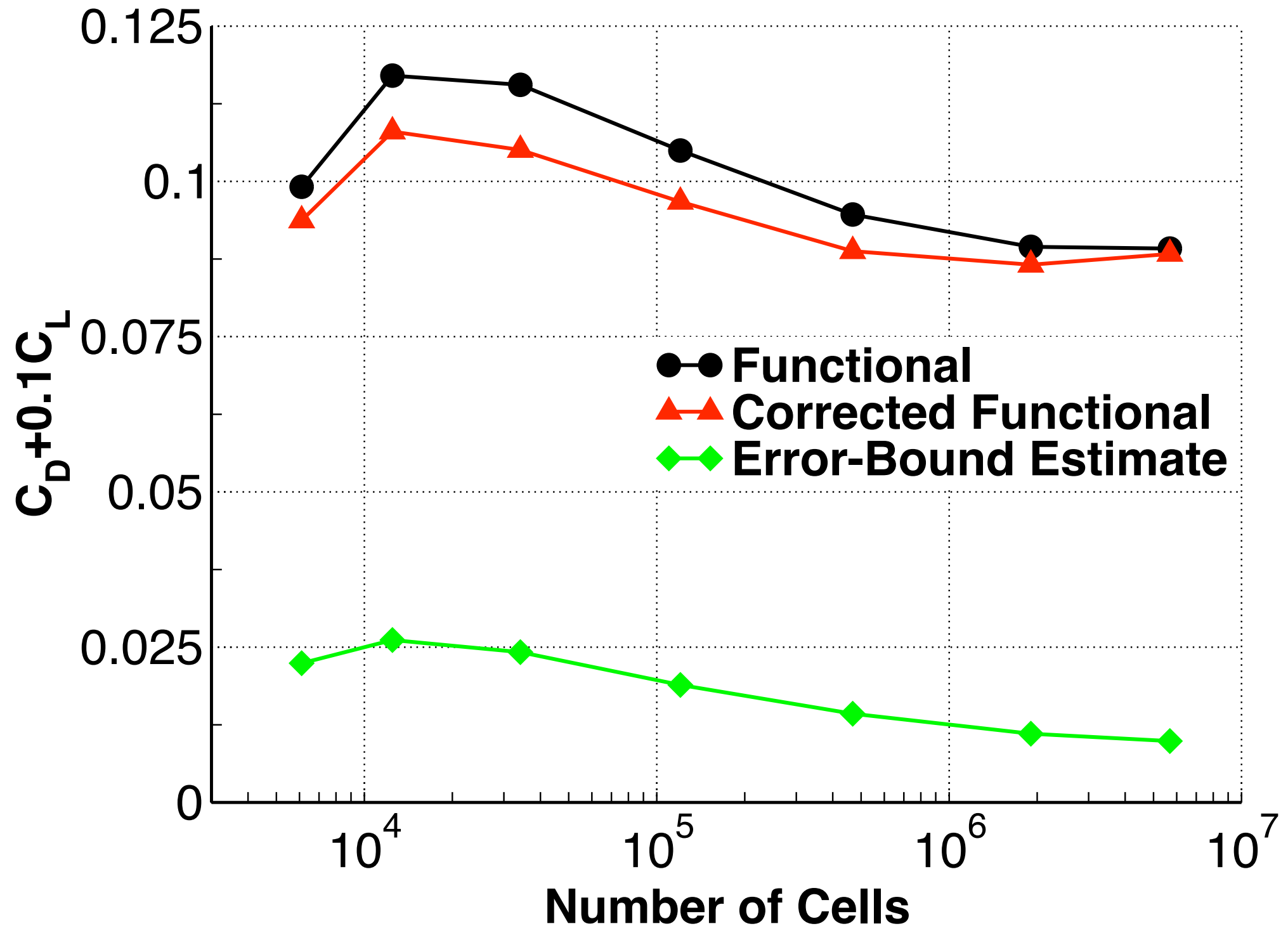


Transport Aircraft

- Transonic flow: $M_\infty = 0.8$, $\alpha = 2^\circ$
- Functional: $C_D + 0.1C_L$
- Initial mesh ~6k cells
- Final mesh ~5.7M cells (6 adaptations)



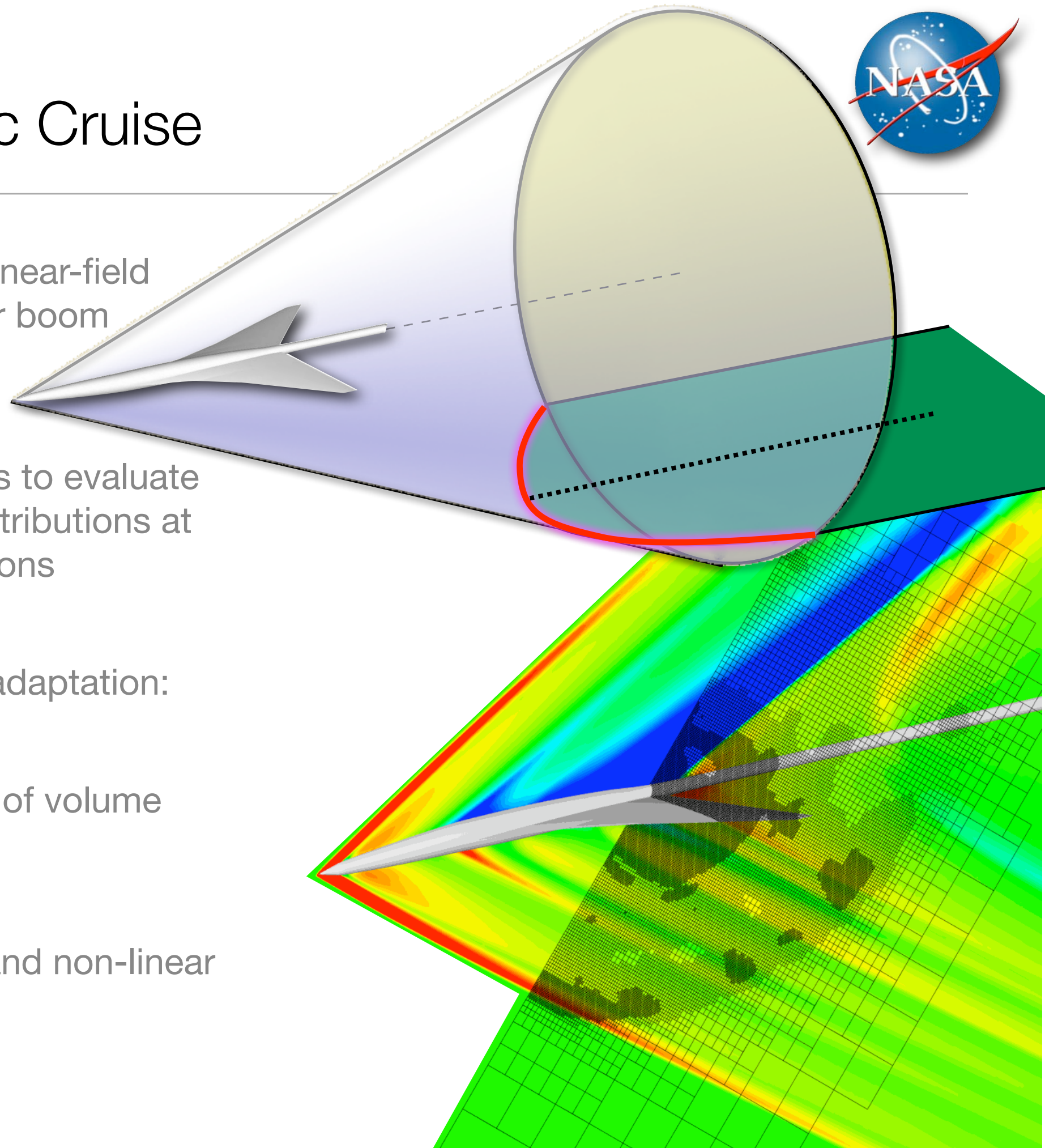
Transport Aircraft Functional Convergence





Quiet Supersonic Cruise

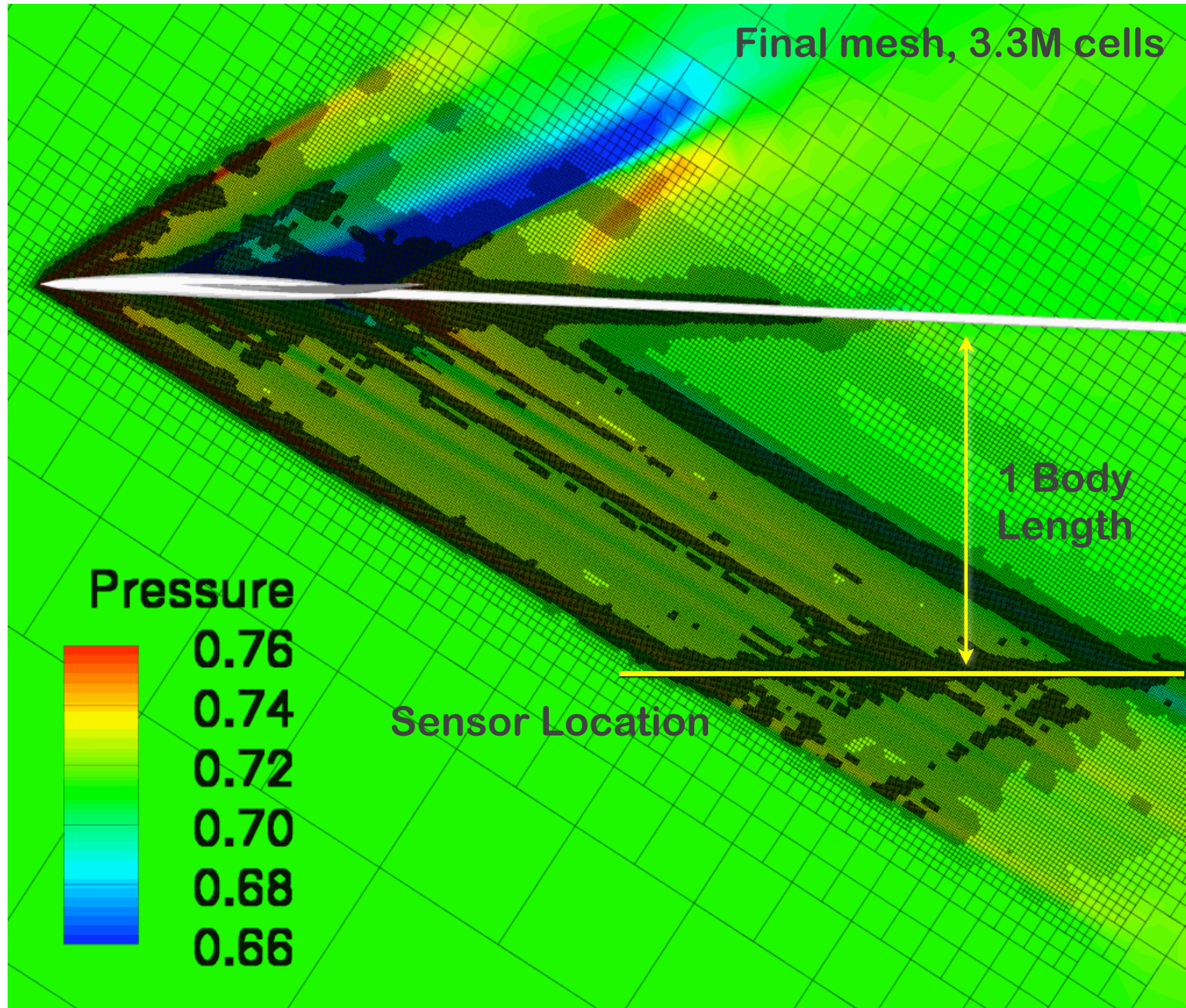
- Goal is determination of near-field pressure distributions for boom prediction (“N”-waves)
- Use adjoint error analysis to evaluate accuracy of pressure distributions at specified “sensor” locations
- Ideal problem for mesh adaptation:
 - ★ Extensive refinement of volume mesh
 - ★ Many length-scales and non-linear flow features





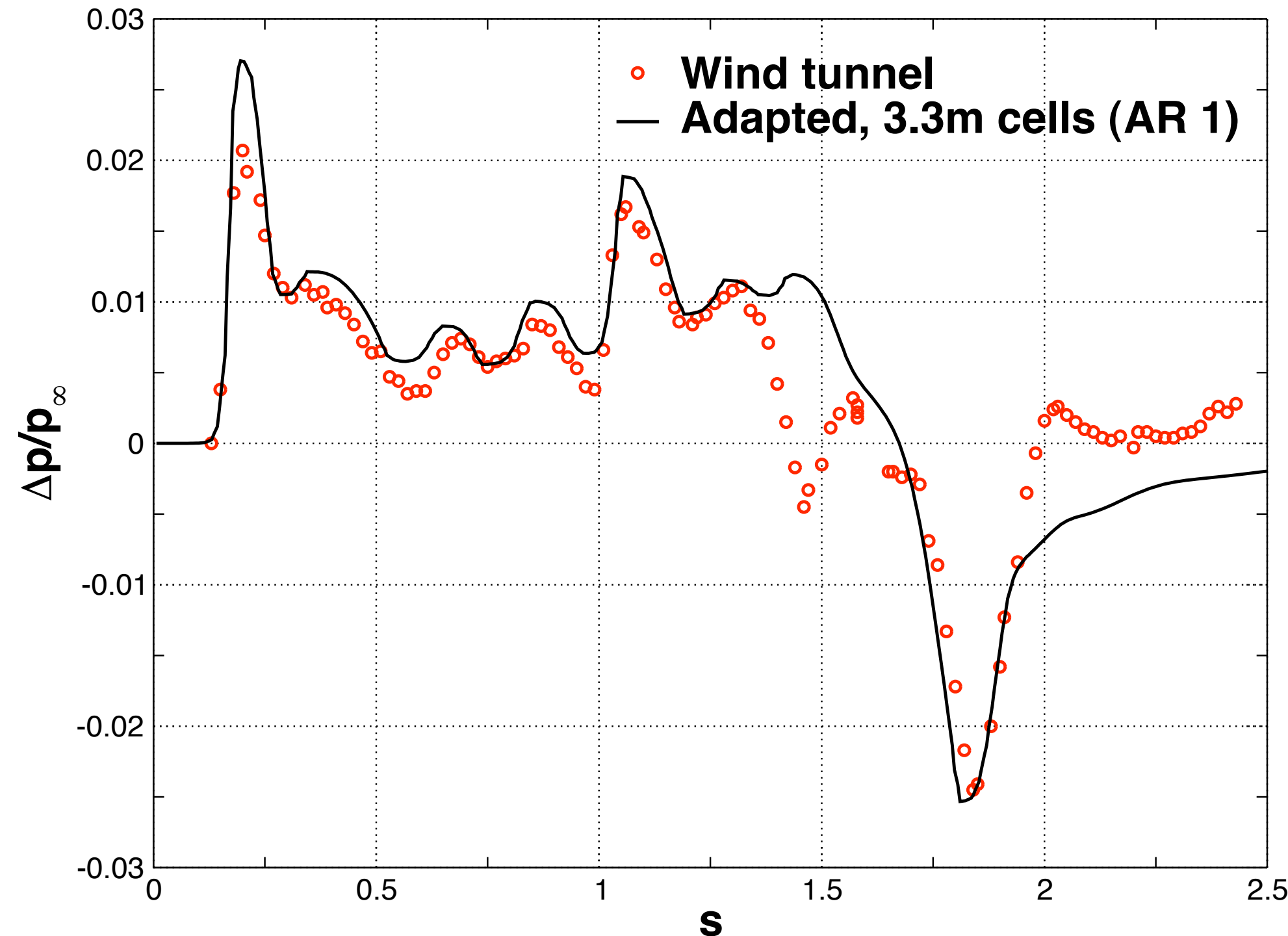
SLSLE Low-Boom Configuration

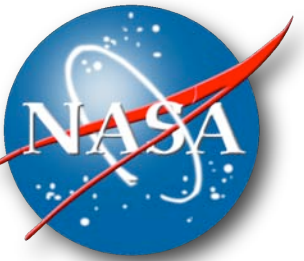
- $M_\infty = 2.0, \alpha = 2.03^\circ$
- Rotate mesh to freestream Mach angle to improve wave propagation to sensor
- Stretch initial mesh along freestream Mach angle (not shown)





SLSLE Pressure Signature





Results

Focus on practical cases

Part A. Classic examples

1. Typical Launch Abort Vehicle database
2. Parametric studies of Launch Vehicles
3. Transport Aircraft
4. Quiet Supersonic Cruise

Part B. Most recent (preliminary) work on cases with jets

1. Axial Flow Jet
2. Nozzle-Guide-Vane Missile
3. Launch Abort Vehicle with Abort Control Motor Jets



Axial Flow Jet - Problem Setup

- Initial Mesh: ~17k cells

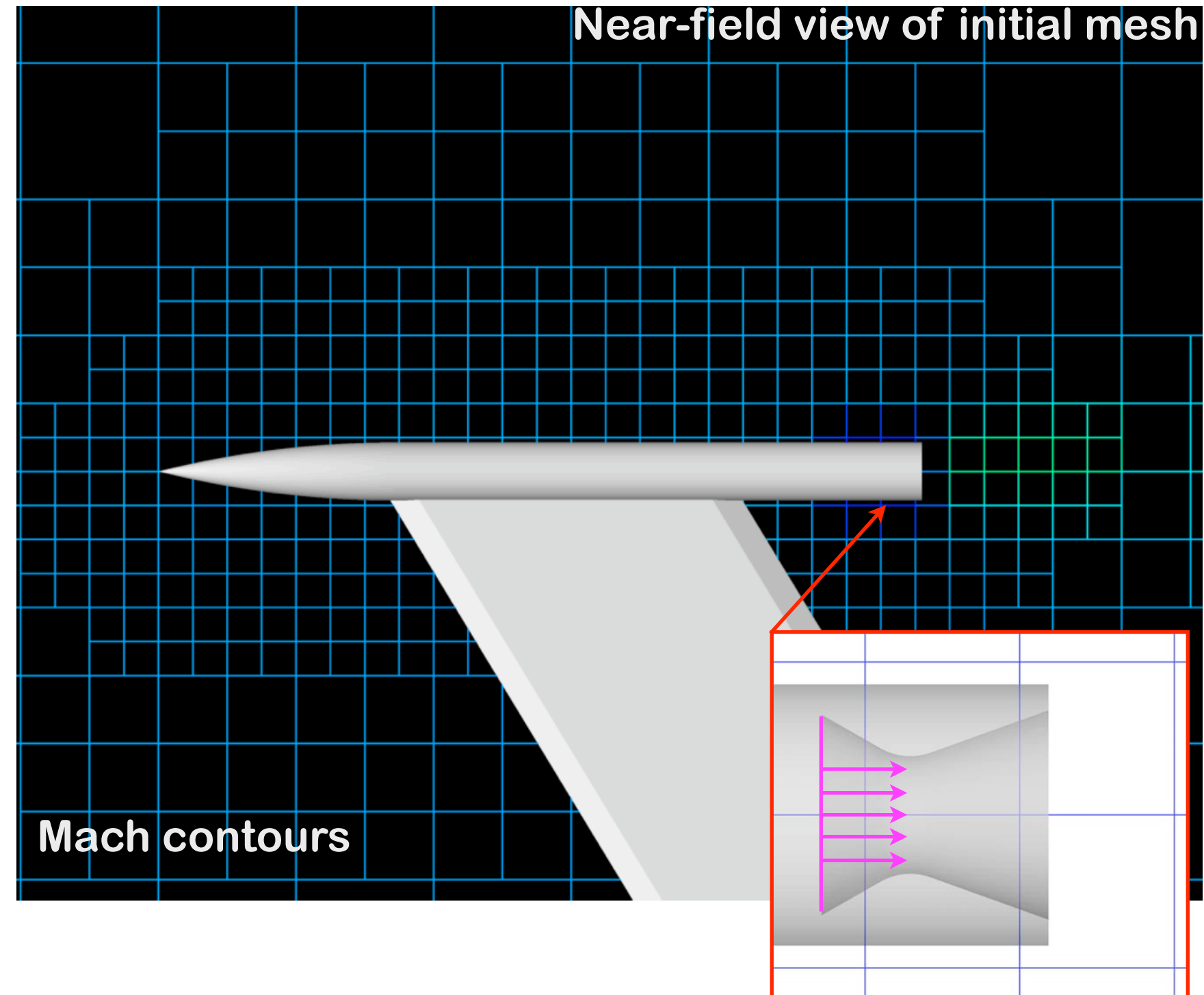
- Functional: C_A

$$M_\infty = 0.9$$

$$M_{Jet} = 2.7$$

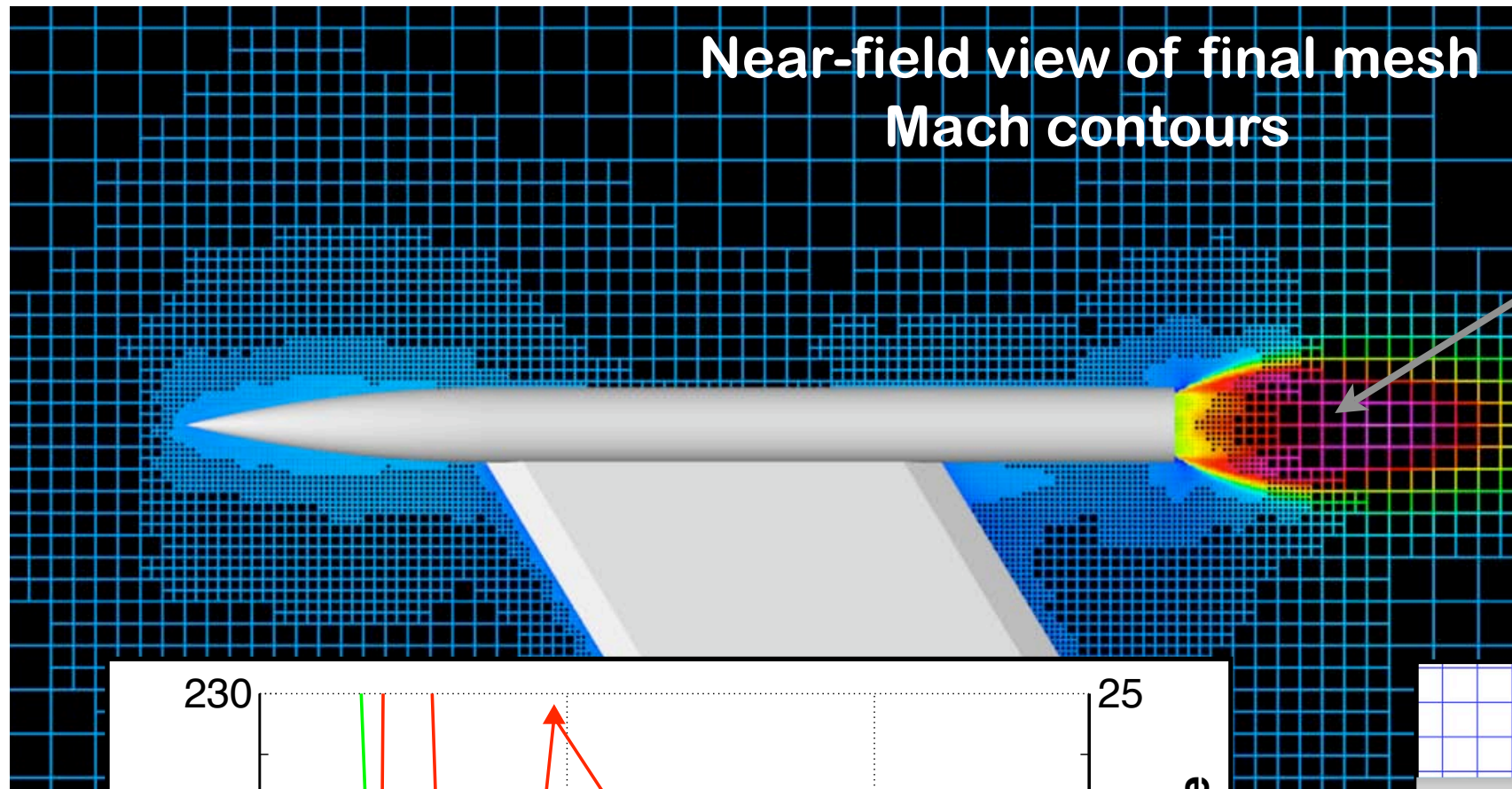
$$P_{Plen.}/P_\infty = 88$$

- Power boundary conditions applied at plenum face

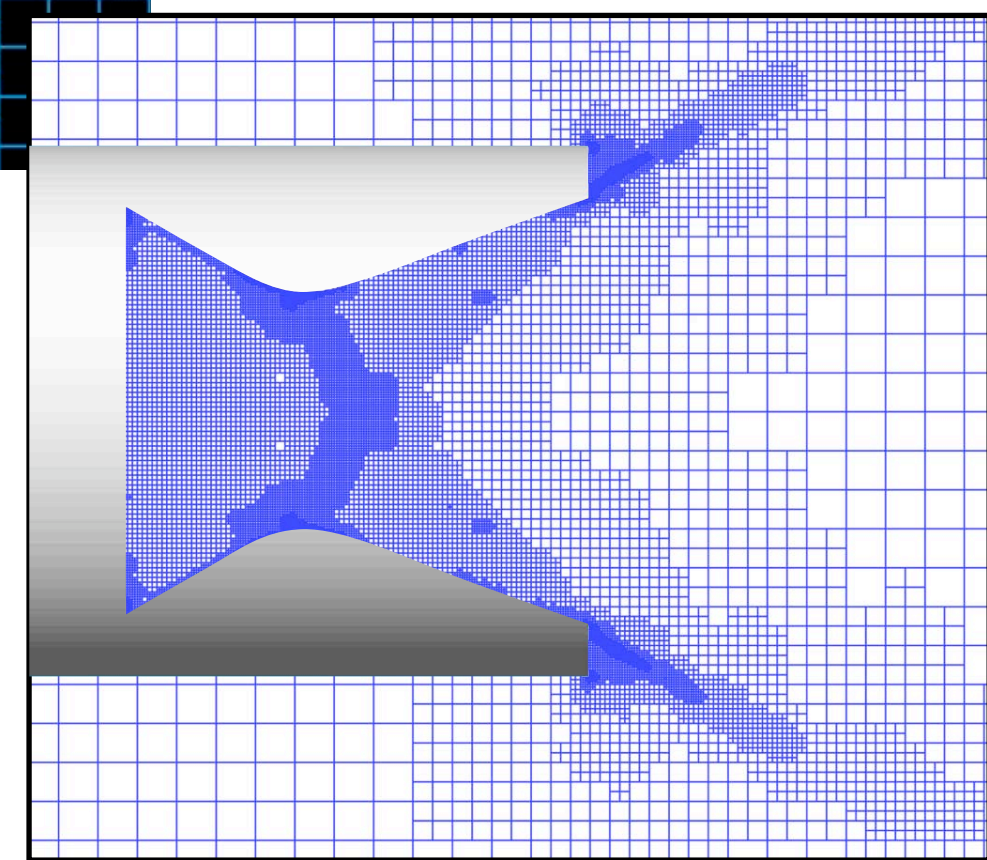
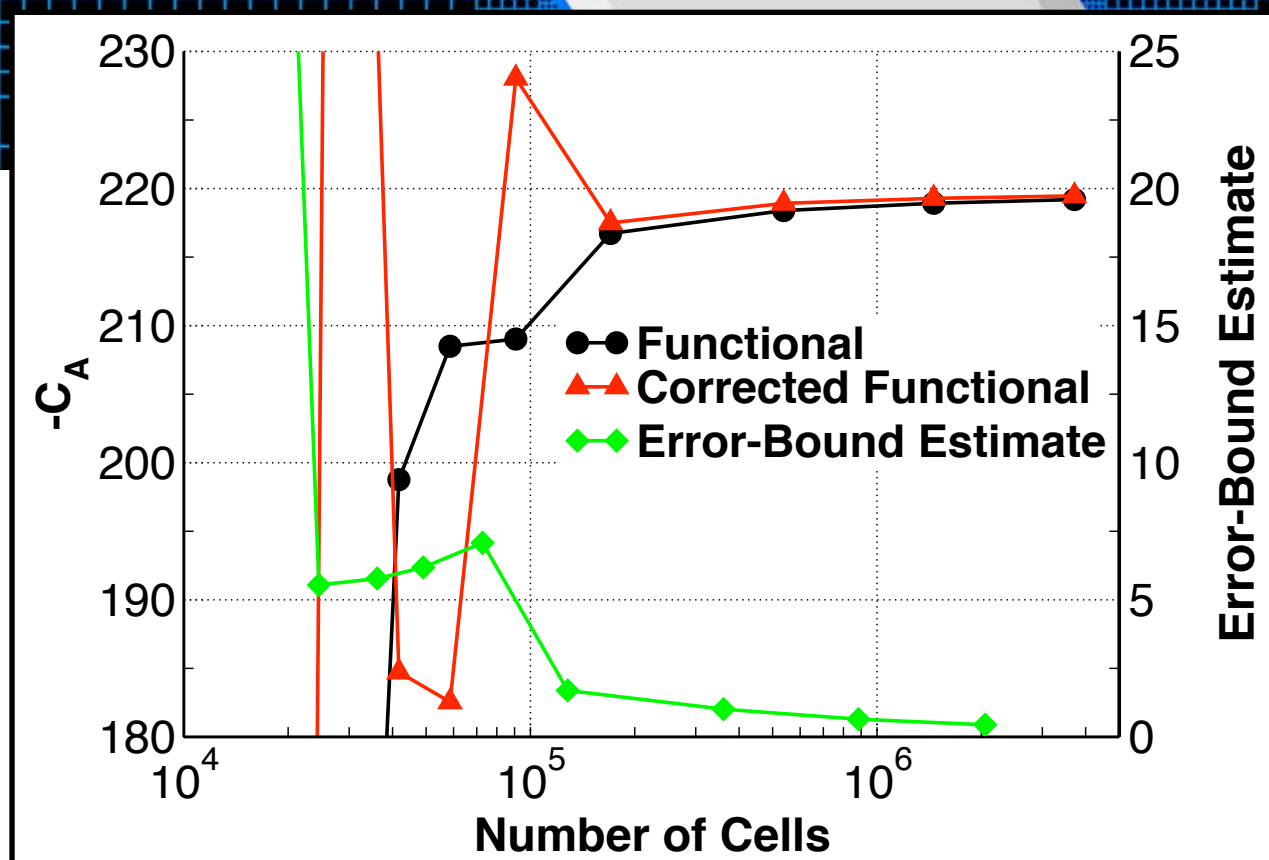




Final Mesh (Functional C_A , TOL=0.5%)



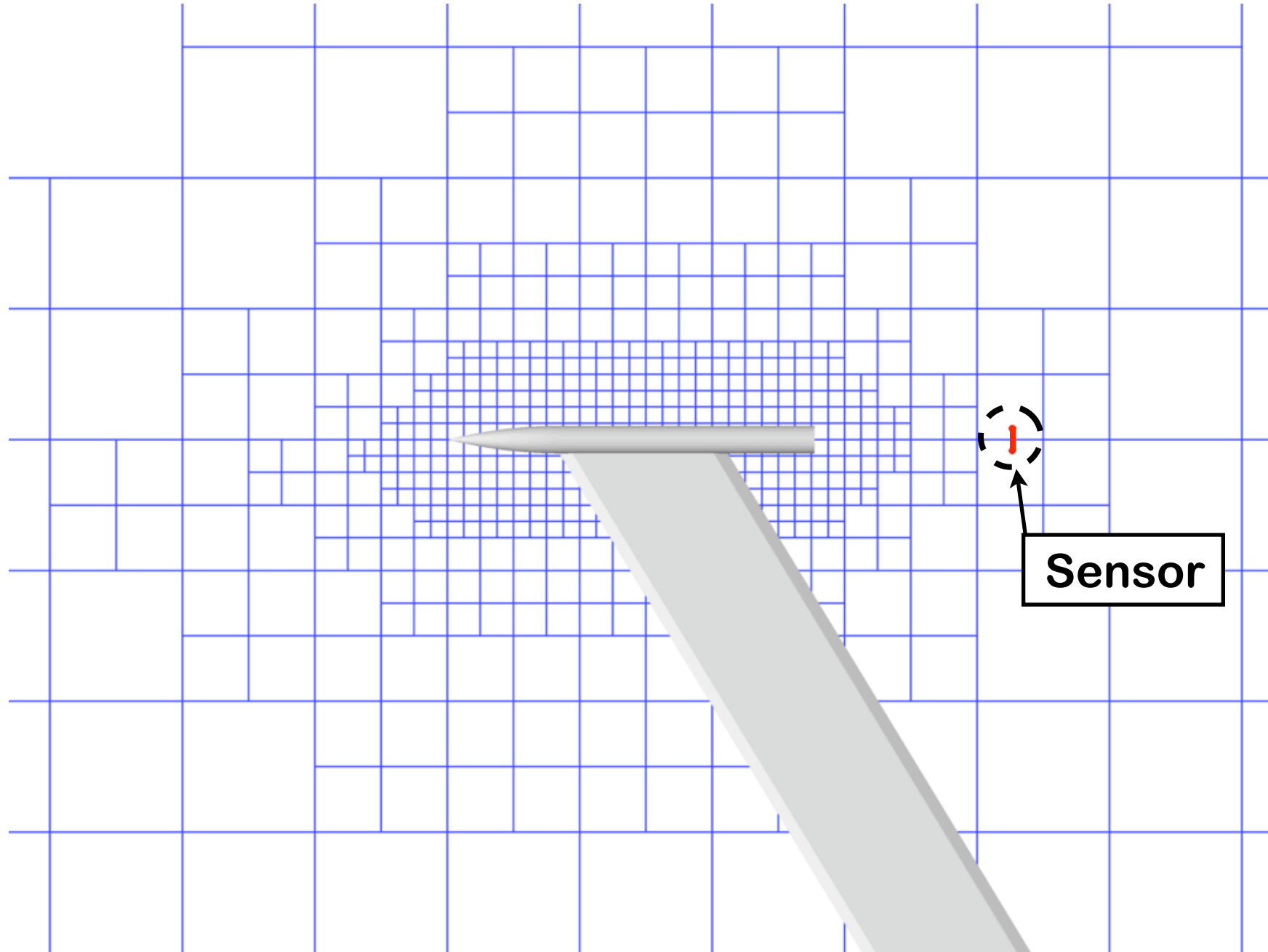
Note rapid coarsening of mesh due to small influence of discretization errors on axial force





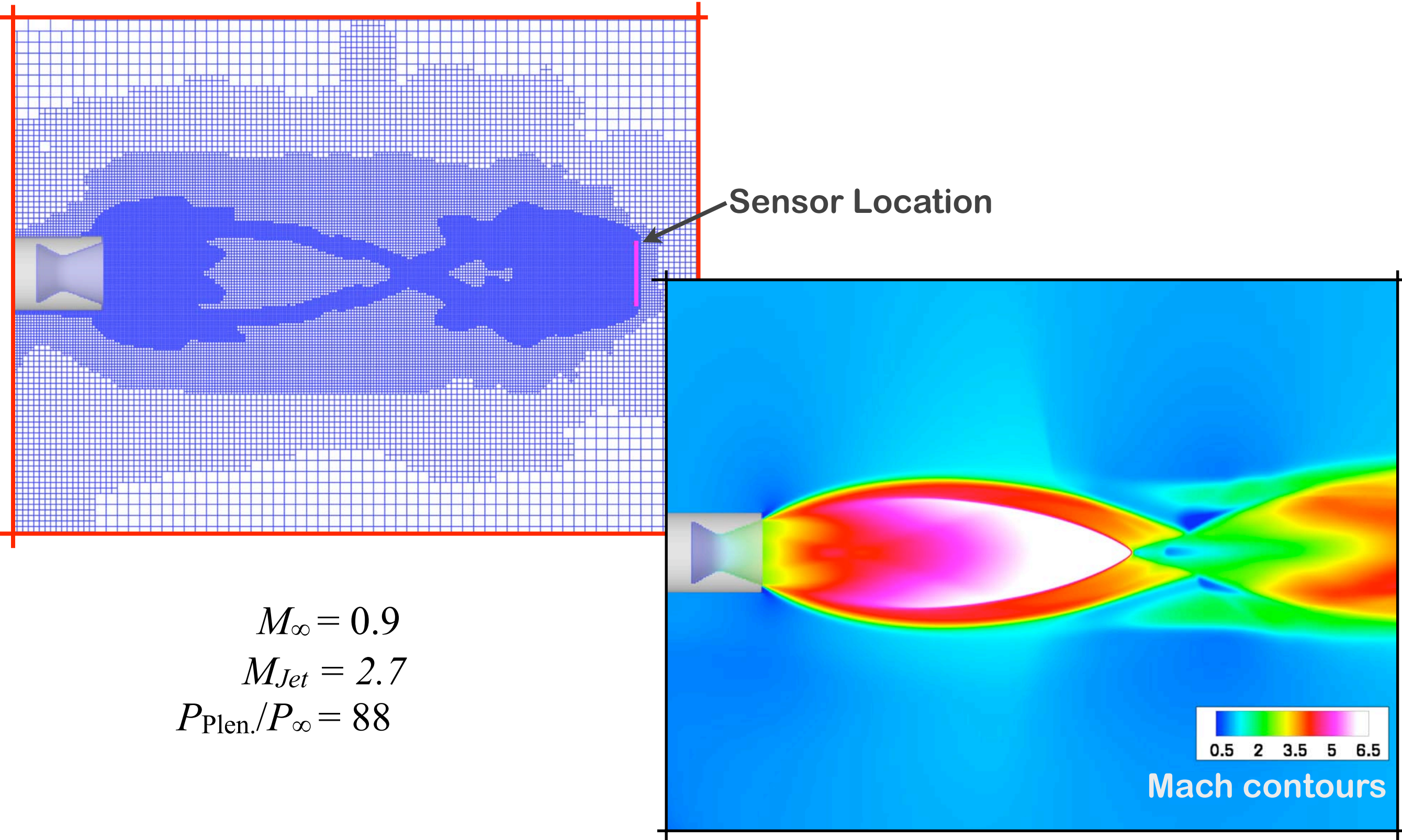
Axial Flow Jet - Field Functional

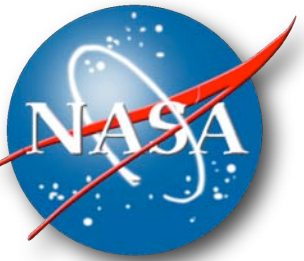
- Example case to demonstrate field functional capability
- Use integral of pressure along a fictitious line sensor to obtain accurate solution in nozzle plume
- Coarse initial mesh (~17k cells)
- Transonic flow conditions





Final Mesh (~9M cells)

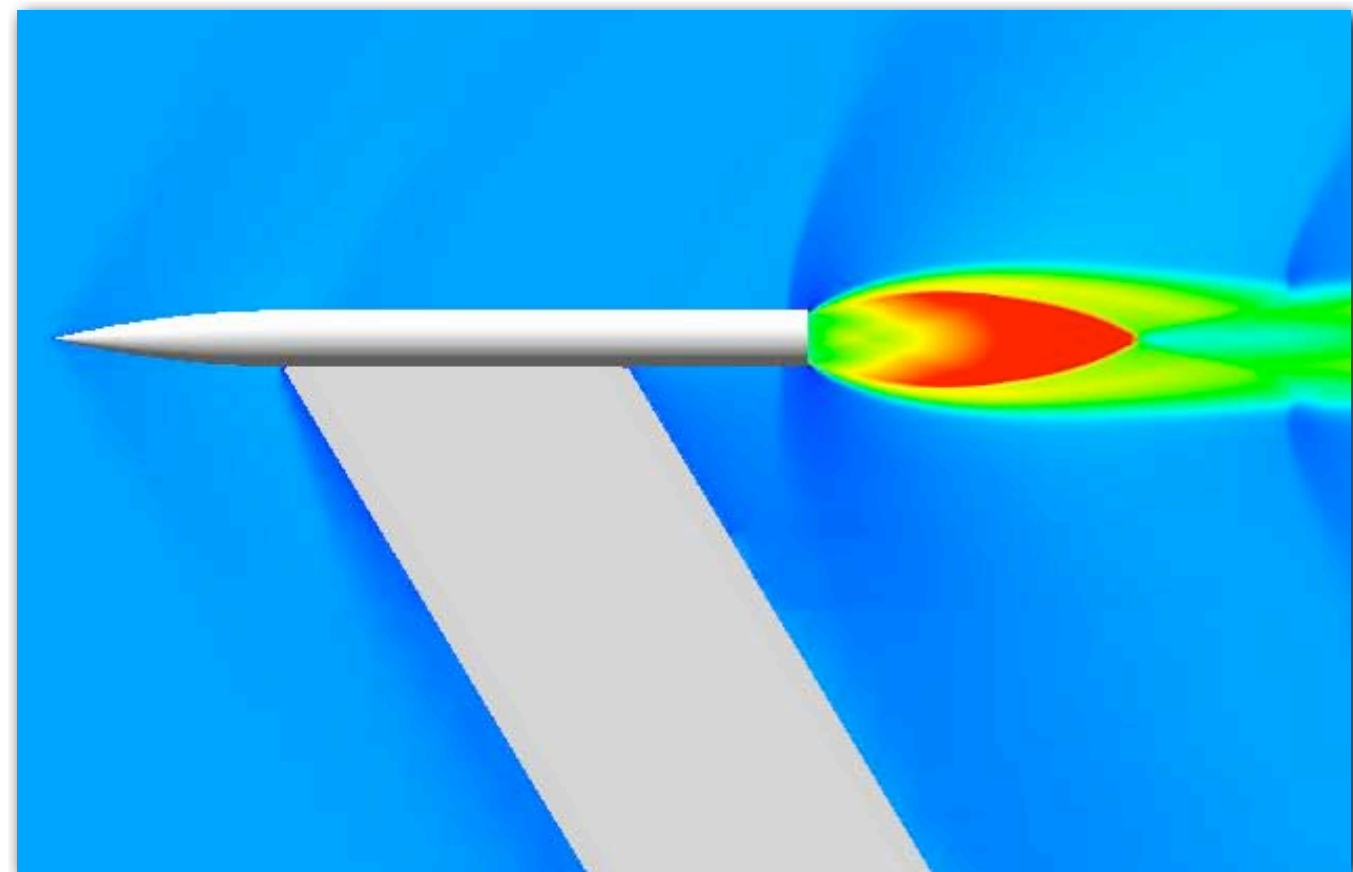




Propulsive Deceleration

- Model problem for propulsive deceleration and control jets

$$\begin{aligned} M_{\infty} &= 2.0 & \xrightarrow{\hspace{1cm}} \\ M_{Jet} &= 2.7 & \xrightarrow{\hspace{1cm}} \\ P_{Plen.}/P_{\infty} &= 88 & \xrightarrow{\hspace{1cm}} \end{aligned}$$

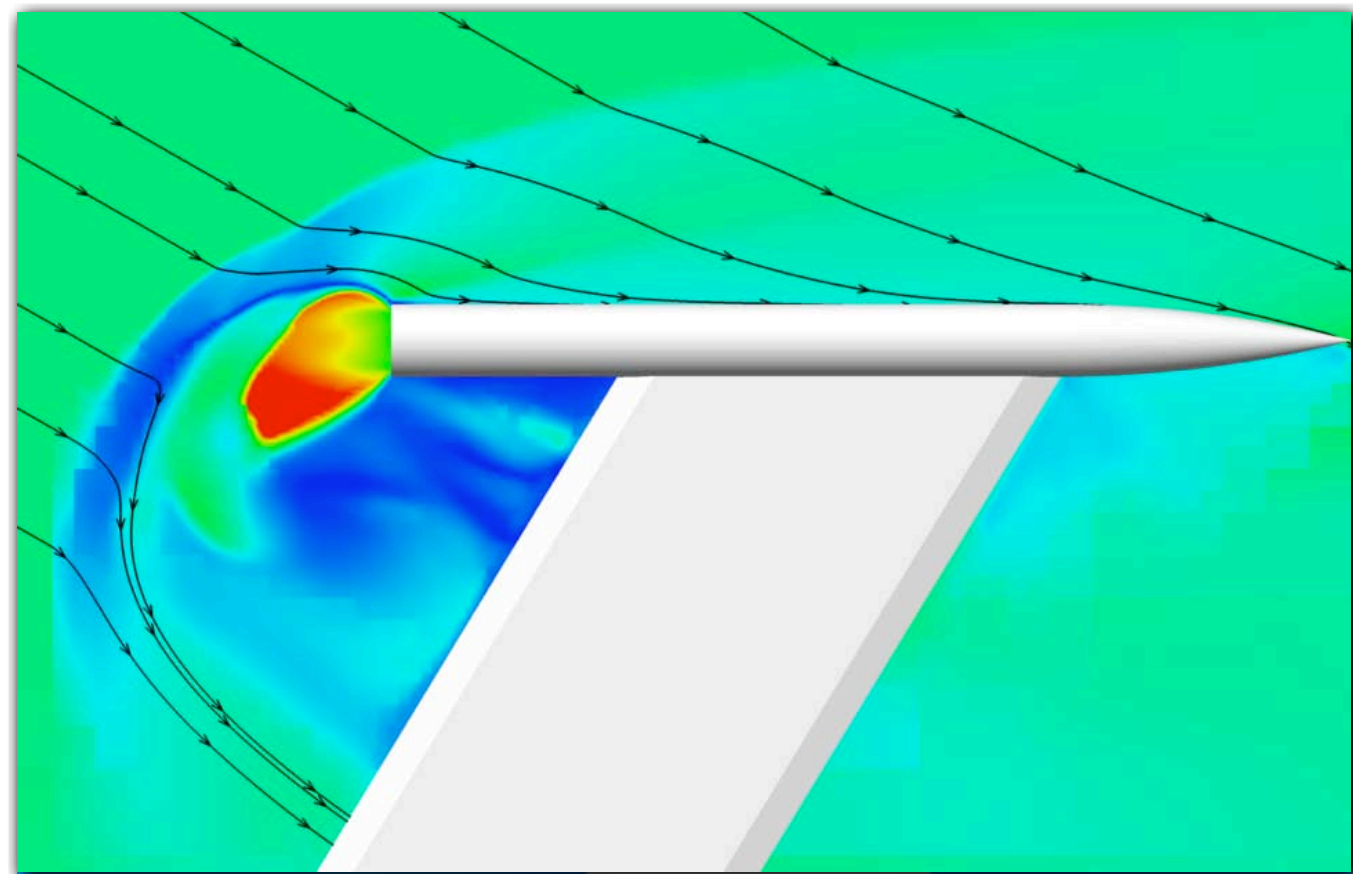




Propulsive Deceleration

- Model problem for propulsive deceleration and control jets

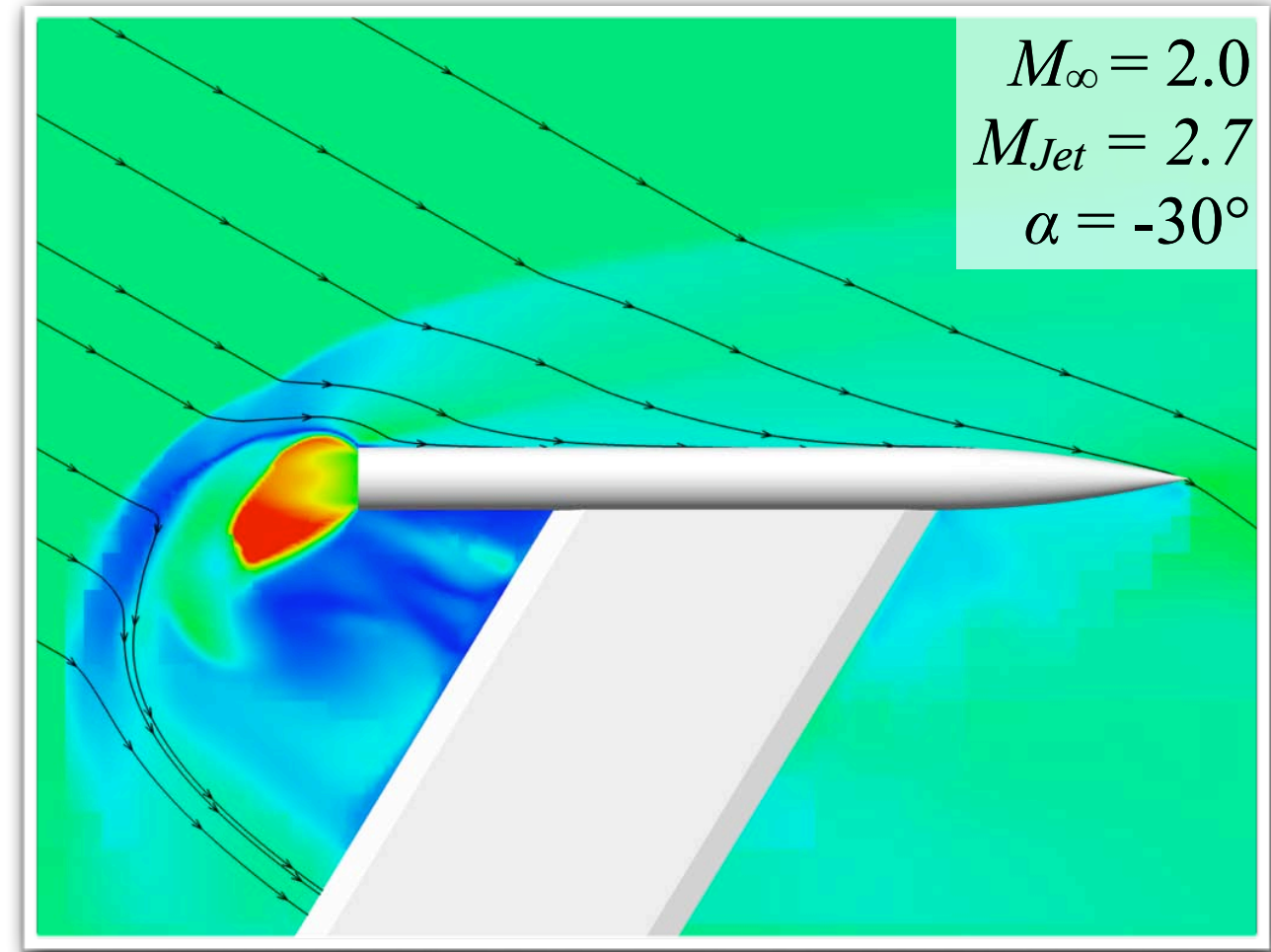
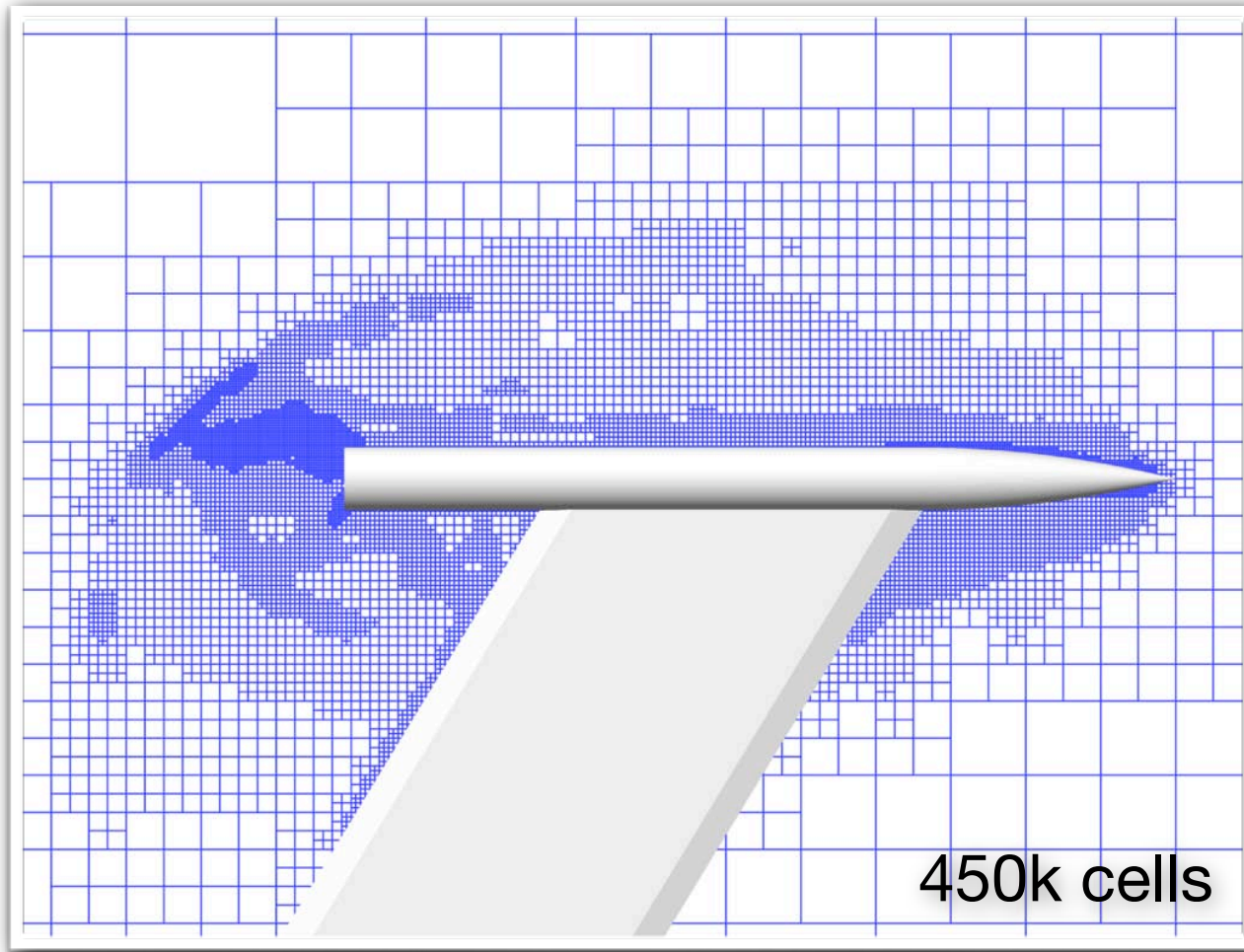
$$\begin{aligned} M_{\infty} &= 2.0 \\ M_{Jet} &= 2.7 \\ P_{Plen.}/P_{\infty} &= 88 \end{aligned}$$





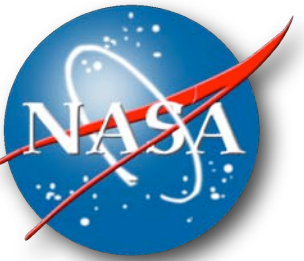
Propulsive Deceleration

- Model problem for propulsive deceleration and control jets

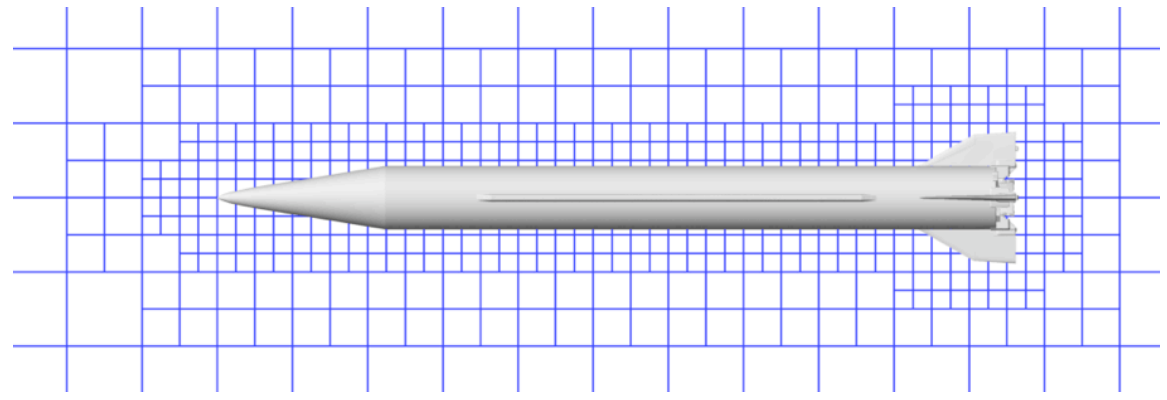


NGV Missile

Functional: Axial force

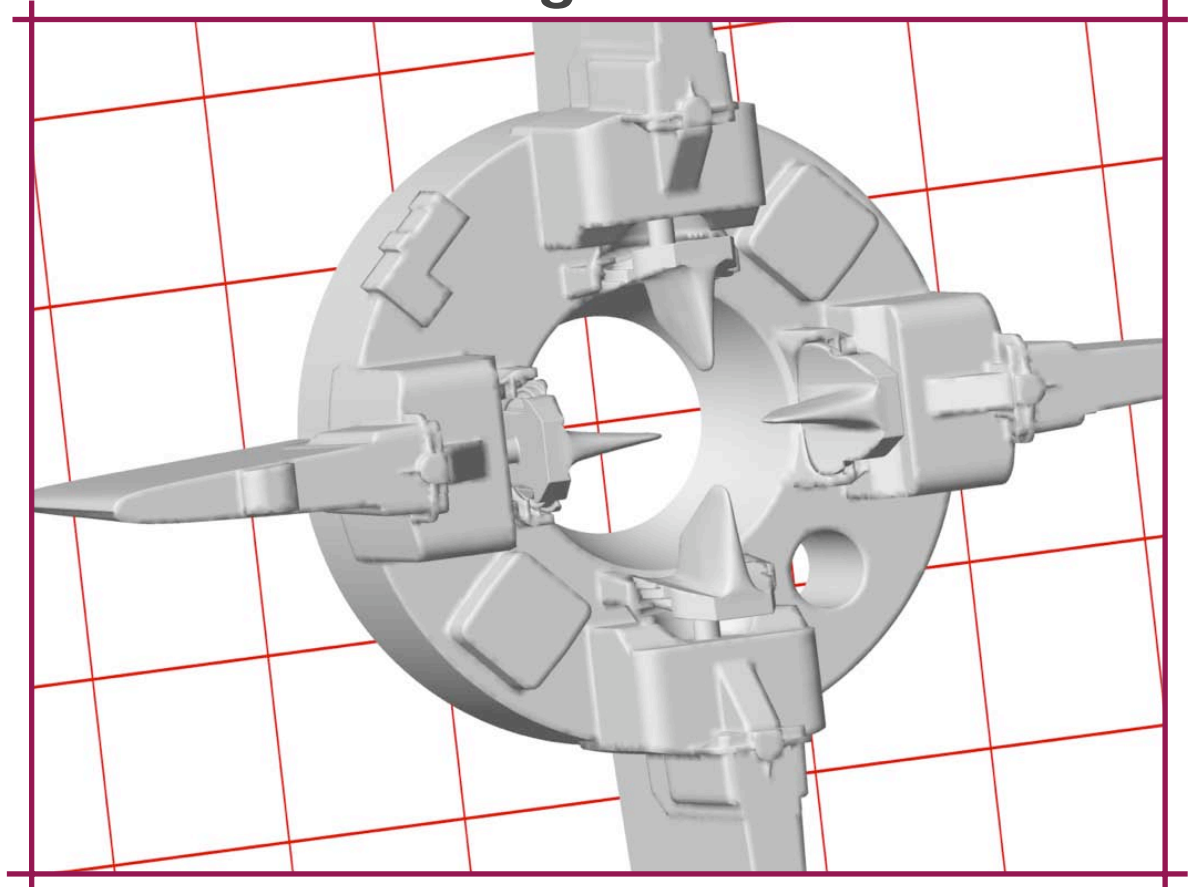


- Initial mesh: ~5k cells
- Supersonic flow: $M_\infty = 2$, $\alpha = 0^\circ$
- Power boundary conditions applied at plenum face

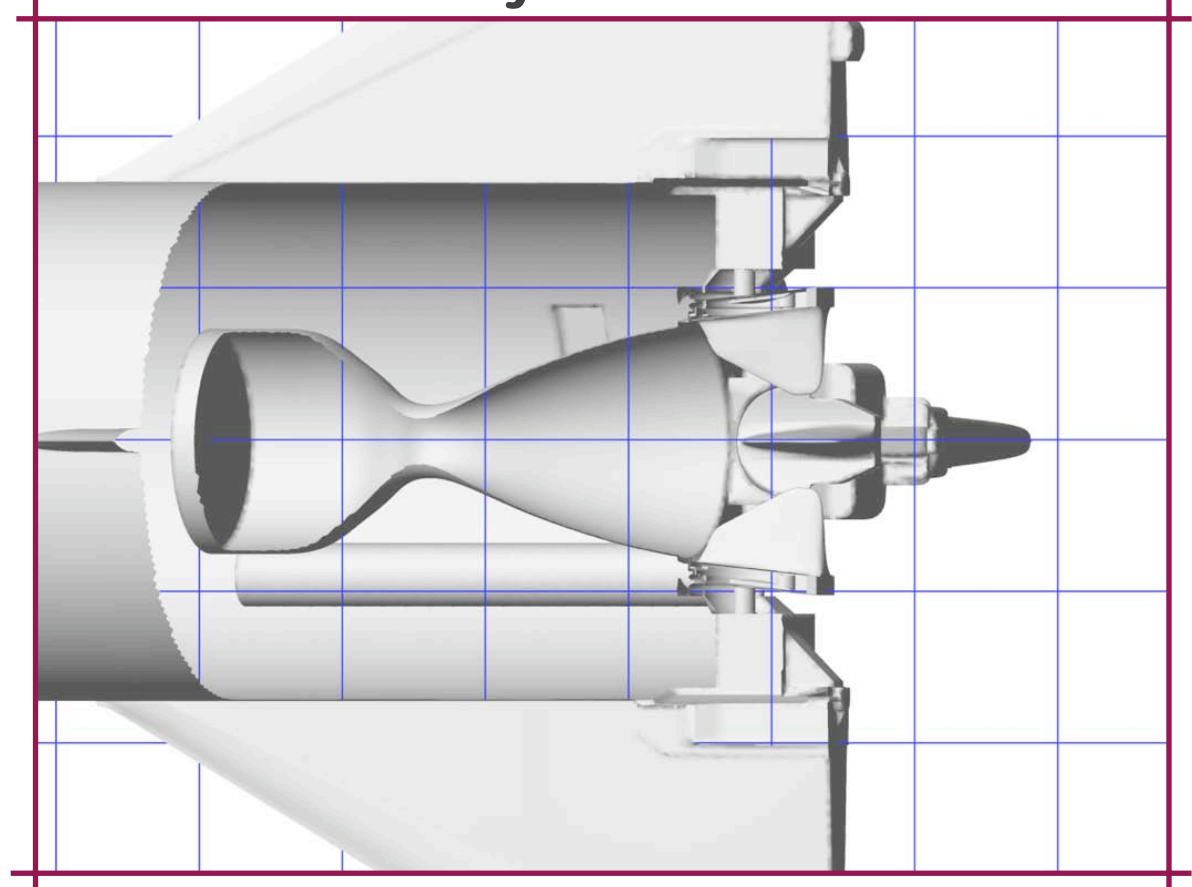


Near-body view of initial mesh

Fins and nozzle guide vanes



Nozzle cutaway

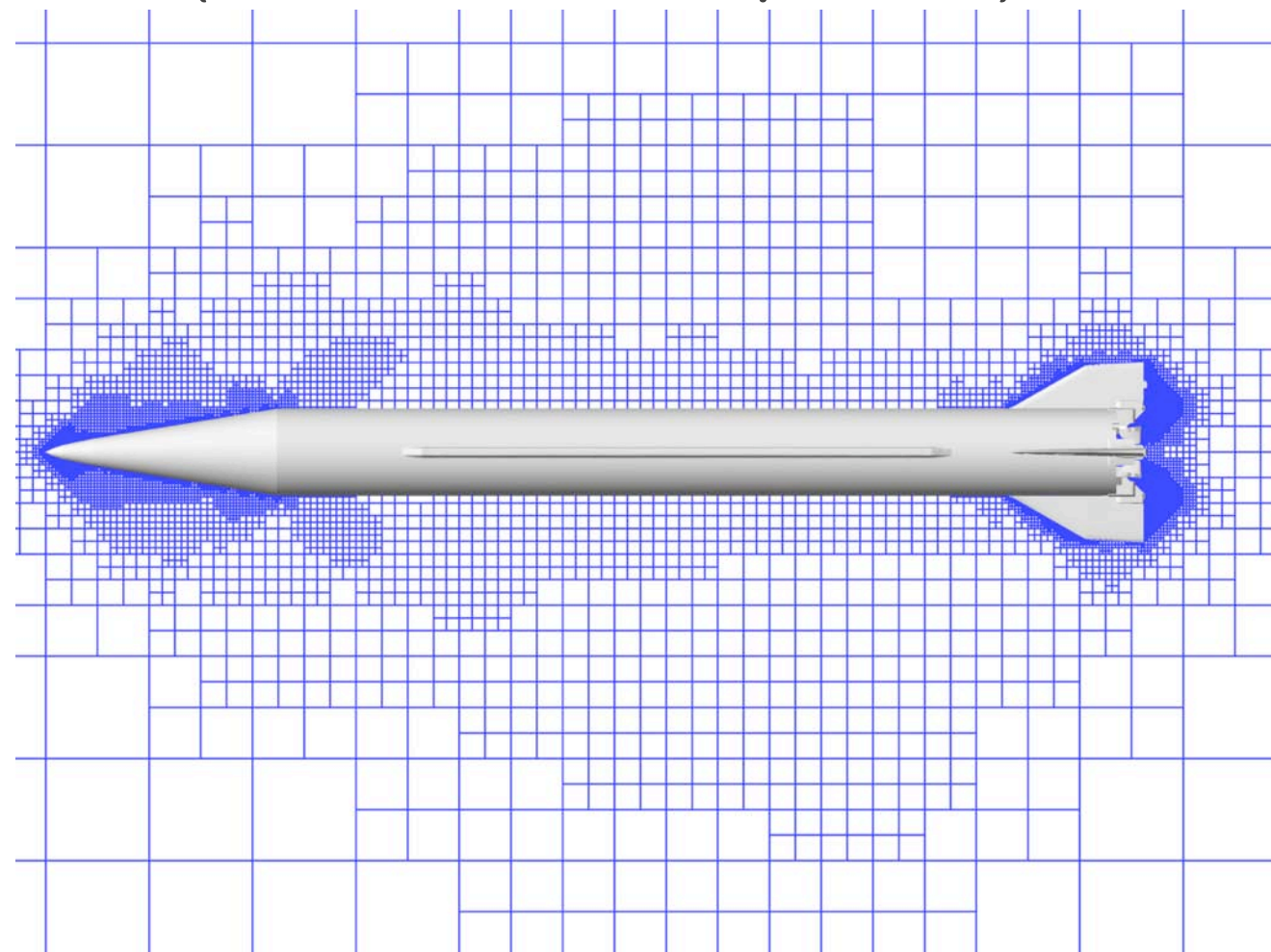


NGV Missile

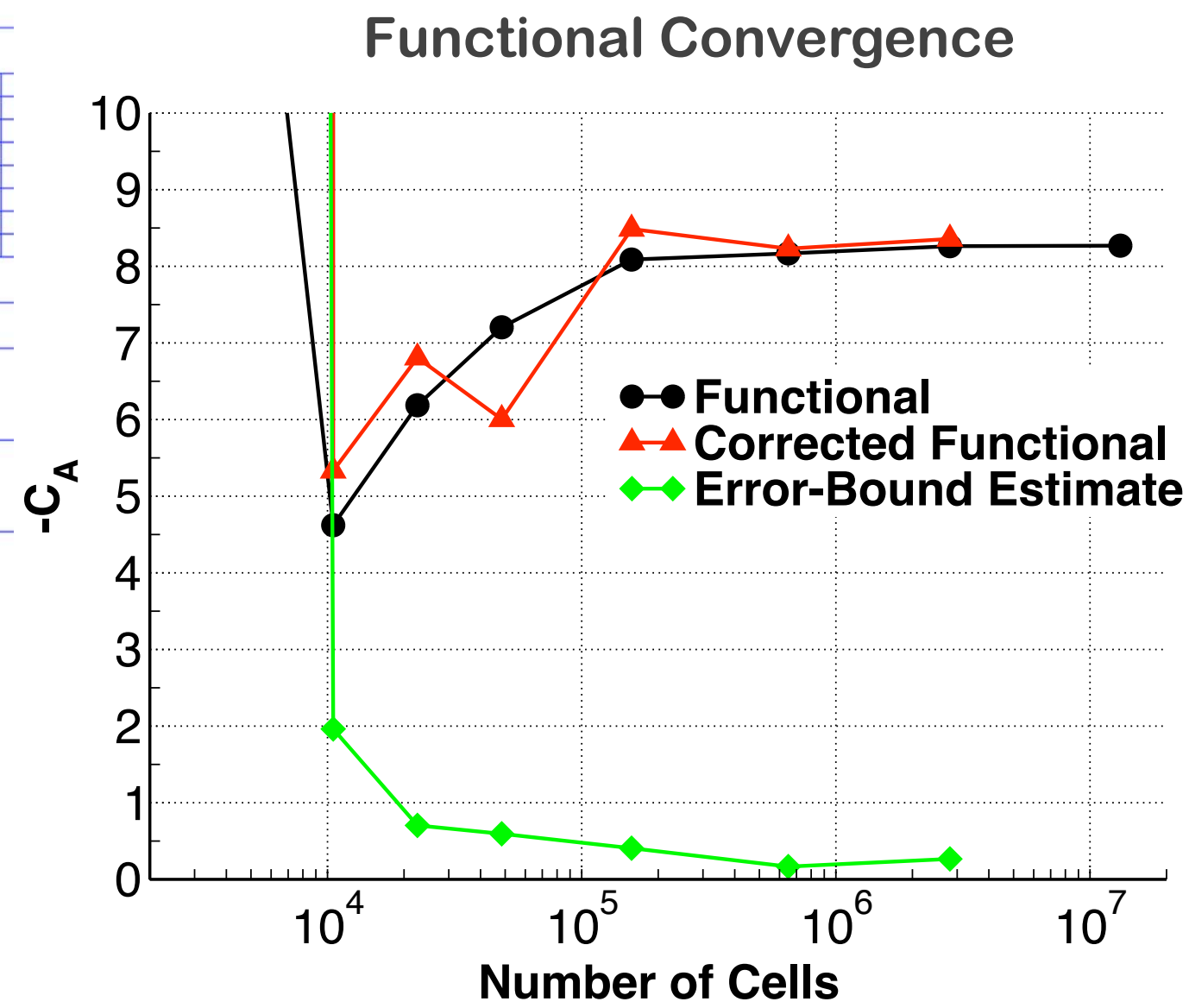
Functional: Axial force



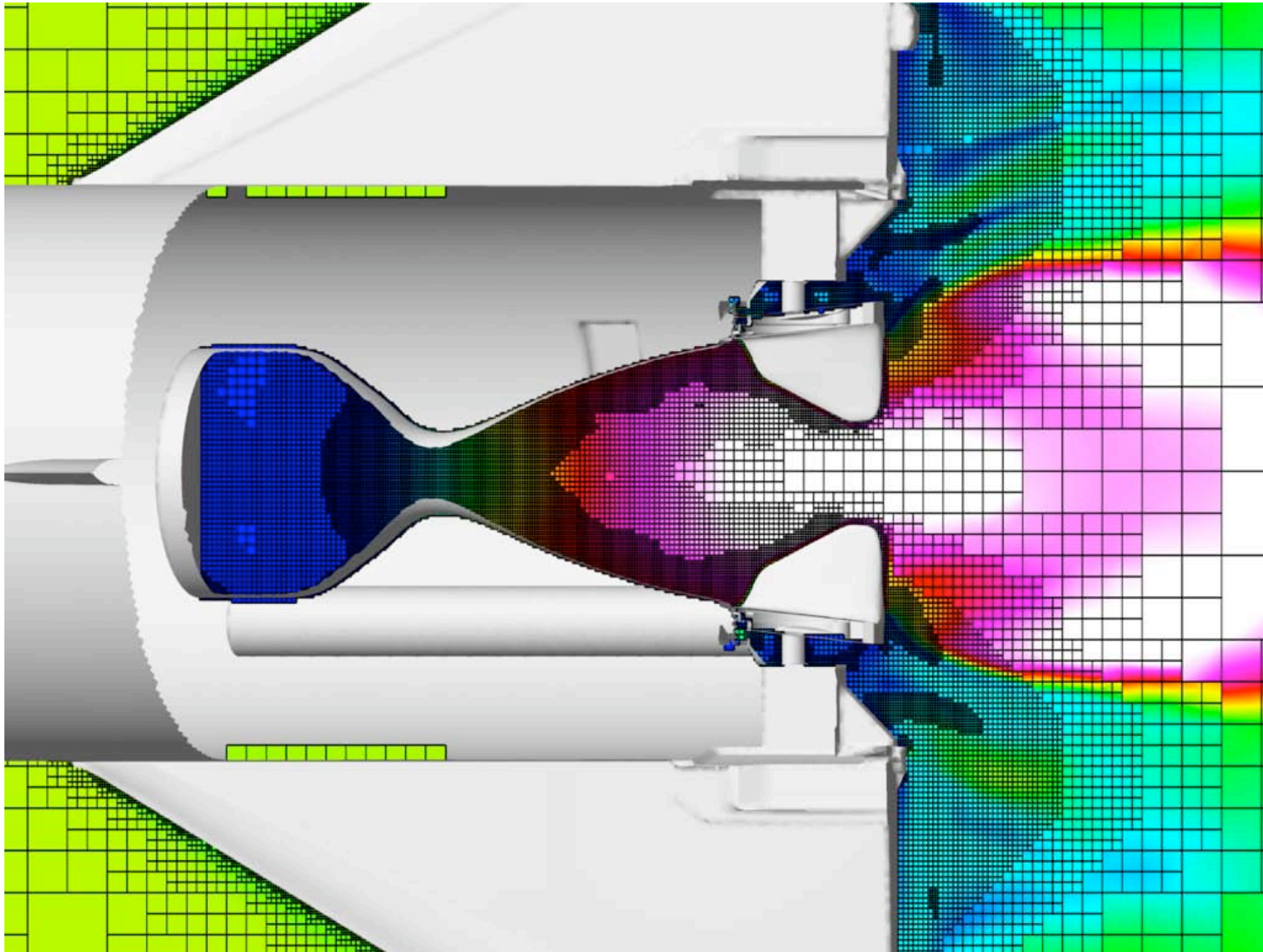
Near-body view of final mesh
(~ 2.7M cells, 6 adaptations)



$M_\infty = 2, \alpha = 0^\circ$

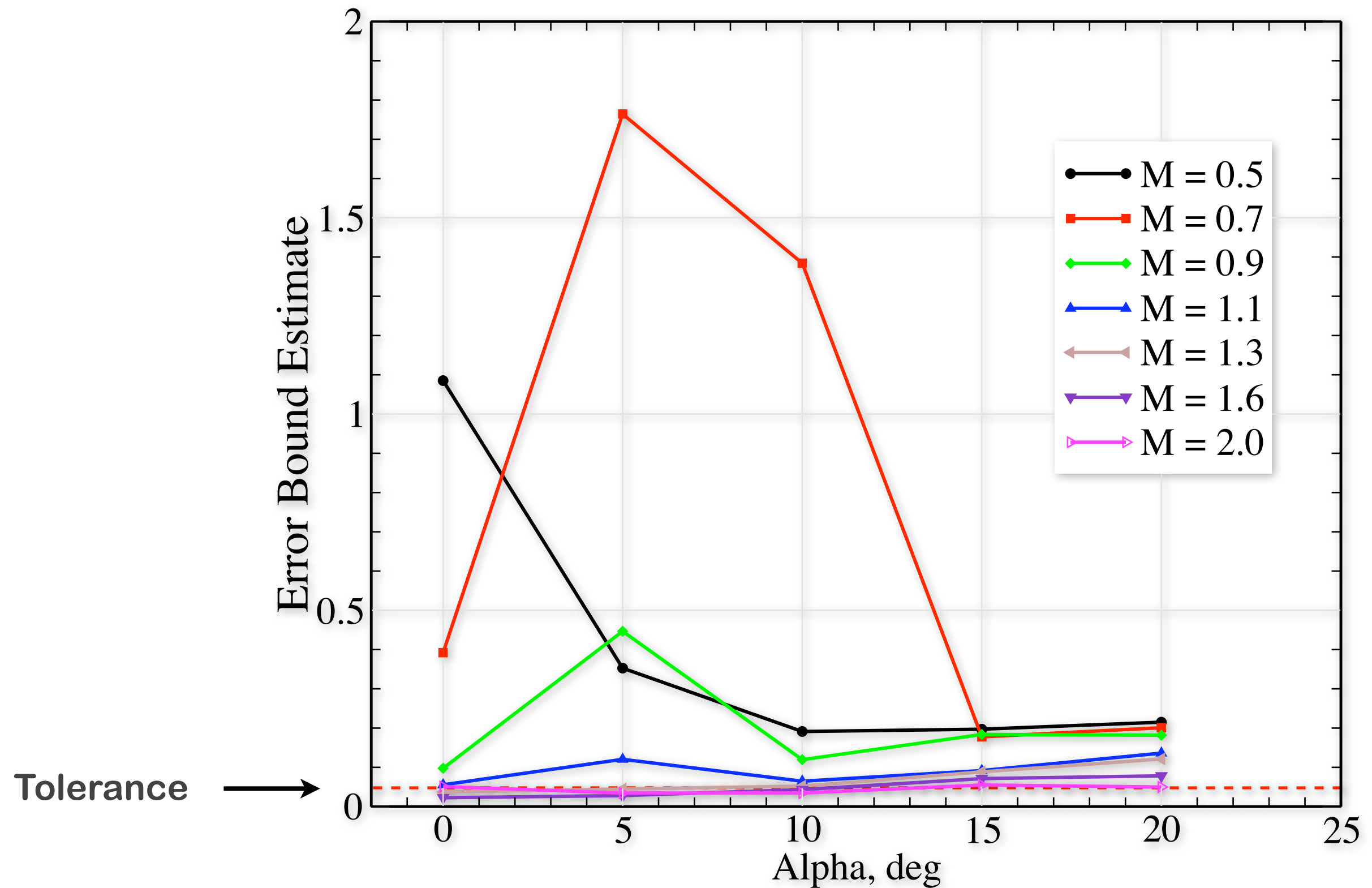


NGV Missile Nozzle cutaway (6 adaptations, Mach contours)



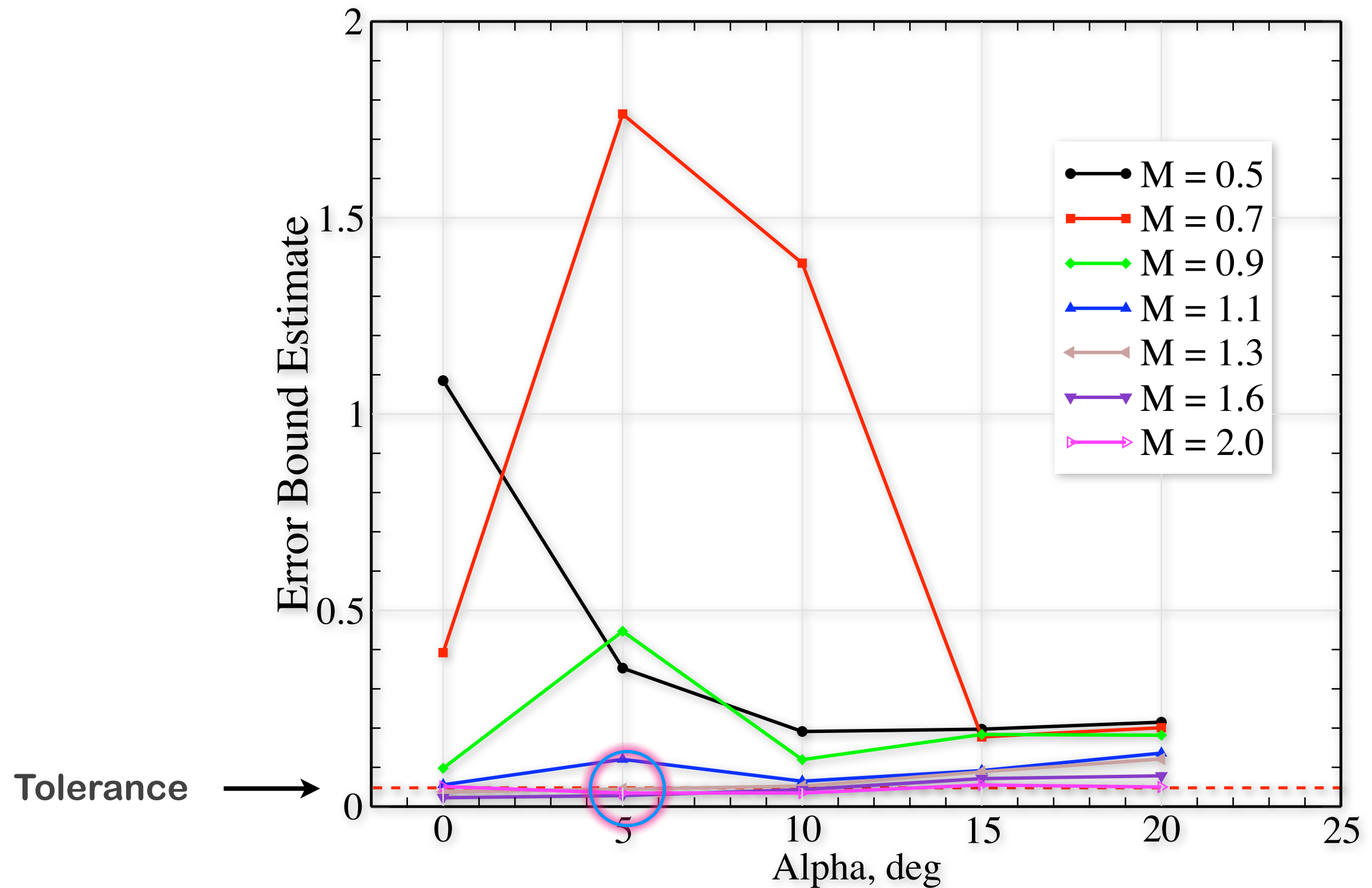


Error Controlled Database



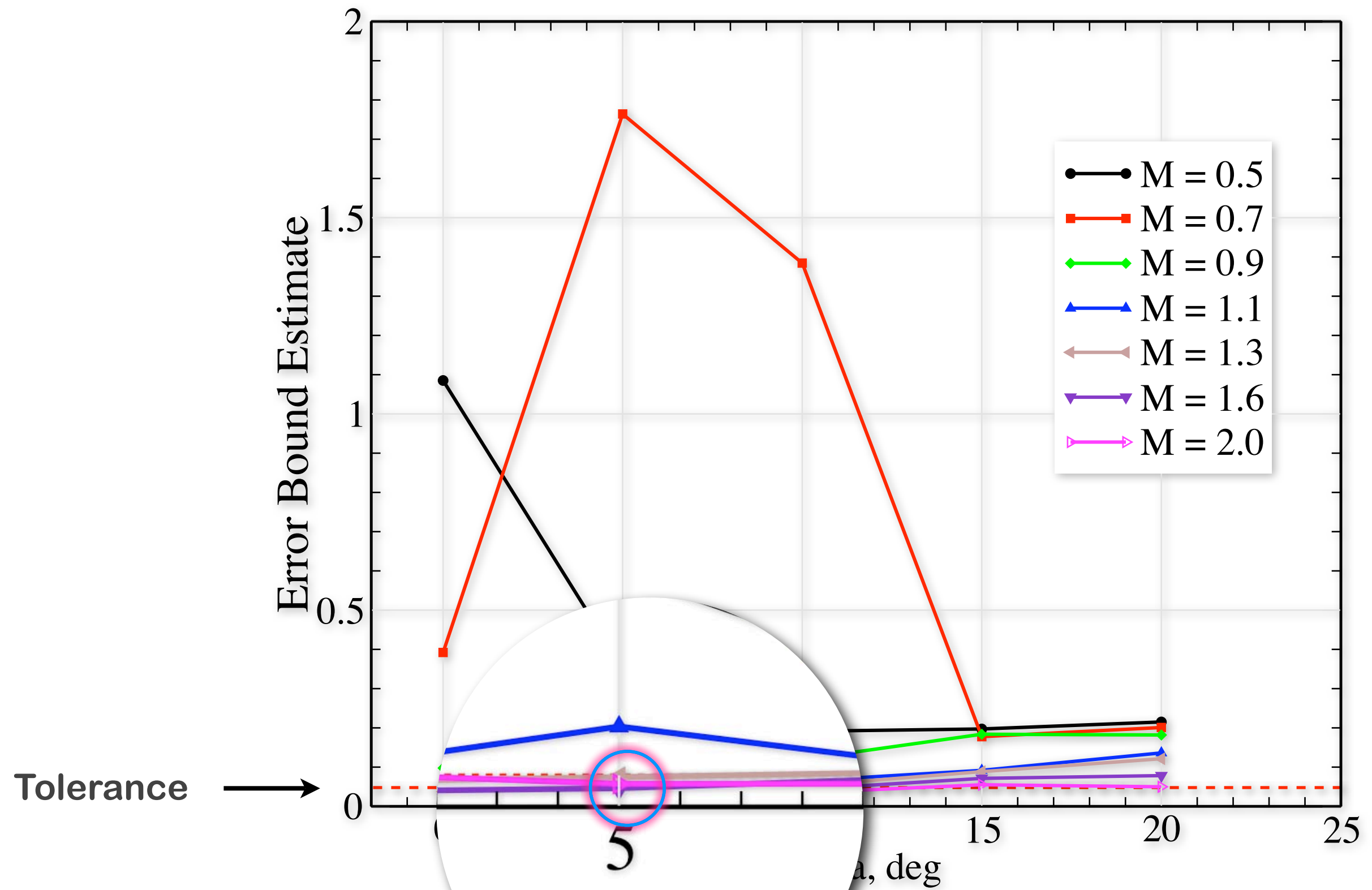


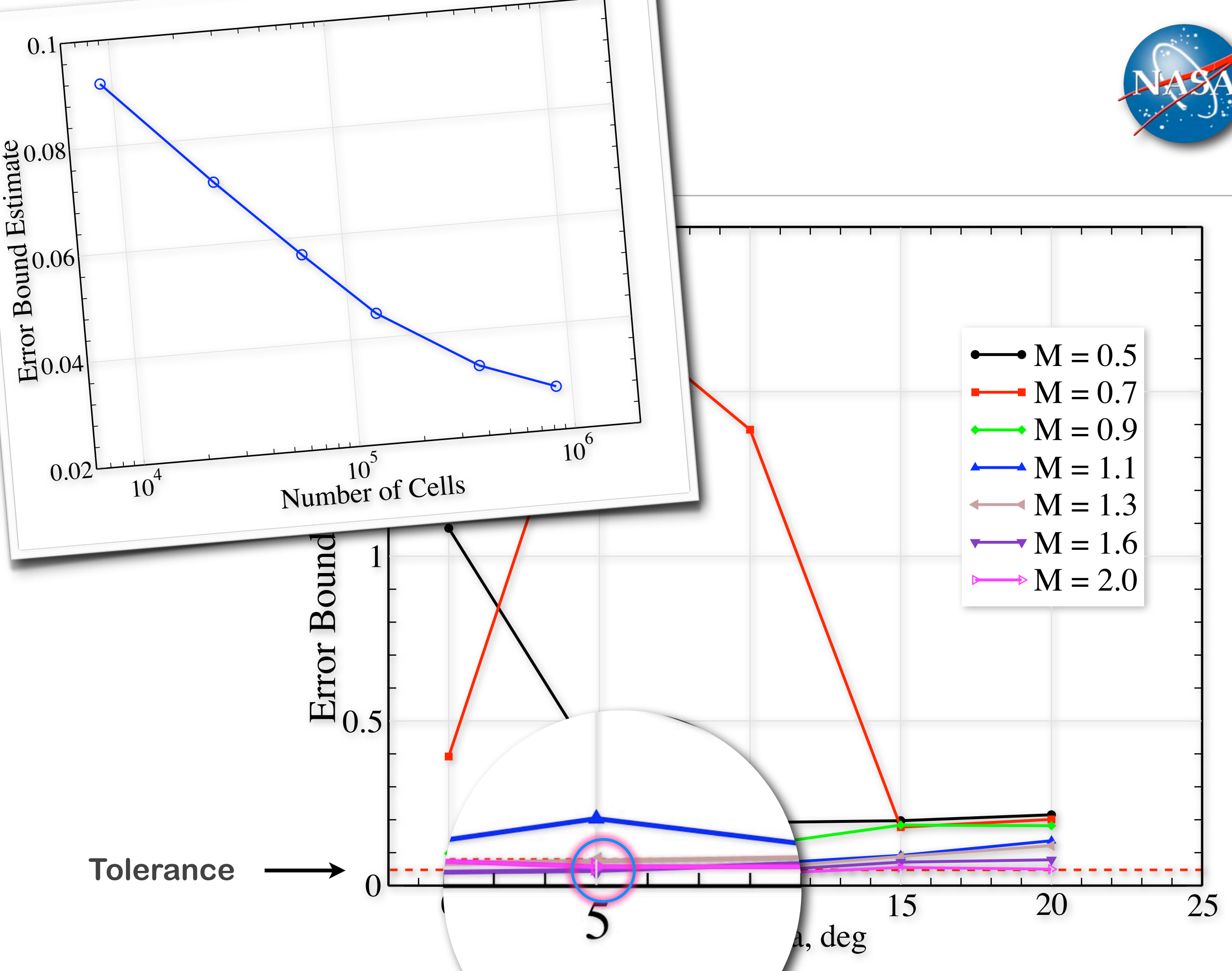
Error Controlled Database

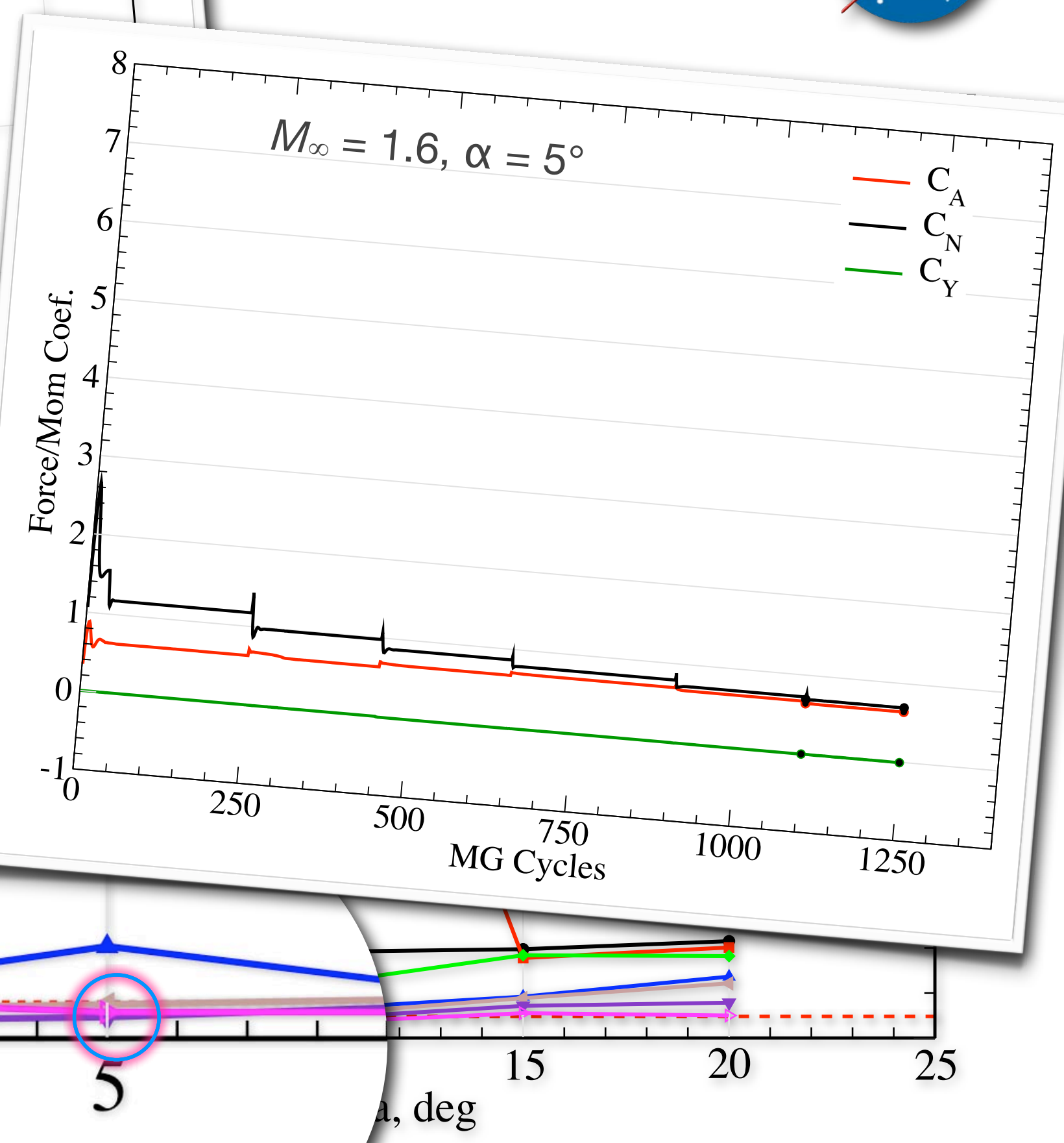
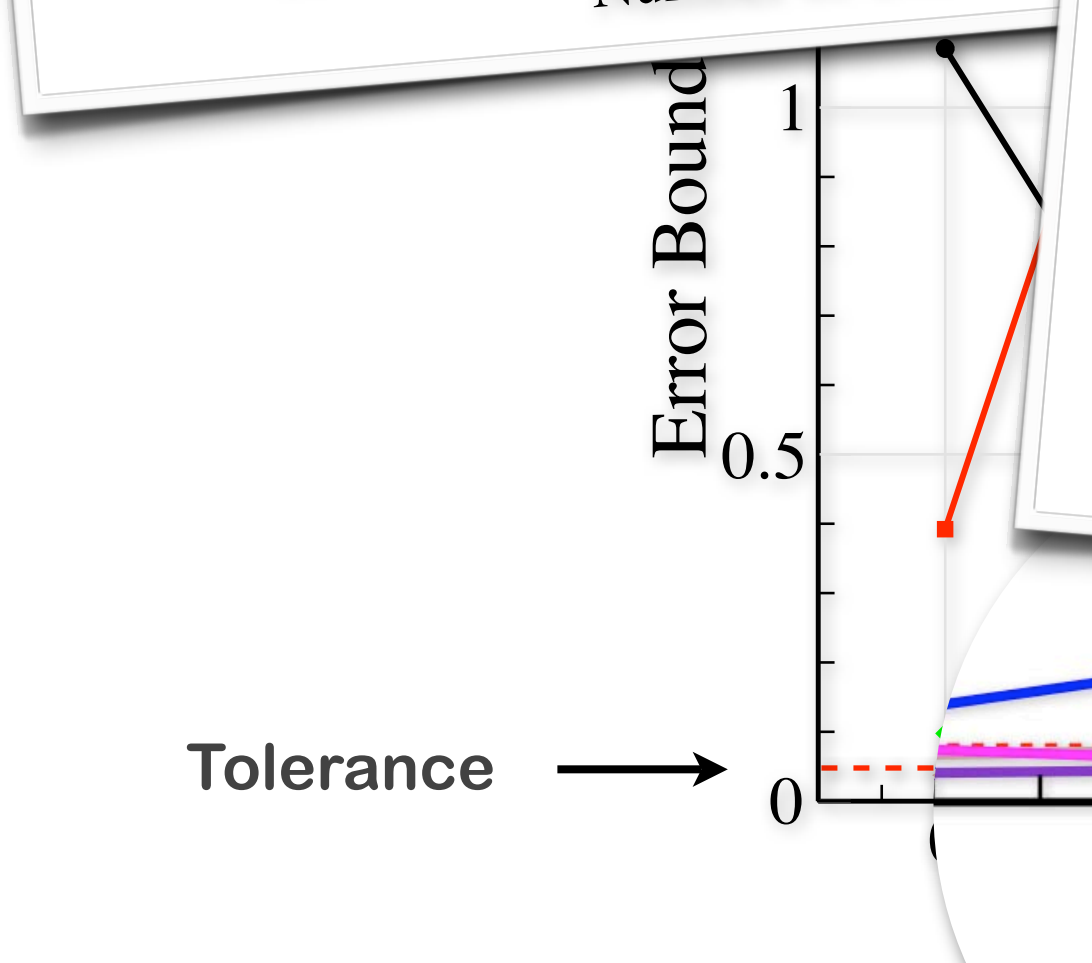
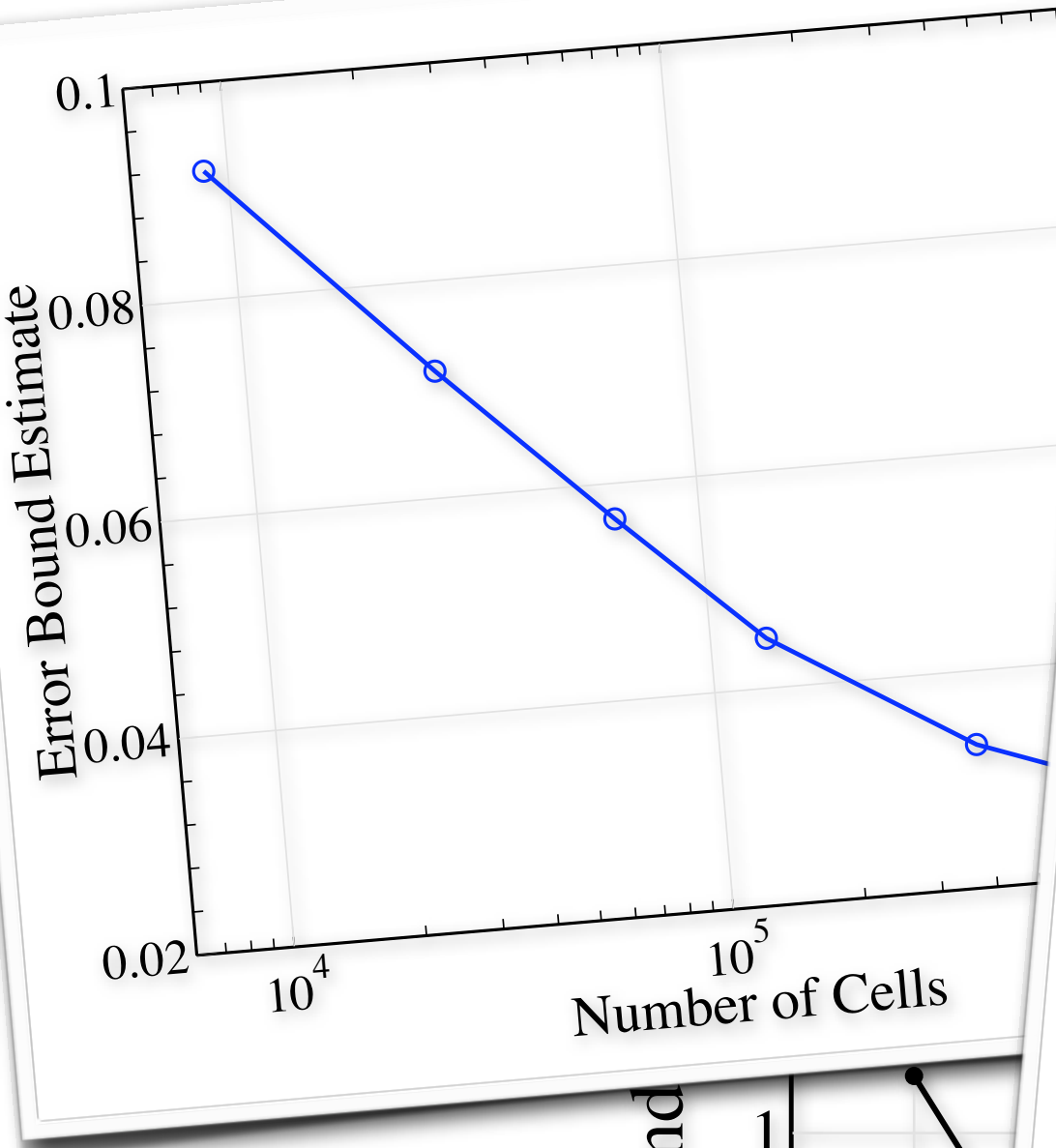




Error Controlled Database

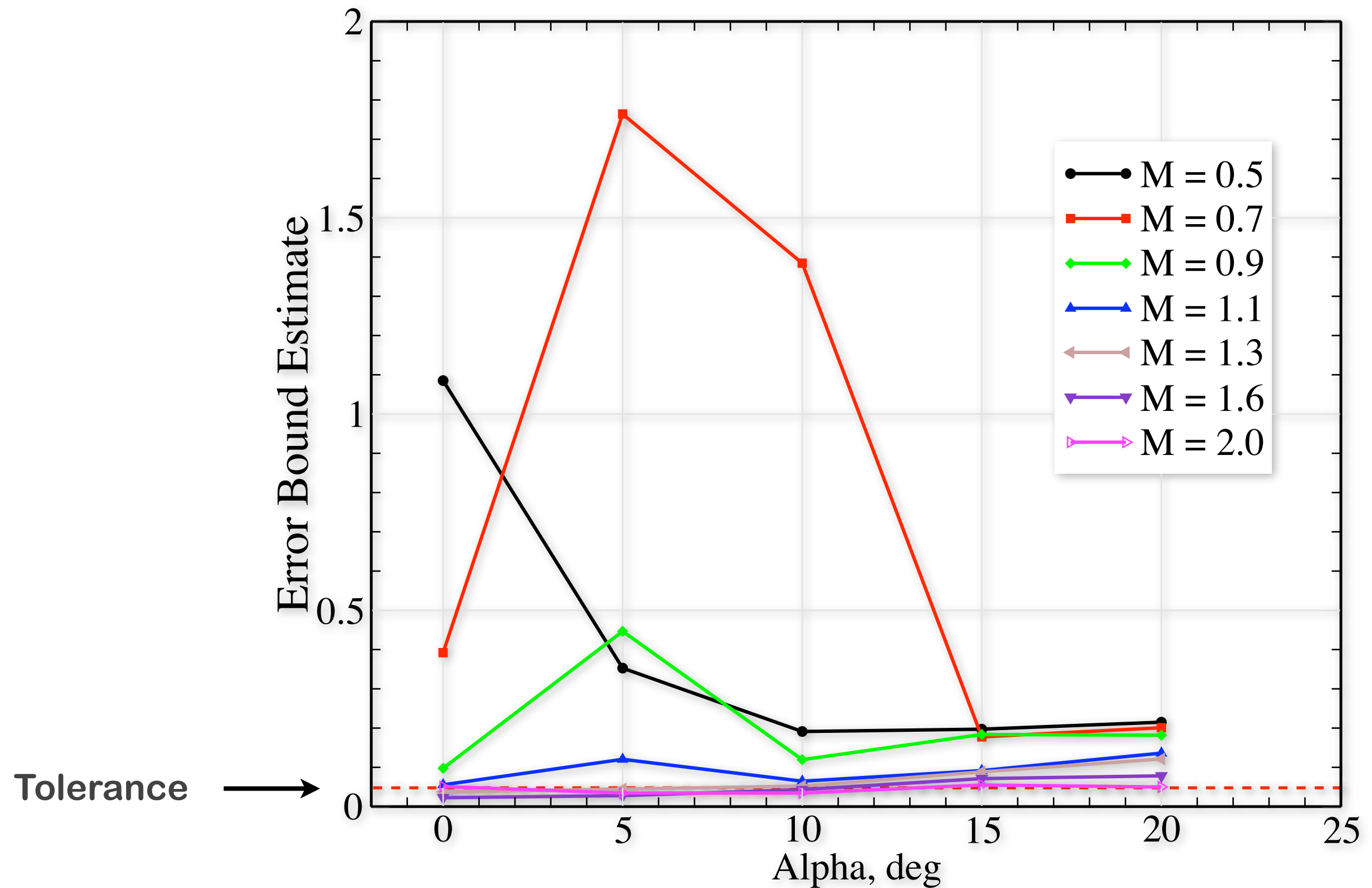






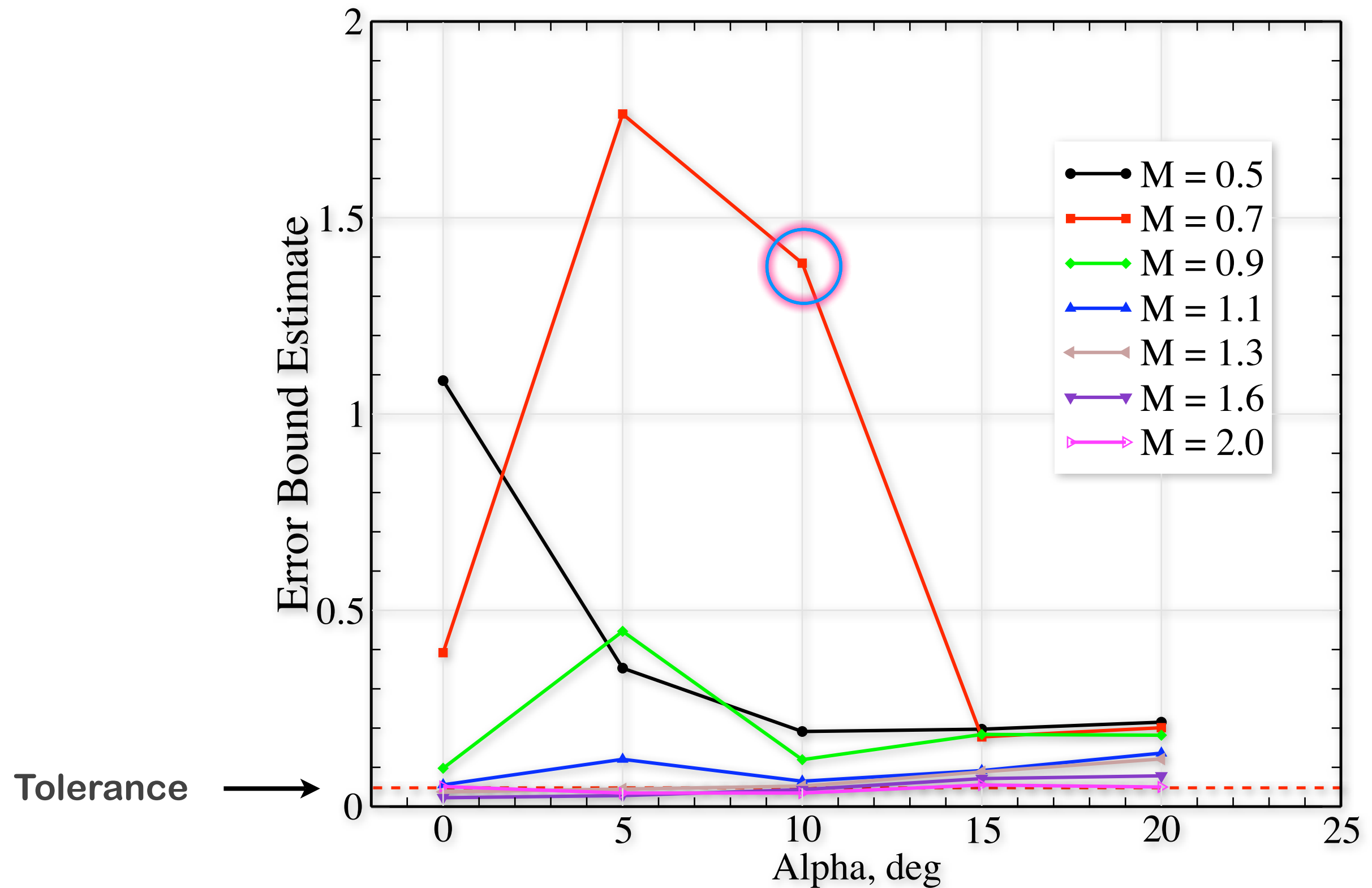


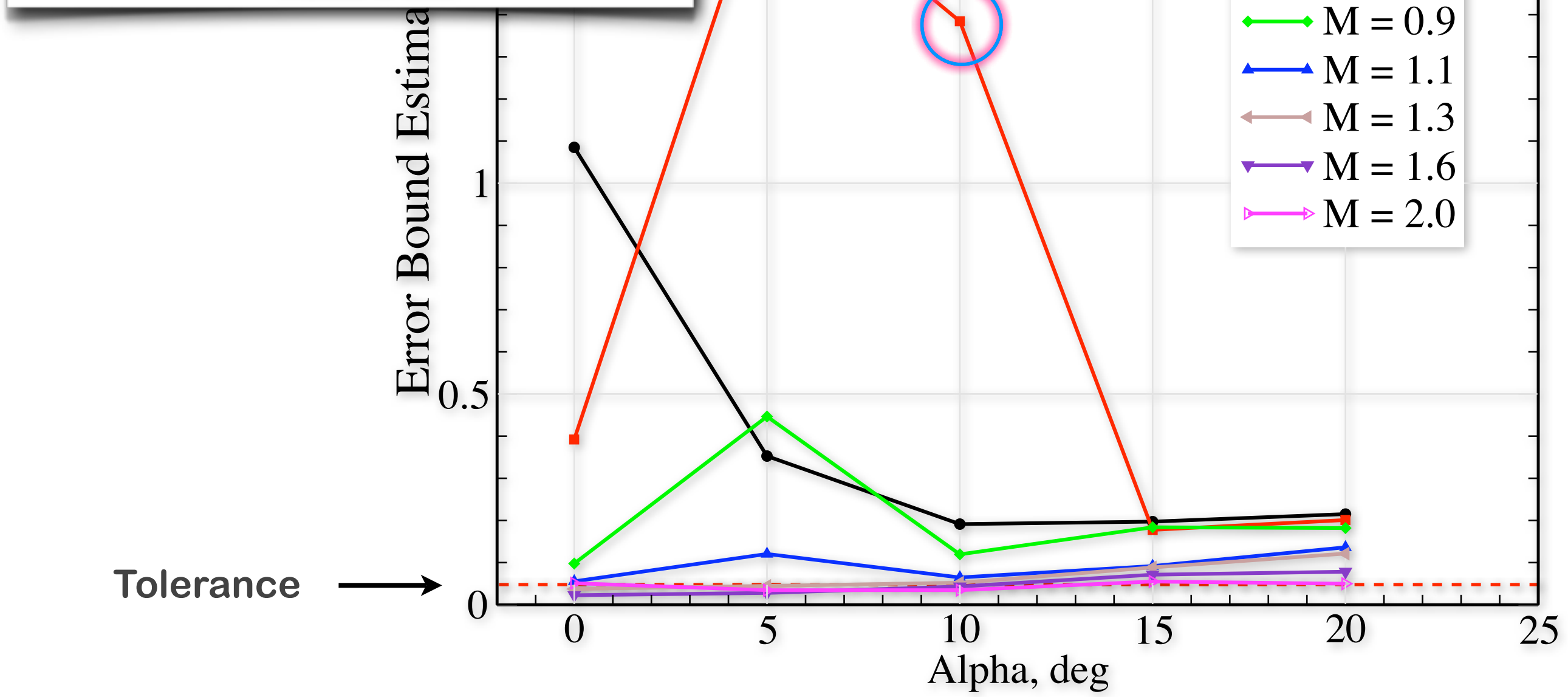
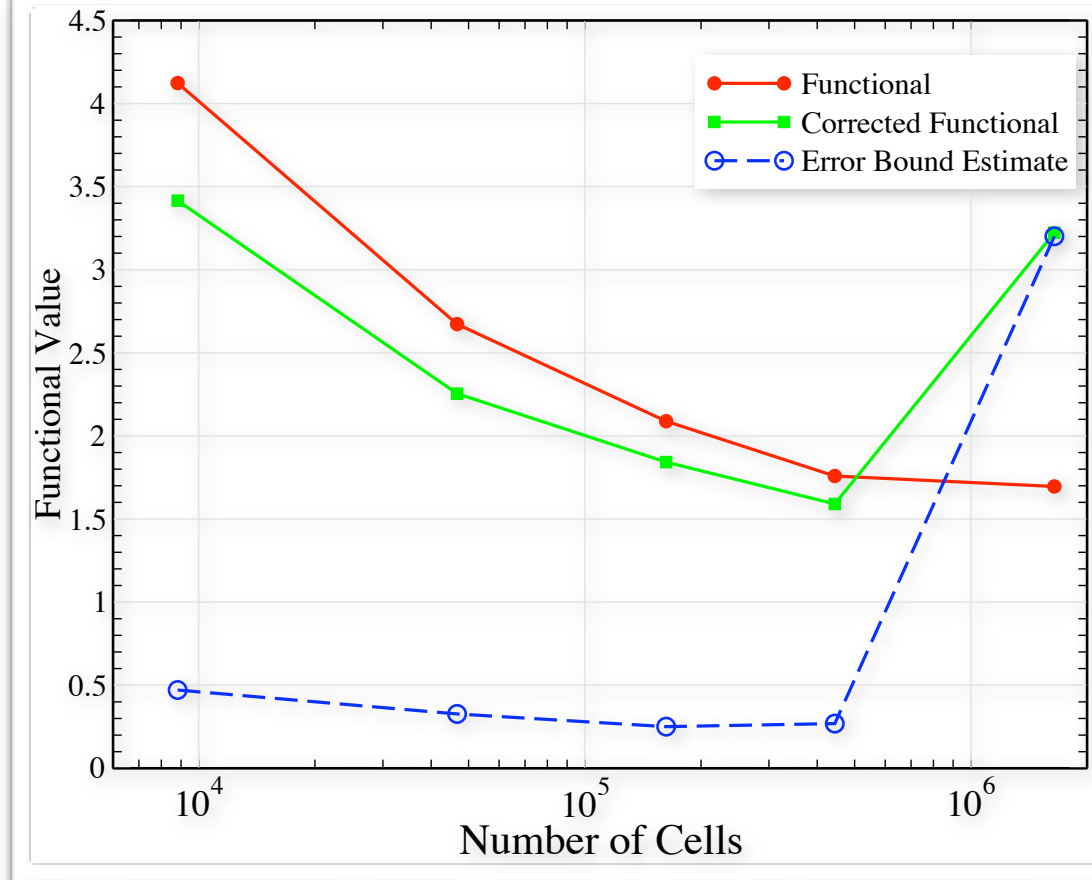
Error Controlled Database

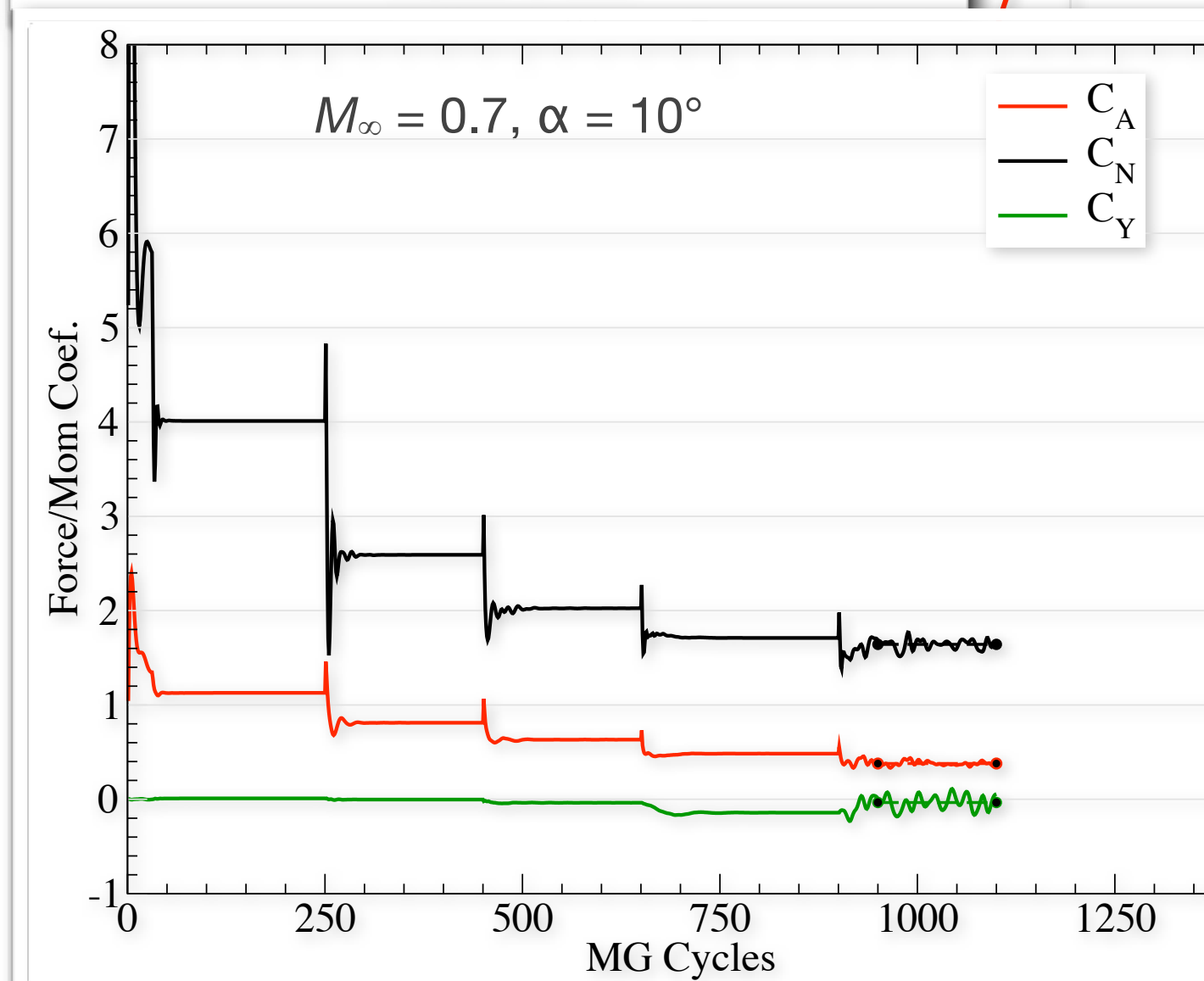
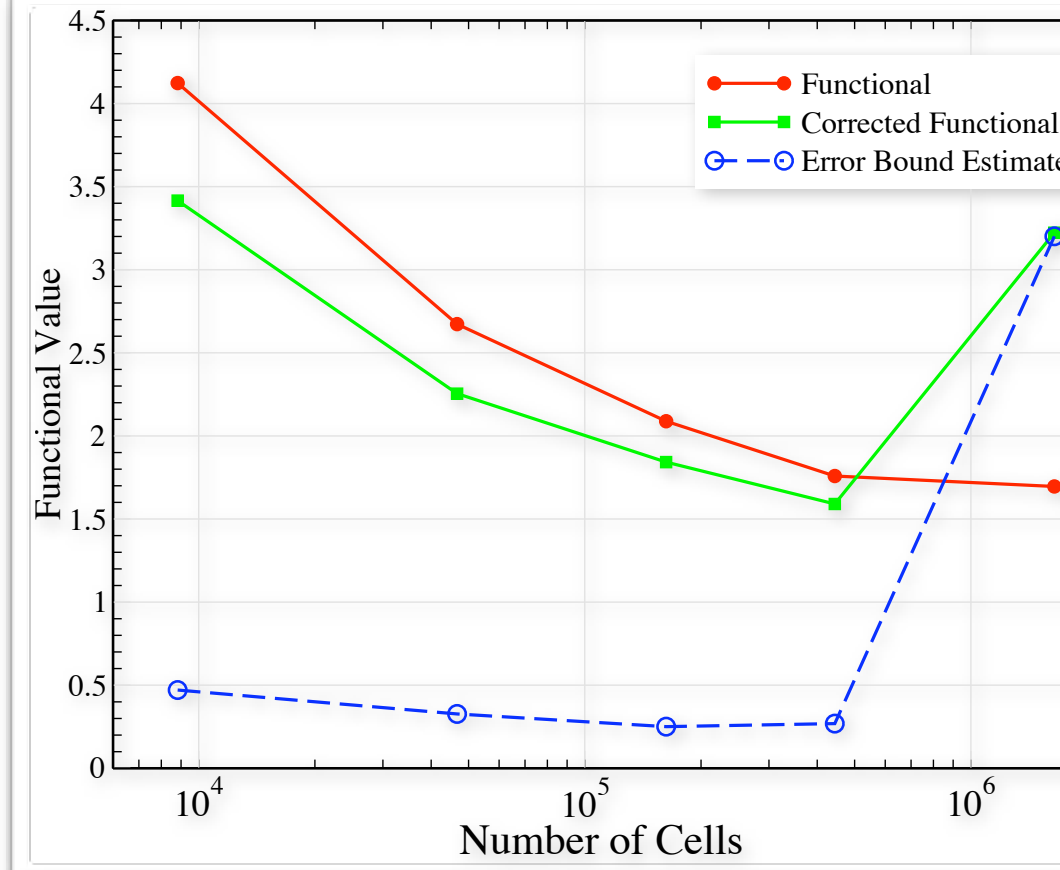




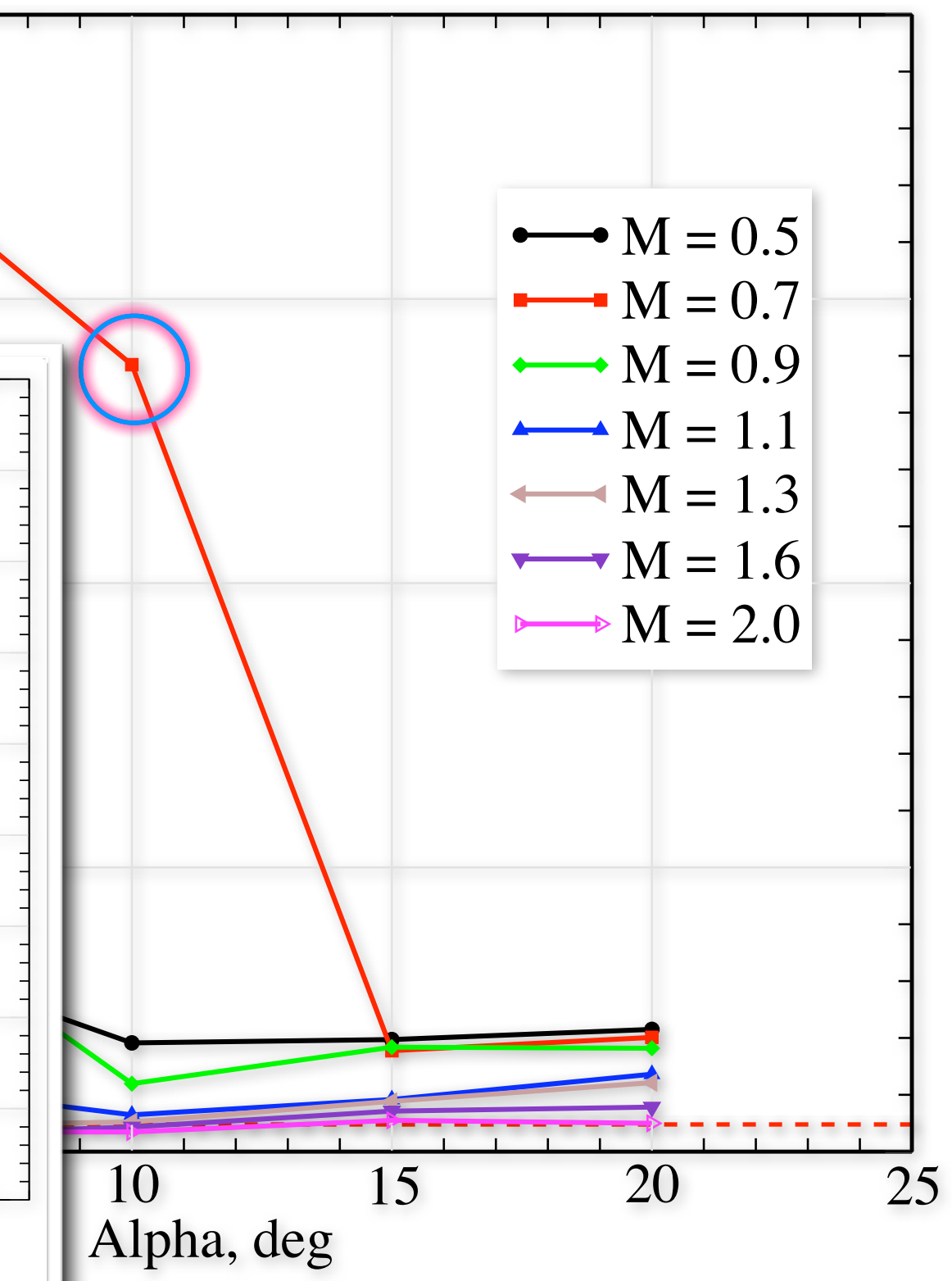
Error Controlled Database



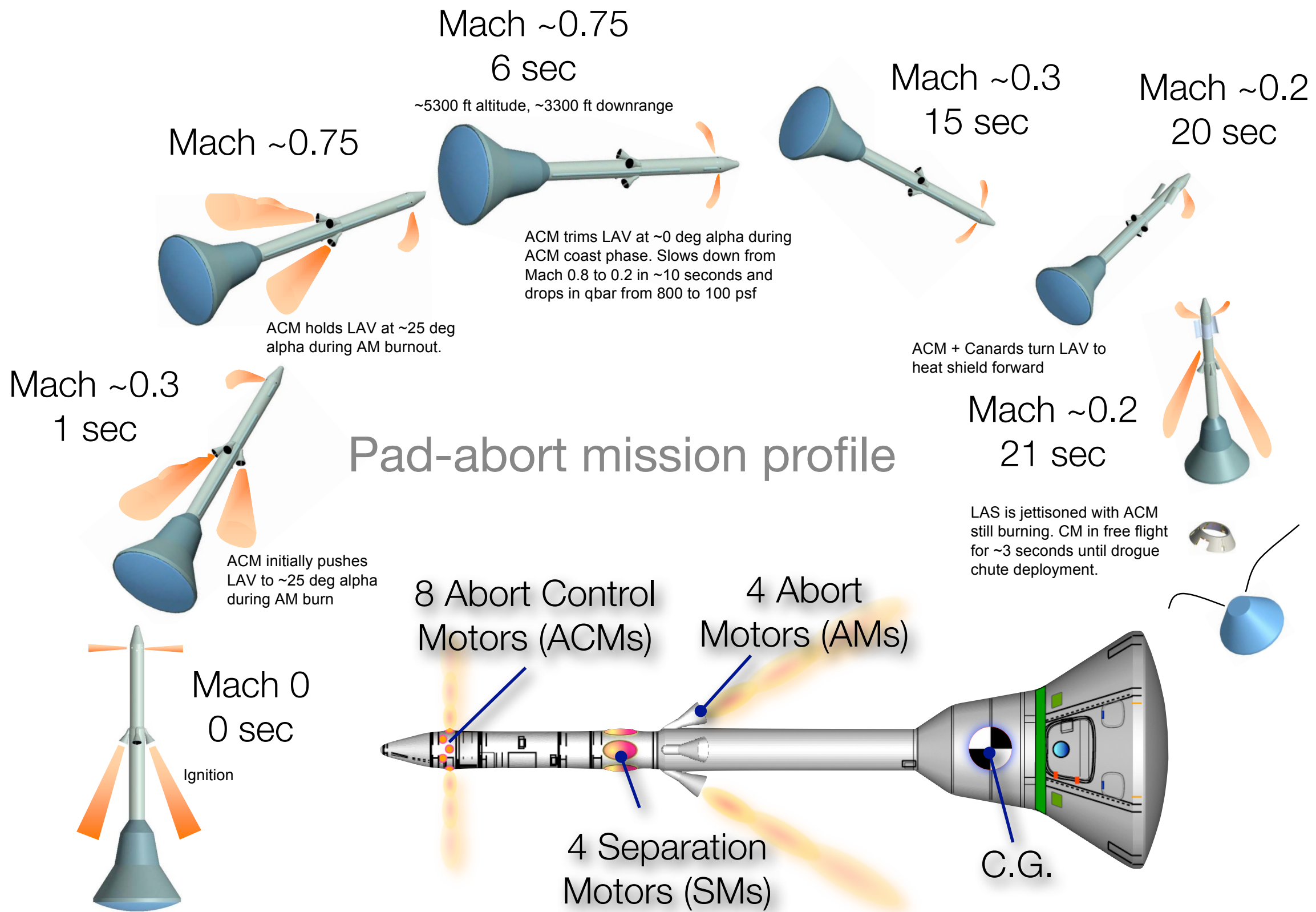




base



Launch Abort Vehicle with ACM Jets



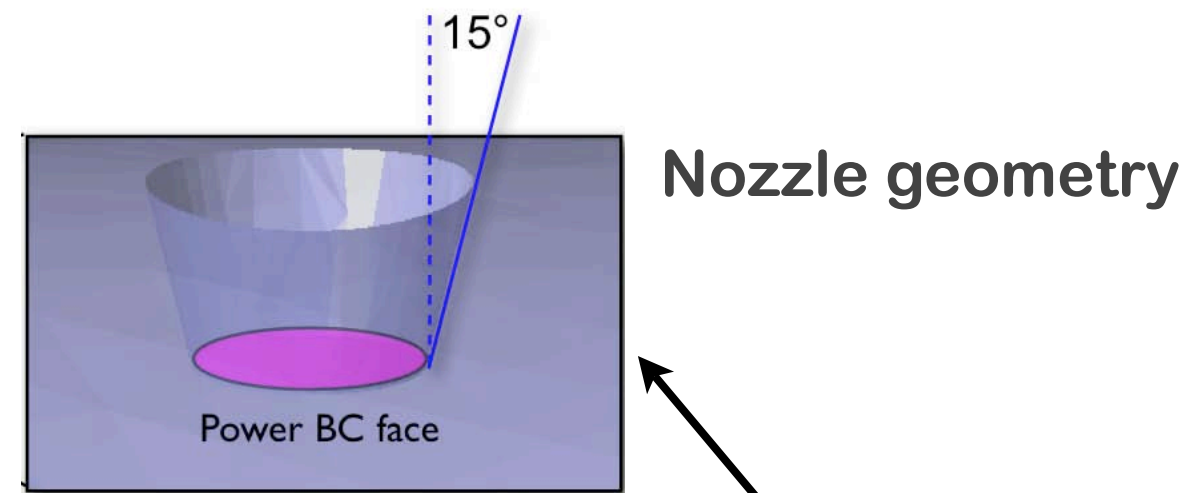
Launch Abort Vehicle with ACM Jets

Problem Setup

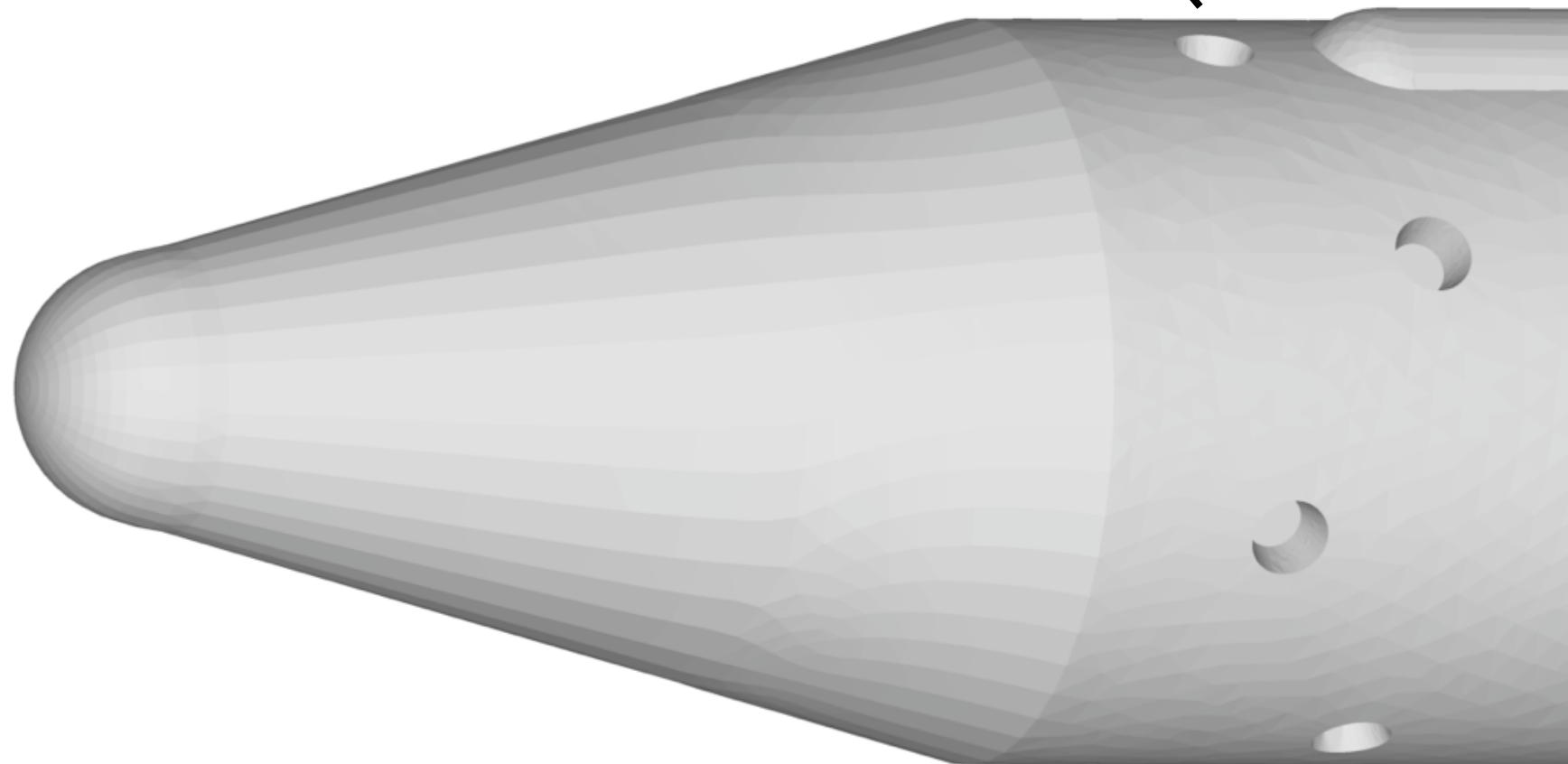
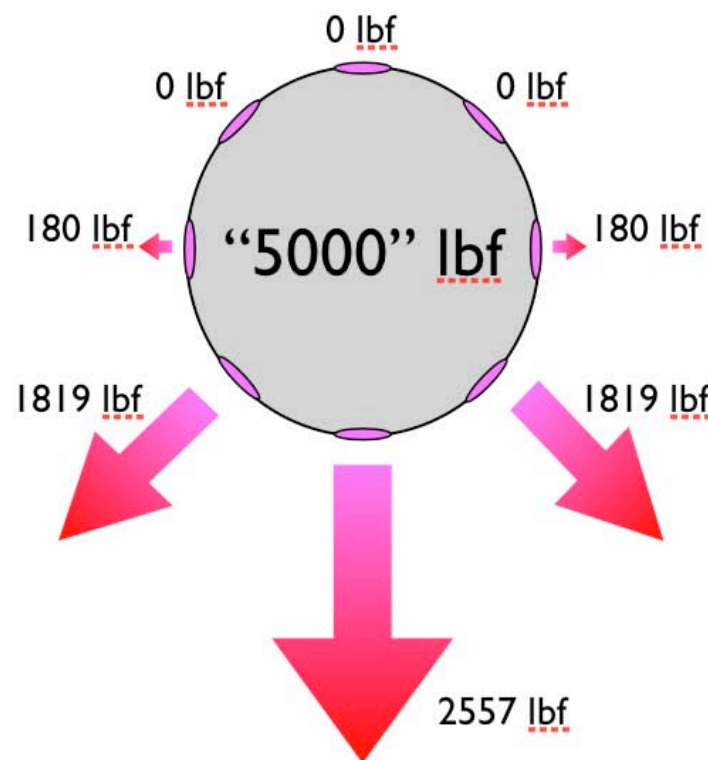


- Examine aerodynamic performance with ACM jets (AIAA 2008-1281)
- Selected case: $M_\infty = 4$, $\alpha = 20^\circ$, due to significant plume penetration
- Power boundary conditions applied at plenum face (assumes perfect gas)

- Functional: $C_N + 0.4C_A$

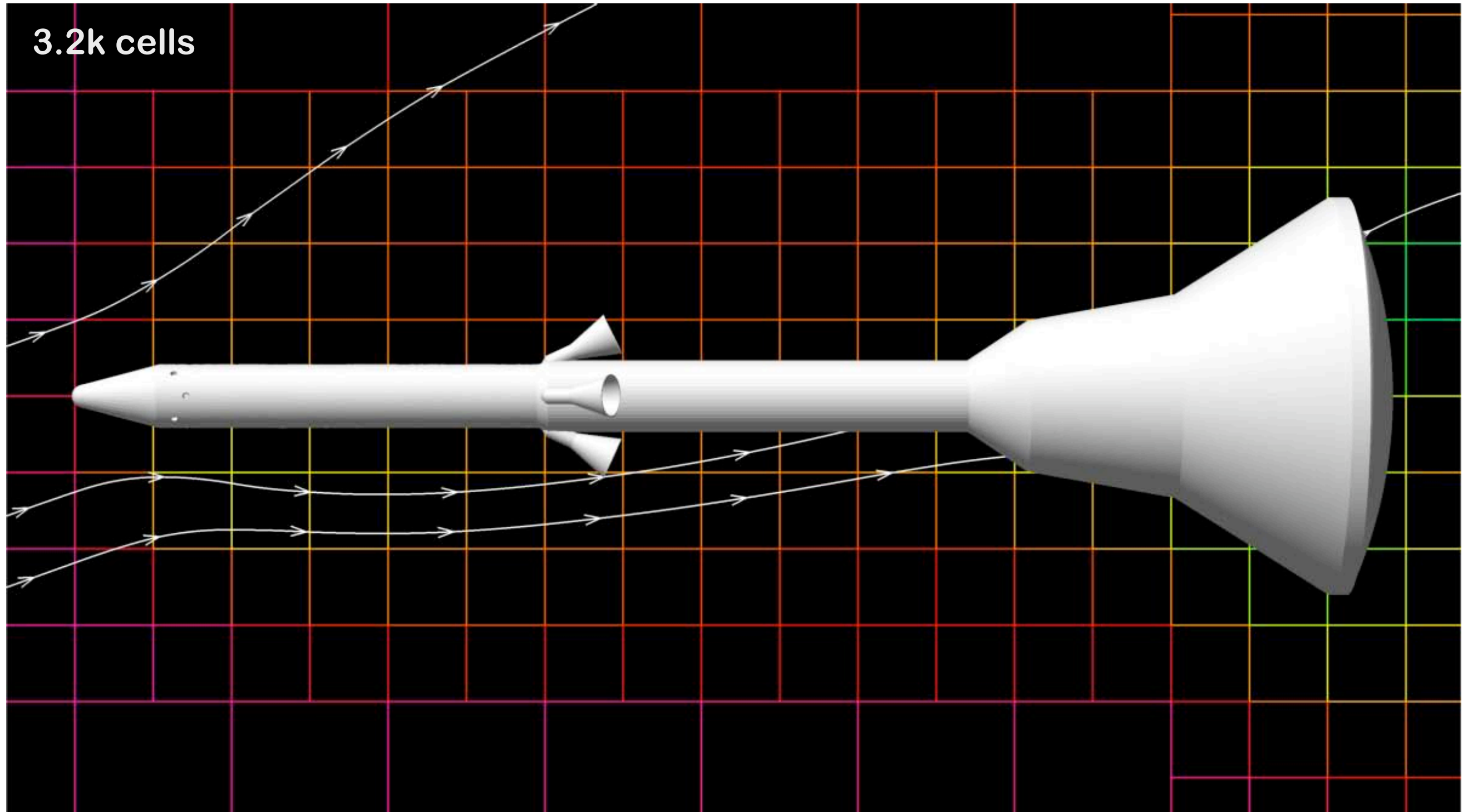


Thrust setting



Launch Abort Vehicle

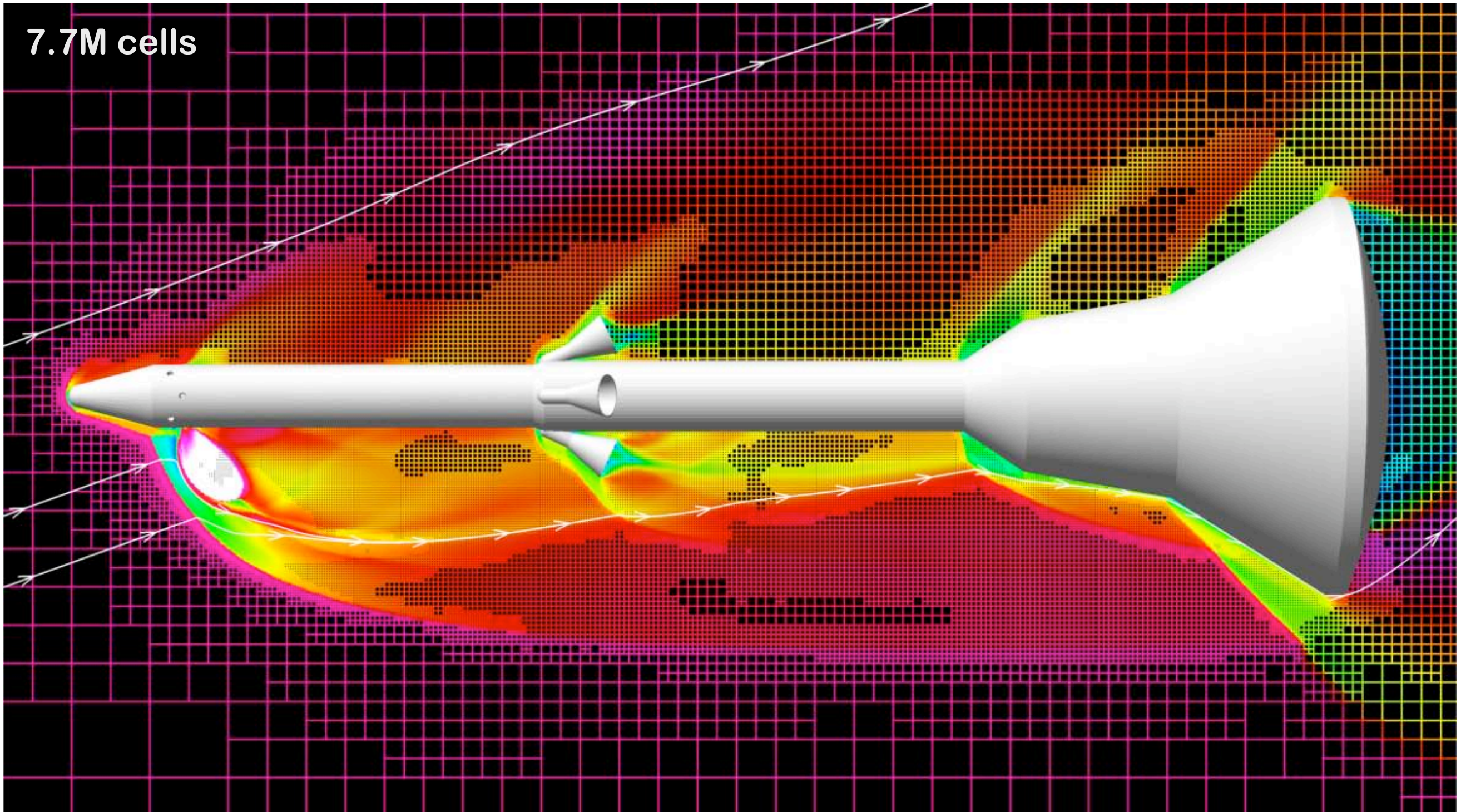
Initial mesh and solution on symmetry plane



Mach contours, $M_\infty = 4$, $\alpha = 20^\circ$

Launch Abort Vehicle

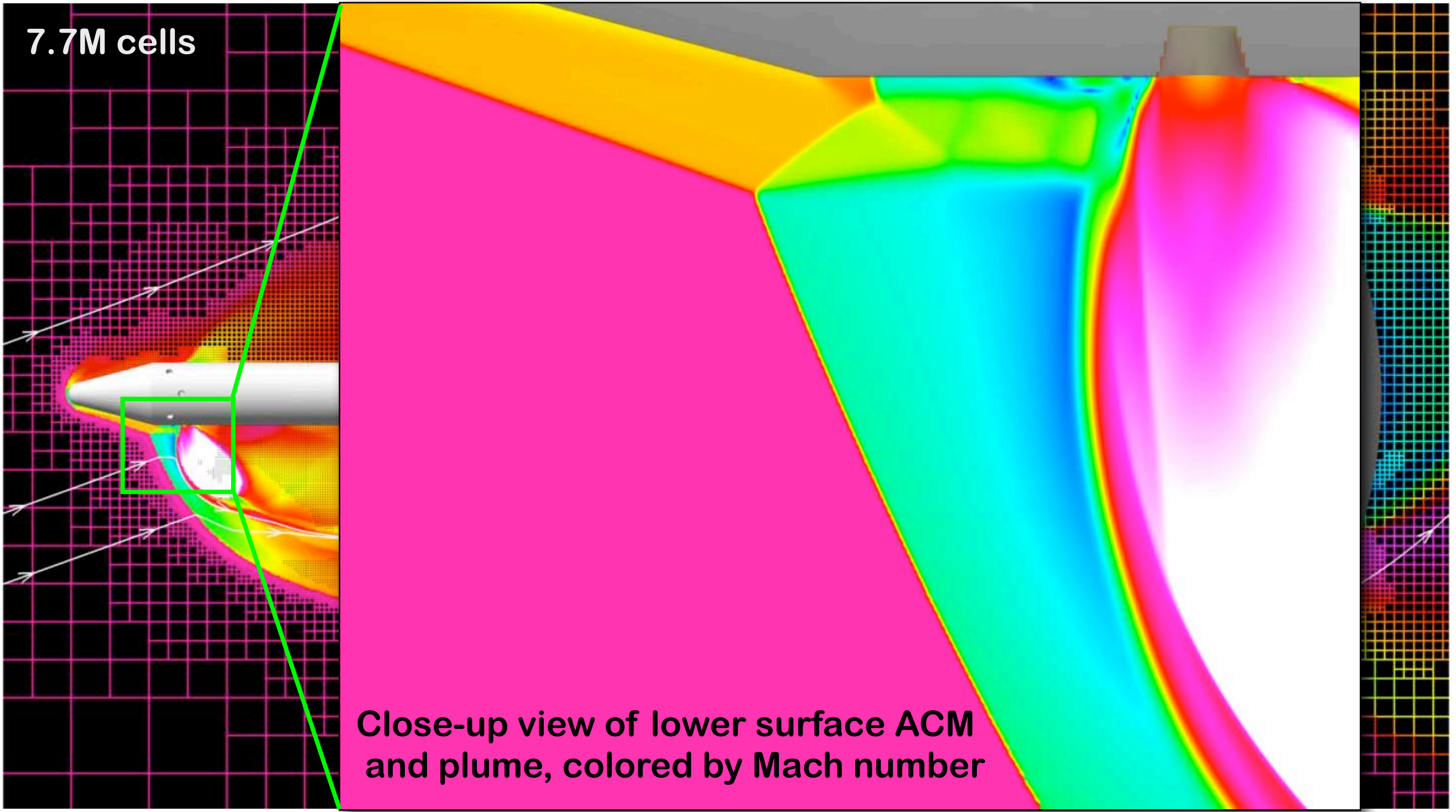
Final mesh and solution on symmetry plane



9 adaptations, Mach contours, $M_\infty = 4$, $\alpha = 20^\circ$

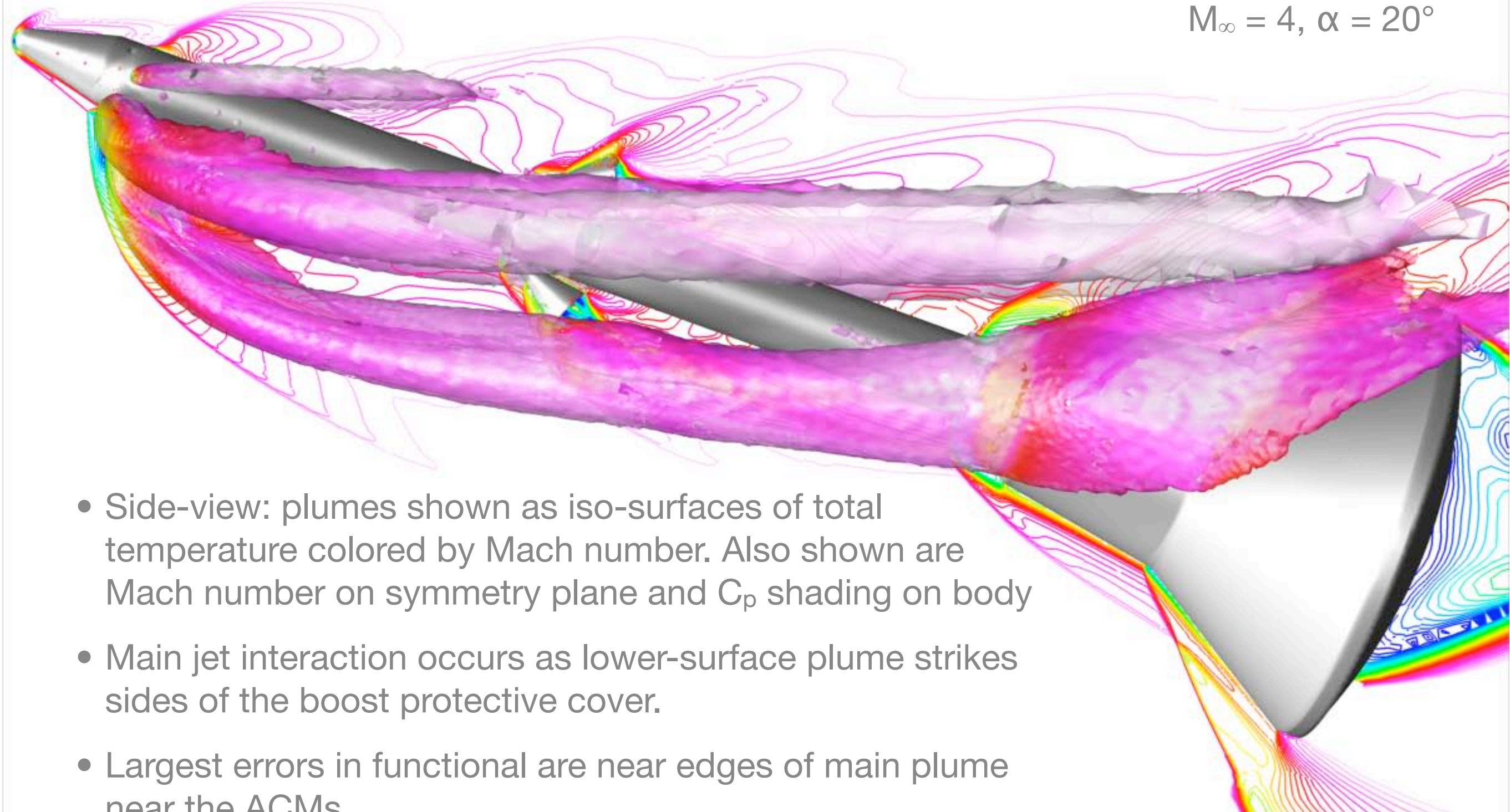
Launch Abort Vehicle

Final mesh and solution on symmetry plane



9 adaptations, Mach contours, $M_\infty = 4$, $\alpha = 20^\circ$

Launch Abort Vehicle Plume Visualization on Final Mesh (~7.7M cells)

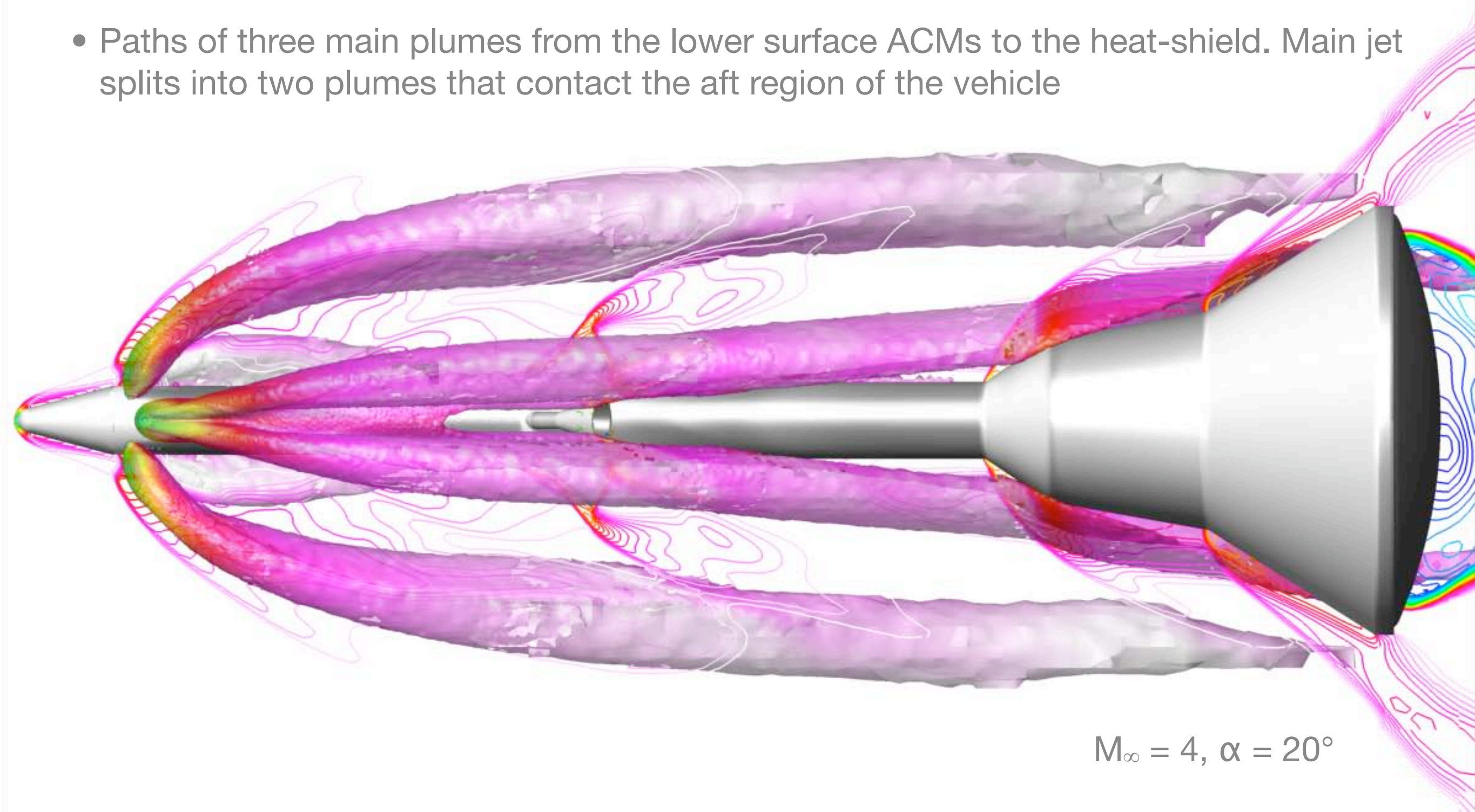


Launch Abort Vehicle

Bottom view of plumes on final mesh



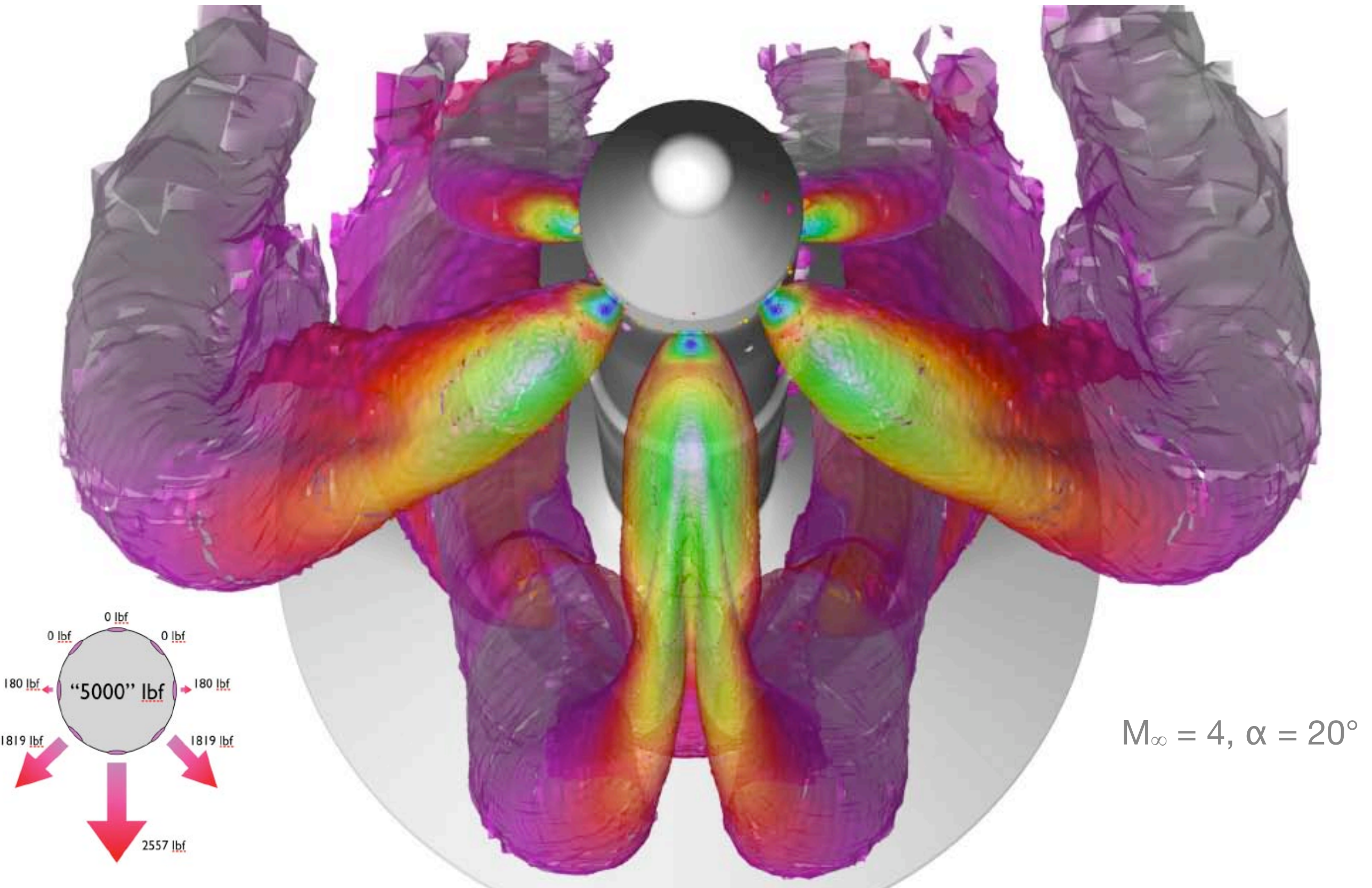
- Paths of three main plumes from the lower surface ACMs to the heat-shield. Main jet splits into two plumes that contact the aft region of the vehicle



$$M_{\infty} = 4, \alpha = 20^\circ$$

Launch Abort Vehicle

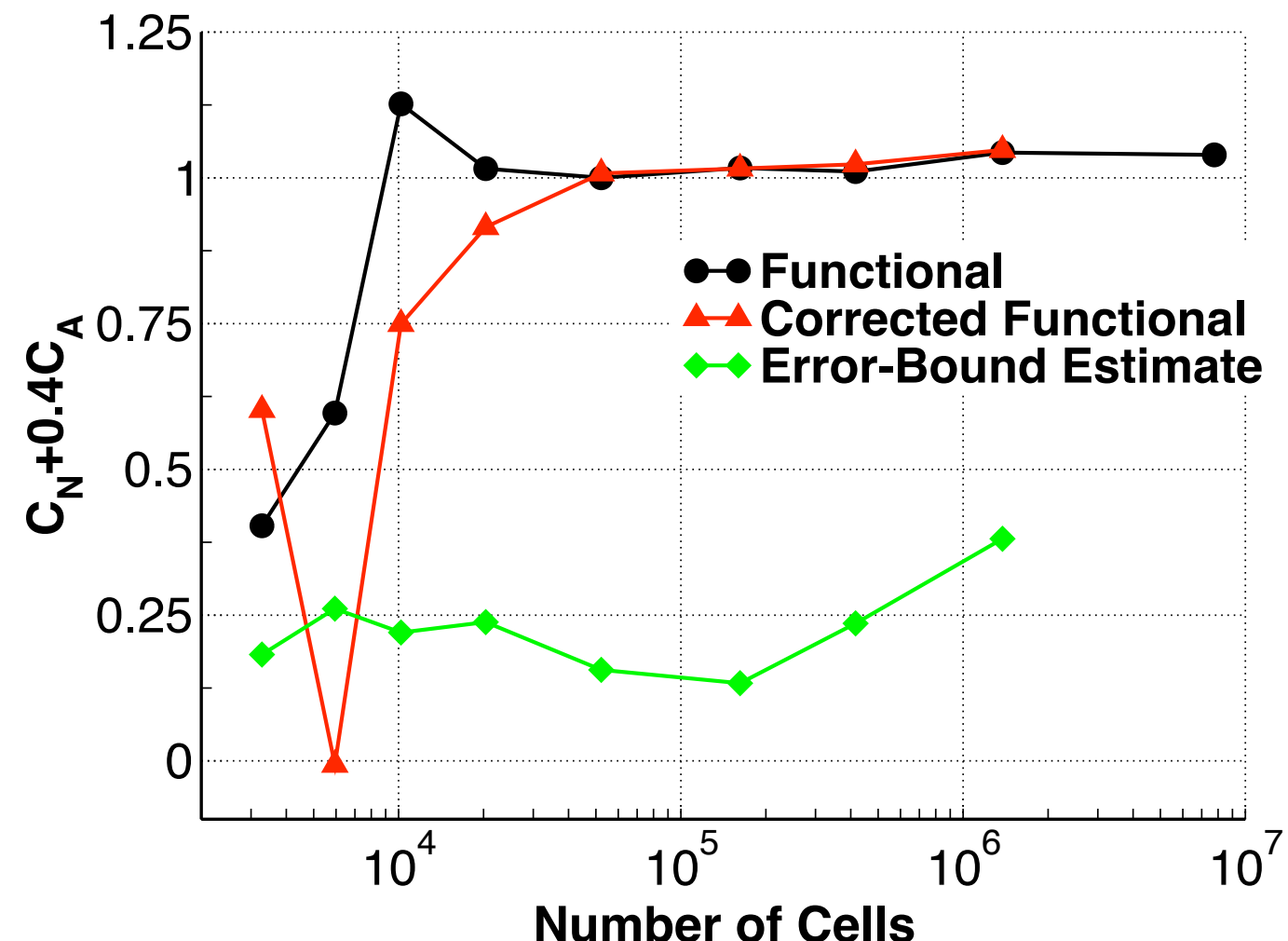
Front view of plumes on final mesh



Launch Abort Vehicle Functional Convergence



- Determination of plume paths and appropriate refinement of plume edges is not possible *a-priori*, yet these features determine the “aerodynamic shape” of the vehicle
- Adjoint error analysis identifies regions where jet interaction effects are important for the computation of aerodynamic coefficients and triggers mesh refinement
- Functional convergence settles down at ~1M cells, however, additional research is required to improve estimates of the error-bound





Summary

Presented a reliable and efficient approach for error estimates and mesh refinement of complex geometry problems

1. Handles complex geometry problems in an automatic fashion
2. Tolerant of coarse initial meshes
3. Behavior of functional, correction, and error estimate provide an indication of errors due to lack-of-convergence in steady simulations

→ **It is our best mesh generator ... refinement complements and surpasses expert knowledge**

→ **Allows users to focus on data validation and analysis instead of mesh generation**



Future Work

- Sonic-boom applications (Mathias Winzter)
- Address unsteadiness issues in difficult cases
 - Affordable mesh refinement and error bound for “mildly” unsteady flow
 - Formal unsteady adjoint development
- Control accuracy of objective functions in optimization studies

Acknowledgments

- Scott Murman, NASA Ames
- Tom Pulliam, NASA Ames
- Shishir Pandya, NASA Ames
- Goetz Klopfer, NASA Ames
- NASA Ames contract NNA06BC19C



Questions?



Marian.Nemec@nasa.gov

<http://people.nas.nasa.gov/~aftosmis/cart3d>